Diffusion in the titanium-aluminium system

DIFFUSION IN THE TITANIUM-ALUMINIUM SYSTEM

F.J.J. van Loo

DIFFUSION IN THE TITANIUM-ALUMINIUM SYSTEM

DIFFUSION IN THE TITANIUM-ALUMINIUM SYSTEM

PROEFSCHRIFT

ter verkrijging van de graad van doctor in de technische wetenschappen aan de Technische Hogeschool te Eindhoven, op gezag van de rector magnificus, prof. dr. ir. A.A. Th. M. van Trier, voor een commissie uit de senaat in het openbaar te verdedigen op vrijdag 17 september 1971 te 16.00 uur

door

Frans Johan Jozef van Loo

geboren te Heerlen

Dit proefschrift is goedgekeurd door de promotor
prof. dr. G.D. Rieck

Aan de nagedachtenis van mijn moeder
Aan mijn vader

Tekeningen : H.J. van der Weijden
Fotografisch werk: L.J. Horbach
Correctie Engels : H.J.A. van Beckum
Typewerk : mevr. Th. de Meijer-van Kempen

Alle leden van de groep Fysiche Chemie hebben bijgedragen aan het tot stand komen van dit proefschrift. In het bijzonder wil ik hierbij noemen de heer J.H. van der Ham, die met grote toewijding en inventiviteit vanaf het eerste begin heeft meegewerkt aan het preparatieve en metallografische gedeelte van dit onderzoek. Aan allen mijn welgemeende dank!

Bovenal echter dank ik mijn vrouw die mij zo voortreffelijk heeft gesteund, mij vele waardevolle adviezen heeft gegeven en die zich zoveel opofferingen heeft moeten getroosten.

CONTENTS

CHAPTER VI EVALUATION OF THE EXPERIMENTAL RESULTS

LIST OF SYMBOLS

a_i = activity of component i = $\gamma_i N_i$

a_g = mean radius of a grain or half the mean distance between dislocation pipes in cm

C_i = concentration of component i in moles/cm^3

C_i^- = initial concentration of component i on the left-hand side of the diffusion couple

C_i^+ = initial concentration of component i on the right-hand side of the diffusion couple

D = interdiffusion coefficient (also called chemical diffusion coefficient or, simply, diffusion coefficient) in cm^2/sec

D_c = apparent or macroscopic diffusion coefficient (see section 2.6.) in cm^2/sec

D_i^s = self-diffusion coefficient of component i in cm^2/sec

D_o = frequency factor in cm^2/sec

D_v = true volume diffusion coefficient in cm^2/sec

$D_{int.}$ = integrated diffusion coefficient in cm^2/sec (see section 2.4.1.)

d_γ = width of layer γ in µm or cm

d_l = layer width during the linear growth period

I_i = corrected intensity for component i in an alloy in microprobe analysis

I_i^o = corrected intensity for component i in the pure metal i in microprobe analysis

J_i = flux of atoms of component i across a section, fixed with respect to the origin (see section 2.2.1.) in moles /cm^2 sec

J_i^m = flux of atoms of component i across a marker interface (usually the Kirkendall interface, see section 2.2.2.) in moles /cm^2 sec

K_i = I_i/I_i^o

k_γ = penetration constant for the growth of layer γ in cm^n/sec

k_l = penetration constant for the layer growth during the "linear" growth period in cm^n/sec

k_p = penetration constant for the layer growth during the parabolic growth period in cm^2/sec

N_i = mole fraction of component i. For superscript - or +, see C_i

n = exponent in the relation $d_\gamma^n = k_\gamma t$

Q = energy of activation in cal/mole

R = gas constant = 1.986 cal/mole deg

T = temperature in ^{o}K unless stated otherwise

t = diffusion duration in sec

t_l = duration of the linear growth period in sec

V_i = specific molar volume of component i in cm^3

$\overline{V}_i$ = partial molal volume of component i in cm^3

V_m = molar volume in cm^3. For superscript - or +, see C_i

VH100 = Vickers hardness number, using a 100 g load

v = velocity of flow, determined by the instantaneous velocity of local markers, in cm/sec

v_m = velocity of markers, mostly inserted in the Kirkendall interface, in cm/sec

x = coordinate in the diffusion direction in cm

x_o = coordinate of the origin (see section 2.2.1.)

x_m = coordinate of the Kirkendall interface

Y = concentration unit for component i = $(N_i - N_i^-)/(N_i^+ - N_i^-)$

γ_i = activity coefficient of component i

$\lambda(C_i)$ = Boltzmann function = $x/t^{\frac{1}{2}}$

μ_i = chemical potential of component i per mole

An asterisk (as in C_i^*, x^*, Y^*) refers to a definite value of the quantity in question.

All percentages are given in atomic or mole per cent unless stated otherwise.

CHAPTER I

INTRODUCTION

1.1. INTERDIFFUSION IN METAL SYSTEMS

If two metals are in contact with each other at a sufficiently high temperature they interdiffuse. Dependent on the nature of the starting materials, temperature and duration, a new concentration distribution will be set up. If for such a system a well-defined interdiffusion coefficient is available as a function of concentration and temperature, this new distribution may be predicted[1-3].

At the moment, such data have been determined for a number of binary systems. If more than two components are present, then only incomplete data are on hand, since in this case experiments are extremely time-consuming.

Knowledge of diffusion data is important in many cases:

(a) In metallurgy several processes are controlled by diffusion, e.g. homogenisation, non-martensitic phase transformation, precipitation, oxidation and sintering.

(b) In coating and finishing techniques as well as in various brazing and welding processes the interaction between base metal and applied metal at elevated temperatures must be known.

(c) The diffusion coefficient may supply much information on fundamental physical and thermodynamic phenomena, like point defects in crystals and thermodynamic activities of the components.

Another application of interdiffusion experiments is the examination of the phase diagram of a binary system. As will be seen, this method is not completely reliable, but, performed in a careful way, interesting results may be obtained.

Various methods are known to determine the diffusion process by experiment, e.g. from measured penetration curves as carried out in this thesis, but also by means of radioactive tracers and by internal friction. Generally, the results agree satisfactorily.

1.2. THE OBJECT OF THIS THESIS

Titanium can only be used as a structural material up to about 550 ^{o}C

despite its high melting point of 1670 °C[4-8]. There are two reasons for this:

(1) Mechanical properties, like strength, deteriorate above 550 °C. This might be overcome by alloying, although investigations in this field conducted during the last fifteen years have produced only little result.

(2) Above this temperature, gases like oxygen and nitrogen diffuse into titanium, causing deterioration of its properties. This can be surmounted by coating titanium with a protective layer[4,6,9-13].

This study of the interdiffusion in the titanium-aluminium system is carried out for several reasons:

(a) Titanium alloys used in practice almost invariably contain aluminium in various percentages, so a better knowledge of these alloys is desirable.

(b) The phase diagram, especially the titanium-rich part, was little known at the beginning of the present investigation. The thesis wants to contribute to a better knowledge on the subject.

(c) Aluminide coatings, as referred to in point (2) above might be used in the case of titanium for future applications (as with niobium at the moment)[9,10,13]. In this connection quantitative determination of the various diffusion coefficients and activation energies may be very helpful. Also, the growth kinetics and the mechanical properties of diffusion layers between various starting materials have to be known.

(d) There is a great deal of confusion in the literature concerning the determination of diffusion coefficients when partial molal volumes are not constant. Part of the present thesis has been devoted to this problem.

CHAPTER II

THEORY OF INTERDIFFUSION

2.1. DIFFUSION MECHANISMS

A number of possible mechanisms has been suggested for explaining diffusion in a crystalline solid. Manning[14] gives an excellent survey, from which an abstract is given below:

diffusion in crystalline solids	volume diffusion	no imperfections needed	exchange mechanism
			ring mechanism
		interstitial atoms involved	interstitial mechanism
			interstitialcy mechanism
		vacancies involved	vacancy mechanism
			divacancy mechanism
	short-circuit diffusion	surface diffusion mechanism	
		grain boundary diffusion mechanism	
		dislocation pipe diffusion mechanism	

In this chapter only volume diffusion in regions of regular lattice structure in binary metal systems will be discussed in detail. Because of its low activation energy short-circuit diffusion may be important at lower temperatures. Therefore, it must be kept in mind in the analysis of the experimental results.

In volume diffusion, the exchange and ring mechanism could be important in very loosely packed crystals. In these mechanisms, two or more atoms simply change places. New lattice sites are not formed and therefore, it is obviously impossible to obtain a nett displacement of atoms relative to the crystal lattice. In practice, however, these displacements are very common (Kirkendall effect, see section

2.2.2.). Therefore, exchange or ring mechanism is improbable in most metal systems.

Mechanisms involving interstitial atoms are not in contradiction to the Kirkendall effect. However, interdiffusion between two metals involving interstitial atoms would cause a decrease in the total number of lattice sites. Experimentally, this is not found in most binary metal diffusion studies[14]. Besides, the formation of pores which is often observed in the diffusion zone cannot be explained satisfactorily by an interstitial mechanism. Moreover, interstitial as well as exchange mechanisms are also unlikely for energetic reasons, since the theoretically calculated activation energy for these processes is considerably higher than the actually measured energy. In some sort of structures, however, these mechanisms may play an important part, e.g. in very loosely packed crystals or in systems where a great difference in atomic radius occurs.

Mechanisms involving vacancies are the most probable, explaining both the observed Kirkendall effect as the observed activation energy. In the case of a simple vacancy mechanism, atoms exchange with vacant sites (vacancies). The number of these vacancies is normally in thermodynamic equilibrium with the volume of the metal.

Generally, atoms of one component exchange more readily with vacancies than atoms of the other, so sources as well as sinks for vacancies must be operating to retain the equilibrium number. Possible sources and sinks are the surface of the metal, grain boundaries and dislocations. Since the Kirkendall effect is the same in samples with large and small grains respectively, and is also independent of the vicinity of a surface[3], it is believed that dislocations are the main sources and sinks for vacancies.

In regions where a large number of vacancies have to vanish,it might be found that dislocations are insufficient for this purpose, and cavities by combination of vacancies occur, which become stable above some critical size and grow into microscopically observable voids or pores of mostly crystallographic shape. The reverse effect, i.e. volume expansion to create vacancies, is also observed.

The divacancy mechanism seems to contribute to a considerable extent only at high temperatures[15].

In this chapter the following assumptions will be made:

(a) Diffusion is proceeding according to a simple vacancy mechanism. Vacancies are in thermodynamic equilibrium in the entire diffusion system, so no formation of pores occurs.

(b) The cross-section of the "diffusion couple" remains constant[16].

(The term diffusion couple will henceforth be used to denote a system of two interdiffusing materials).

(c) The diffusion process will not extend to the ends of the couple ("infinite diffusion couple"). Therefore, the concentrations at the ends remain constant.

(d) Diffusion takes place only in the direction perpendicular to the contact interface between the two metals. This will be called the x-direction.

2.2. DIFFUSION IN SINGLE-PHASE SYSTEMS ASSUMING CONSTANT PARTIAL MOLAL VOLUMES

If at a certain elevated temperature two metals 1 and 2 form a solid solution over the whole range of concentration, diffusion between these metals will cause a smooth penetration curve for both components. The

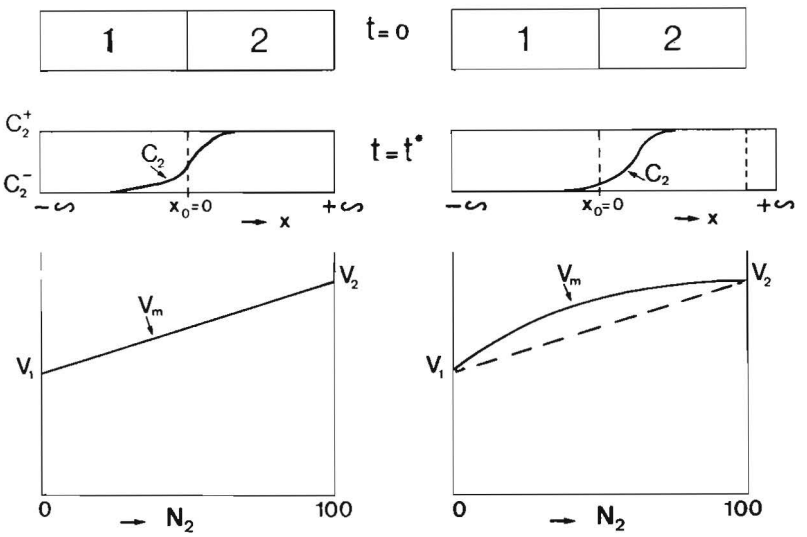

Fig.2.1,a. In the metal system 1-2 $\bar{V}_1$ and $\bar{V}_2$ are independent of concentration; consequently, the total volume of the couple remains constant after diffusion time t .

Fig.2.1,b. A metal system is shown in which $\bar{V}_1$ and V_2 depend on concentration; therefore, the total volume of the couple has changed after diffusion time t. (In this example the couple expands since the molar volume is larger than represented by the dotted line).

total volume of the couple will not change if the partial molal volumes are constant. If this condition does not apply, the volume will either expand or contract (see fig.2.1.a,b; for explanation of the symbols see page 5).

2.2.1. The choice of the frame of reference; Fick's laws and their solutions

In this thesis the origin of the coordinate system $x_o = 0$ is fixed with respect to the non-diffused left-hand end of the diffusion couple, formally referred to as $x = -\infty$ at any instant t. As shown in fig.2.1,a,b at time t= 0 the plane $x_o = 0$ coincides with the contact interface between the two metals, or more generally, between the two "starting materials".

If the total volume remains constant, this particular choice is in fact immaterial. However, if the total volume expands or contracts (section 2.3.) the choice is very important and is found to be a source of confusion in many papers.

If the total volume remains constant, the flux of moles of component i across any section, fixed with respect to the origin, can be expressed by Fick's first law:

$$J_i = - D(\partial C_i/\partial x) \qquad (1)$$

Experiments show that the interdiffusion coefficient D is a function of C_i and temperature, but is independent of the magnitude of $\delta C_i/\delta x$ (see also section 2.5.). Eq.(1) is often referred to as a definition of the interdiffusion coefficient, although it must be emphasised that this is only true is the total volume of the couple is constant (see section 2.3.1.).

Combination of Fick's first law and the law of conservation of matter leads to Fick's second law

$$\frac{\partial C_i}{\partial t} = \frac{\partial}{\partial x}\left(D \frac{\partial C_i}{\partial x} \right) \qquad (2)$$

A solution of Eq.(2) is given by Boltzmann[17] and first applied to interdiffusion problems by Matano[18] (the Boltzmann-Matano solution). This allows D to be calculated as a function of duration t, concentration C_i and coordinate x.

Using the boundary conditions

$$\begin{aligned} C_i &= C_i^- \quad x<0 \quad t = 0 \\ C_i &= C_i^+ \quad x>0 \quad t = 0 \end{aligned} \tag{3}$$

and substituting the function $\lambda\,(C_i) = x/t^{\frac{1}{2}}$ in Eq. (2), the latter can be solved:

$$D(C_i^*) = -\frac{1}{2t}\left(\frac{\partial x}{\partial C_i}\right)^* \int_{C_i^-}^{C_i^*} x\,dC_i \tag{4}$$

If $C_i^* = C_i^+$, Eq.(4) reduces to

$$\int_{C_i^-}^{C_i^+} x\,dC_i = 0 \tag{5}$$

In fact, Eq.(5) defines the plane $x_o = 0$, called the Matano interface. Eqs.(4) and (5) can be solved graphically from the measured penetration curve (see fig.2.2.). It must be emphasised that the

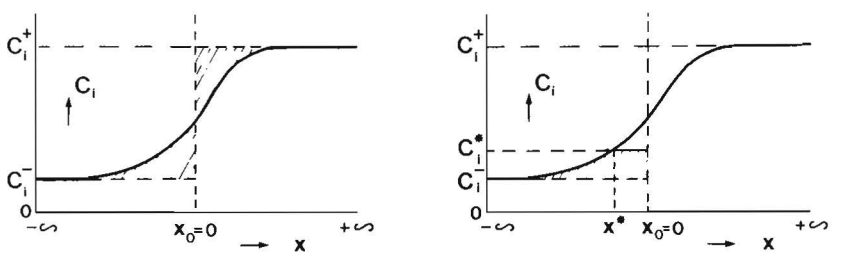

Fig.2.2,a. The Matano interface $x_o=0$ is found by making the shaded areas equal (Eq.(5)).

Fig.2.2,b. The value of the integral in Eq.(4) is equal to the shaded area.

Boltzmann substitution $\lambda(C_i) = x/t^{\frac{1}{2}}$ is only allowed if the initial conditions can be described in terms of $\lambda(C_i)$. The solution implies that each concentration C_i^* is connected with a constant value of $x^*/t^{\frac{1}{2}}$. This means that the coordinate x^* for each concentration C_i^* moves proportionally to $t^{\frac{1}{2}}$, with a different value for the proportionality constant for each coordinate.

Table 2.1

List of standard equations (for derivation see e.g. Trimble[60])

a) $C_i = N_i/V_m$

b) $N_1\overline{V}_1 + N_2\overline{V}_2 = V_m$

c) $C_1\overline{V}_1 + C_2\overline{V}_2 = 1$

d) $N_1 d\overline{V}_1 + N_2 d\overline{V}_2 = 0$

e) $C_1 d\overline{V}_1 + C_2 d\overline{V}_2 = 0$

f) $\overline{V}_1 dC_1 + \overline{V}_2 dC_2 = 0$

g) $dC_1 = (\overline{V}_2/V_n^2)\, dN_1$

Eq.(4) can also be written in a form in which the coordinate x figures only as a differential. This has the advantage that there is no need to determine the Matano interface by Eq.(5).

This expression for D may be found by partial integration of Eq.(4):

$$D(C_i^*) = -\frac{1}{2t}\left(\frac{\partial x}{\partial C_i}\right)^* \left[x^*(C_i^* - C_i^-) - \int_{-\infty}^{x^*}(C_i - C_i^-)\, dx\right] \qquad (6)$$

From fig.2.3 it is seen that

$$x^*(C_i^+ - C_i^-) = \int_{-\infty}^{x^*}(C_i - C_i^-)dx - \int_{x^*}^{+\infty}(C_i^+ - C_i)dx \qquad (7)$$

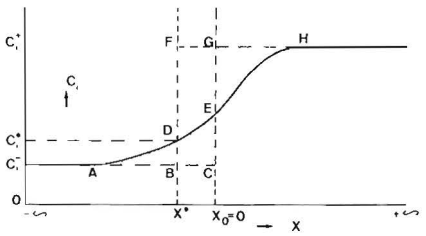

Fig.2.3. Since the shaded areas are equal, area BCGF = area DFH minus area ABD (Eq.(7)).

Substitution of Eq.(7) in Eq(6) leads to

$$D(C_i^*) = +\frac{1}{2}t\left(\frac{\partial x}{\partial C_i}\right)^* \frac{1}{(C_i^+ - C_i^-)}\left[(C_i^+ - C_i^*)\int_{-\infty}^{x^*}(C_i - C_i^-)dx + \right.$$

$$\left. + (C_i^* - C_i^-)\int_{x^*}^{+\infty}(C_i^+ - C_i)dx\right] \qquad (8)$$

This has also been derived in another way by Sauer and Freise[19] and by Den Broeder[20].

Eq.(4) or (8) can be simplified in particular circumstances:

(a) If D is constant and independent of concentration, Fick's second law can be solved with the result

$$C_i = \frac{C_i^+ + C_i^-}{2} + \frac{C_i^+ - C_i^-}{2}\,\mathrm{erf}\left(\frac{x}{2(Dt)^{\frac{1}{2}}}\right) \qquad (9)$$

The error function erf (ψ) is defined by

$$\mathrm{erf}(\psi) = \frac{2}{\pi^{\frac{1}{2}}}\int_0^{\psi}\exp(-\eta^2)d\eta$$

Error functions are available in tabular form.

From Eq.(9) it is seen that the penetration curve is symmetrical with respect to the Matano interface, where the concentration gradient reaches a maximum value.

Eq.(9) can be useful in predicting a penetration curve in particular diffusion problem using an average value of D. Since in many systems the diffusion coefficient is a function of concentration, this is generally a rather rough approximation.

(b) If the molar volume V_m is constant (this means $\bar{V}_1 = \bar{V}_2 = V_m$), the concentration C_i becomes proportional to the mole fraction N_i). Therefore, in Eqs.(4) and (8) C_i may then be replaced by N_i (see table 2.1).

2.2.2. Intrinsic diffusion coefficients; the Kirkendall effect

As mentioned in section 2.1., interdiffusion is often accompanied by a nett displacement of atoms relative to the crystal lattice. This was first demonstrated in the famous experiments of Kirkendall and Smigelskas[61] by marking the contact interface between two interdiffusing materials, viz. copper and brass, with molybdenum wires. After a certain diffusion duration this marker interface (or Kirkendall interface) showed a pronounced displacement relative to a fixed point outside the diffusion zone. This phenomenon is called the Kirkendall effect.

Darken[21] explained these experiments by introducing the conception of unequal diffusion coefficients for both components. Assuming this view, the material transport of e.g. component 1 through a section fixed with respect to $x_o = 0$ originates from two sources. First, there is flux of atoms of component 1 diffusing in the direction which is determined by its concentration gradient.

Secondly, there is a uniform translation of an entire region through this section. If, for instance, component 1 diffuses at a larger rate than component 2, contraction will occur on the side of component 1 and expansion on the side of component 2.

This can be written mathematically as

$$J_i = - D_i\left(\frac{\partial C_i}{\partial x}\right) + C_i v_m \qquad (10)$$

The first term on the right gives the flux of atoms of component i across the marker interface. D_i is called the intrinsic diffusion coefficient of component i, and is a function of only concentration and temperature. The second term represents the uniform translation as measured by the marker movement relative to $x_o = 0$; v_m is the marker velocity.

The molar flux J_i in Eq.(10) can be replaced by a volume flux of component i by multiplying by the partial molal volume $\bar{V}_i$.

$$J_i\bar{V}_i = - D_i\bar{V}_i\left(\frac{\partial C_i}{\partial x}\right) + \bar{V}_i C_i v_m \qquad (11)$$

Since the nett volume flux relative to $x_o = 0$ is zero, Eq.(11) yields

$$- D_1\bar{V}_1\left(\frac{\partial C_1}{\partial x}\right) + v_m C_1\bar{V}_1 - D_2\bar{V}_2\left(\frac{\partial C_2}{\partial x}\right) + v_m C_2\bar{V}_2 = 0$$

Using the standard equations c) and f) from table 2.1 , this reduces to

$$v_m = \bar{V}_1\left(\frac{\partial C_1}{\partial x}\right)(D_1 - D_2) \qquad (12)$$

Substitution of Eq.(12) in Eq.(11) leads to

$$J_1 = - (C_2\bar{V}_2 D_1 + C_1\bar{V}_1 D_2)\left(\frac{\partial C_1}{\partial x}\right)$$

This equation is the same as Fick's first law. In fact,

$$D = C_2\bar{V}_2 D_1 + C_1\bar{V}_1 D_2 \qquad (13)$$

Eq.(13) is frequently used as the most general definition of the interdiffusion coefficient D, since it can be applied even when the partial molal volumes are not constant (see section 2.3.).

The intrinsic diffusion coefficients can be determined from Eqs.(12) and (13) by measuring the marker velocity and the interdiffusion coefficient (by means of Eq.(4) or (8)).

The velocity of markers in the Kirkendall interface can be found by measuring the marker displacement x_m, since

$$v_m = \frac{dx_m}{dt} = \frac{d(k_m t^{\frac{1}{2}})}{dt} = \frac{k_m}{2t^{\frac{1}{2}}} = \frac{x_m}{2t} \qquad (14)$$

Eq.(14) is not valid for markers initially inserted outside the Kirkendall interface, since they are overtaken by diffusion after a certain incubation time, after which the Kirkendall effect may displace them. Besides, in experiments of this kind the concentration at these markers varies continuously, contrary to markers in the Kirkendall interface (this follows from the substitution made in the Boltzmann analysis). Therefore, it is difficult to determine in this way the intrinsic diffusion coefficients outside the Kirkendall interface[22,23].

Combination of Eqs.(4), (12), (13) and (14) leads to an expression for the intrinsic diffusion coefficient in the Kirkendall interface

$$D_i(C_i^*) = \frac{1}{2t}\left(\frac{\partial x}{\partial C_i}\right)^* \left[C_i^* x_m - \int_{C_i^-}^{C_i^*} x \, dC_i\right] \qquad (15)$$

Partial integration yields

$$D_i(C_i^*) = \frac{1}{2t}\left(\frac{\partial x}{\partial C_i}\right)^* \left[x_m C_i^- + \int_{-\infty}^{x_m} (C_i - C_i^-) dx\right] \qquad (16)$$

and using Eq.(7), Eq.(16) may be written as

$$D_i(C_i^*) = \frac{1}{2t}\left(\frac{\partial x}{\partial C_i}\right)^* \frac{1}{C_i^+ - C_i^-}\left[C_i^+ \int_{-\infty}^{x_m} (C_i - C_i^-) dx - C_i^- \int_{x_m}^{+\infty} (C_i^+ - C_i) dx\right] \qquad (17)$$

As an advantage, the marker displacement x_m need not be measured when using Eq.(17).

Possible simplifications:

(a) At least one of the starting materials is a pure component, e.g. $C_i^- = 0$. Eqs.(16) an (17) then reduce to

$$D_i(C_i^*) = \frac{1}{2t}\left(\frac{\partial x}{\partial C_i}\right)^* \int_{-\infty}^{x_m} C_i \, dx \qquad (18)$$

This very simple expression for a frequently occurring problem in matters of diffusion has to the author's knowledge not been published up to now.

(b) If $\bar{V}_1 = \bar{V}_2 = V_m$ the concentration C_i can be replaced by N_i/V_m.

This leads to simplification of especially Eqs.(12) and (13)

$$v_m = (D_1 - D_2)\left(\frac{\partial N_1}{\partial x}\right) \qquad (12')$$

$$D = N_2 D_1 + N_1 D_2 \qquad (13')$$

2.3. THE INFLUENCE OF CONCENTRATION-DEPENDENT PARTIAL MOLAL VOLUMES

In 1962, Sauer and Freise[19] derived an equation which permits of calculating the interdiffusion coefficient in the case of a binary system in which the partial molal volumes are concentration-dependent. Recently, Wagner[24] and Den Broeder[20] derived the same equation in a different way.

On the other hand, Balluffi[25] published an equation on the same problem shortly before Sauer and Freise. There is some confusion about the validity of this equation, especially concerning the frame of reference used by Balluffi (see Wagner[22], Crank[26], Guy et al[27,28], van Loo[29]. Sauer and Freise mention the difficulty of measuring the several data to be used in Balluffi's equation. In the analysis below the following points will be demonstrated[30]:

(a) The equation determining the interdiffusion coefficient as given by Balluffi can be converted into that of Sauer and Freise. Consequently, they are equivalent.
(b) In principle, in both formulae the same data are needed and it depends on the experimental conditions which one is preferable.
(c) Balluffi's equations determining the intrinsic diffusion coefficients in the Kirkendall interface can be expressed in the same

variables as were used by Sauer and Freise. In the resulting equations the marker displacement does not occur, which must be considered as a distinct advantage.

In this analysis it is assumed that the interdiffusion coefficient is only a function of concentration and temperature. Therefore, C_i is a single-valued function of $x/t^{\frac{1}{2}}$. This also means that the diffusion couple expands or contracts parabolically with time.

2.3.1. Demonstration of the equivalence of the equations derived by Balluffi, and by Sauer and Freise

The frame of reference chosen by Balluffi is the same as the one defined in this thesis (page 16). The flux of atoms of component i crossing a section fixed in this frame of reference arises from three different sources:

(a) The flux of atoms i arising form the concentration gradient and determined by $- D_i \, \partial C_i/\partial t$.

(b) The flux arising from the Kirkendall effect (see page 20).

(c) The flux because of the total expansion or contraction of the diffusion couple arising from the concentration-dependent partial molal volumes (see fig.2.1.a,b).

The presence of flux (c) invalidates Fick's laws in their simple form. According to Prager[31], Fick's second law can then be written as

$$\frac{\partial C_i}{\partial t} = \frac{\partial}{\partial x}\left[D \frac{\partial C_i}{\partial x} - C_i^* \int_{-\infty}^{x^*} \frac{D}{\bar{V}_2 C_1} \left(\frac{\partial \bar{V}_2}{\partial C_1}\right)\left(\frac{\partial C_1}{\partial x}\right) dx \right] \qquad (19)$$

The velocity of flow v is given by

$$v = \bar{V}_1 (D_1 - D_2) \frac{\partial C_1}{\partial x} + \int_{-\infty}^{x^*} \frac{D}{\bar{V}_2 C_1} \left(\frac{\partial \bar{V}_2}{\partial C_1}\right)\left(\frac{\partial C_1}{\partial x}\right)^2 dx \qquad (20)$$

In both Eq.(19) and Eq.(20) the integral term arises from variations of the partial molal volumes with composition, as can be seen by comparison with Eqs.(2) and (12), respectively.

Balluffi solves Eqs.(19) and (20) by introducing a new function:

$$\theta_i = D_i - vC_i\left(\frac{\partial x}{\partial C_i}\right) \tag{21}$$

The value of θ_i at $C_i = C_i^*$ may be determined by the usual Boltzmann-Matano method

$$\theta_i(C_i^*) = -\frac{1}{2t}\left(\frac{\partial x}{\partial C_i}\right)^* \int_{\bar{C}_i}^{C_i^*} x\, dC_i \tag{22}$$

Using Eqs.(13), (21) and (22) one obtains the expression for the interdiffusion coefficient

$$D(C_1^*) = -\frac{1}{2t}\left(\frac{\partial x}{\partial C_1}\right)^* \left[\left(1 - C_1^*(\bar{V}_1 - \bar{V}_2)\right)\int_{\bar{C}_1}^{C_1^*} x dC_1 + \bar{V}_2 C_1^* \int_{\bar{C}_1}^{C_1^*} \frac{(\bar{V}_1 - \bar{V}_2)}{\bar{V}_1} x\, dC_1\right] \tag{23}$$

and the expressions for the intrinsic diffusion coefficients

$$D_i(C_i^*) = +\frac{1}{2t}\left(\frac{\partial x}{\partial C_i}\right)^* \left[2tv_m C_i^* - \int_{\bar{C}_i}^{C_i^*} x dC_i\right] \tag{24}$$

For markers inserted in the Kirkendall interface this equation is equal to Eq.(15).

As mentioned before, Balluffi's choice of the frame of reference is questioned by several authors, unjustly though, as will be seen in section 2.3.2. Anyhow, Sauer and Freise's equations are valid in any frame of reference, since the x-coordinate occurs only as a differential.

Sauer and Freise's expression for the interdiffusion coefficient is

$$D(Y^*) = \frac{V_m}{2t}\left(\frac{\partial x}{\partial Y}\right)^* \left[(1 - Y^*)\int_{-\infty}^{x^*} \frac{Y}{V_m} dx + Y^* \int_{x^*}^{+\infty} \frac{(1-Y)}{V_m} dx\right] \tag{25}$$

where $Y = (N_1 - N_1^-)/(N_1^+ - N_1^-)$

The position of the plane $x_o = 0$ as defined in fig.2.1 is given by

$$x_o = \bar{V}_m \left[\int_{x_o}^{+\infty} \frac{(1-Y)}{V_m} \, dx - \int_{-\infty}^{x_o} \left(\frac{1}{\bar{V}_m} - \frac{1}{V_m} (1-Y) \right) dx \right] \qquad (26)$$

and can be determined graphically as shown in fig.2.4.

Sauer and Freise do not give an expression for the intrinsic diffusion coefficient.

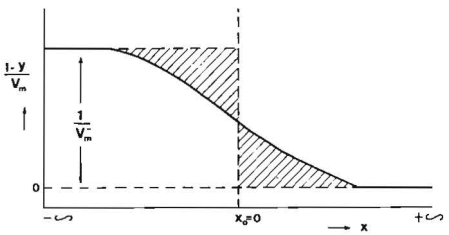

Fig.2.4. According to Eq.(26) the interface $x_o=0$ is situated so that the shaded areas are equal.

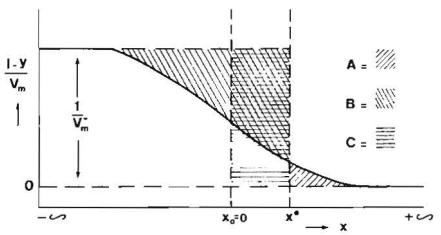

Fig.2.5. Illustration of the validity of Eq.(29). Area A = area B minus area C.

To demonstrate the equivalence of Eqs.(23) and (25) the first equation will be written using Eqs.(13), (21) and (22) as

$$D(C_1^*) = - \frac{V_m^2}{2t} \left(\frac{\partial x}{\partial N_1} \right)^* \left[C_2^* \int_{\bar{C}_1}^{C_1^*} x \, dC_1 - C_1^* \int_{\bar{C}_2}^{C_2^*} x \, dC_2 \right] \qquad (27)$$

Partial integration of this equation yields

$$D(C_1^*) = - \frac{V_m^2}{2t} \left(\frac{\partial x}{\partial N_1} \right)^* \left[(C_1^* \bar{C}_2 - C_2^* \bar{C}_1) \, x^* - C_2^* \int_{-\infty}^{x^*} (C_1 - \bar{C}_1) \, dx + C_1^* \int_{-\infty}^{x^*} (C_2 - \bar{C}_2) \, dx \right] \qquad (28)$$

From fig.2.5 it can be seen that

$$x^* = -V_m^- \left[\int_{x^*}^{+\infty} \frac{(1-Y)}{V_m}\, dx - \int_{-\infty}^{x^*} \left(\frac{1}{V_m^-} - \frac{1}{V_m}(1-Y) \right) dx \right] \qquad (29)$$

Substituting Eq.(29) in (28) and rearranging the latter leads to Eq.(25), proving the equivalence of the Eqs.(23) and (25).

Concerning the intrinsic diffusion coefficients in the Kirkendall interface, partial integrating of Eq.(24) and rearranging leads to:

$$D_i(C_i^*) = \frac{1}{2t} \left(\frac{\partial x}{\partial C_i} \right)^* \left[N_i^+ \int_{-\infty}^{x_m} \frac{Y}{V_m}\, dx - N_i^- \int_{x_m}^{+\infty} \frac{(1-Y)}{V_m}\, dx \right] \qquad (30)$$

In this expression the marker displacement does not occur. If N_i^- is zero (one of the starting components is a pure metal), the expression simplifies to Eq.(18).

The conclusion is that for the interdiffusion coefficient, as well as for the intrinsic diffusion coefficients, Balluffi's equations can be expressed in the same variables as used by Sauer and Freise.

2.3.2. Influence of the end of the diffusion couple to which the frame of reference is fixed

It will now be proved that the value of the diffusion coefficient, determined by Eq.(23), does not depend on the end of the diffusion couple to which the frame of reference is fixed. In fact, this has already been proved by the equivalence of Eqs.(23) and (25). It can also be shown directly by demonstrating the independence of Eq.(24) on the choice mentioned above since then (because of Eq.(13)) the interdiffusion coefficient remains also unchanged.

If x_o is fixed with respect to $x = -\infty$ as was done in the previous pages, Eq.(24) applies:

$$D_i(C_i^*) = +\frac{1}{2t} \left(\frac{\partial x}{\partial C_i} \right)^* \left[2t v_m C_i^* - \int_{C_i^-}^{C_i^*} x\, dC_i \right] \qquad (24)$$

If the frame of reference is fixed with respect to $x = +\infty$ (indicated by an accent) one obtains for the same concentration

$$D_i'(C_i^*) = +\frac{1}{2t}\left(\frac{\partial x}{\partial C_i}\right)^* \left[2tv_m' C_i^* - \int_{C_i^*}^{C_i^+} x' \, dC_i\right] \qquad (24')$$

Now D_i and D_i' are equal if

$$2tC_i^*(v_m - v_m') = \int_{C_i^-}^{C_i^*} x\,dC_i + \int_{C_i^*}^{C_i^+} x'\,dC_i \qquad (31)$$

Since the diffusion couple is assumed to expand or contract parabolically with time, it is easy to see that

$$v_m - v_m' = \Delta x/2t \qquad (32)$$

where $\Delta x = x_o - x_o'$ = total expansion or contraction of the couple (see fig.2.6).

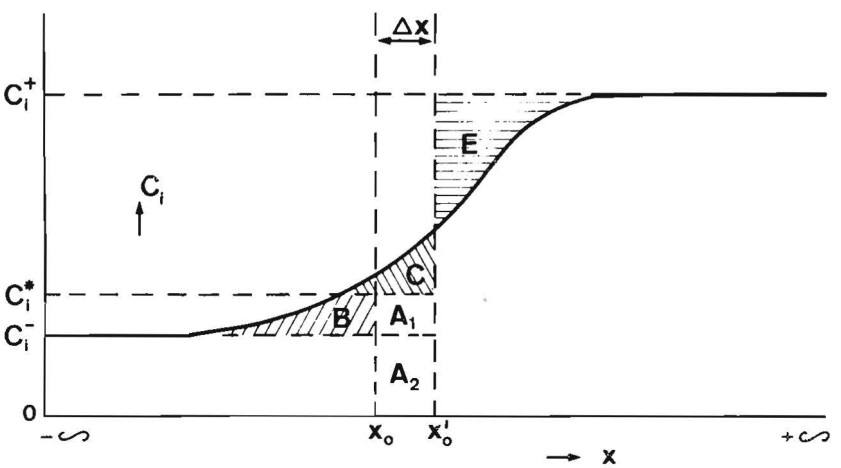

Fig.2.6. Penetration curve of component i. The total expansion of the couple equals Δx. Area $A_1+A_2+B+C=$ area E.

After substitution of Eq.(32) in (31), it is seen that D_i and D_i' are equal if

$$C_i^* \Delta x = \int_{C_i^-}^{C_i^*} x dC_i + \int_{C_i^*}^{C_i^+} x' dC_i \qquad (33)$$

or, see fig.2.6., if

$$\text{Area } A_1 + A_2 + B + C = \text{Area } E \qquad (33')$$

since $A_1 + A_2$ represents $C_i^* \Delta x$

$$B \text{ represents } -\int_{C_i^-}^{C_i^*} x dC_i$$

$$E\text{-}C \text{ represents } \int_{C_i^*}^{C_i^+} x' dC_i$$

From fig.2.6 it is clear that:

Area E denotes the number of moles of component i which crossed the plane x_o' from right to left

Area A_1 + B + C denotes the number of moles of component i which appeared on the left-hand side of x_o' as a result of increase in concentration.

Area A_2 represents the number of moles of component i which appeared on the left-hand side of x_o' as a result of the total expansion of the couple which is directed toward the left, since x_o' is fixed with respect to $x = +\infty$.

The total number of moles of component i which appeared on the left-hand side of x_o' equals $A_1 + A_2 + B + C$.

This must be equal to the number, E, which disappeared from the right-hand side. This shows the validity of Eq.(33), and in consequence the irrelevance of the choice of the end of the couple to which x_o is fixed.

From fig.2.6 one may also see that if $C_i^- = 0$, the plane x_o' coincides with the Matano interface for component i, as defined by Eq.(5), since then A_2 equals zero.

If $C_i^+ = 0$, the Matano interface for component i coincides with x_o. It will be clear that a Matano interface (in the sense of the interface which divides a penetration curve into two equal parts) is a meaningless conception if the partial molal volumes are not constant, since the interface is not the same for both components. For further discussion see also v.d. Broek[32,33].

2.3.3. Applicability of the several equations for the interdiffusion coefficient

In recording the penetration curve by electron microprobe analysis, one actually measures the intensity ratio $K_i = I_i/I_i^o$ where I_i^o represents the corrected intensity for the pure component i, and I_i is the corrected intensity for component i in the diffusion couple.

K_i values can be converted into corresponding values for the concentration by means of standards, prepared by melting a series of alloys of different composition.

When using Balluffi's as well as Sauer and Freise's equations, the molar volume must be known as a function of the concentration. The calibration line can then be given as a plot of K_i vs. N_1, N_2, C_1 or C_2. The penetration curve can therefore be given for both components in mole fraction as well as in moles per unit volume.

From the modified Balluffi equation (27) one may see that all the data may be taken from the measured penetration curve.

The concentration unit Y occurring in Sauer and Freise's Eq.(25) depends on the initial mole fractions N_1^- and N_1^+. This is a disadvantage as it necessitates calculating the penetration curve for each experiment (except when $N_1^- = 0$ and $N_1^+ = 1$, since then $Y = N_1$). On the other hand, in applying Balluffi's equations one has to know the exact position of the plane $x_o = 0$. If Eq.(25) is used the position of this plane is immaterial.

Three cases may be distinguished:

(a) The starting materials are pure components. Then, both Eq.(25) and Eq.(27) are easy to apply. The Matano interface for component i can be

brought to coincidence with the plane $x_o = 0$ if one chooses $C_i^+ = 0$. (see fig.2.6.). Eq.(25) is slightly to be preferred since it does not demand a determination of the Matano interface.

(b) One of the starting materials is a pure component. The Matano interface again coincides with $x_o = 0$ if one chooses $C_i^+ = 0$. Therefore, no problem is offered when evaluating D from Eq.(27). Since Sauer and Freise's Eq. (25) requires more calculation, it is preferable to use Eq. (27).

(c) If the starting materials are both alloys, the plane $x_o = 0$ can only be found by insertion of markers outside the diffusion zone as references or by calculation based on Eq.(26). In both cases Sauer and Freise's Eq. (25) is easier to use than Eq. (27).

This section will be concluded by making reference to the most important equations derived in the preceding pages (table 2.2).

TABLE 2.2

Reference to the most important equations derived in sections 2.2. and 2.3. The equations for the intrinsic diffusion coefficients are valid for the Kirkendall interface in the couple.

	Starting materials are both alloys	Simplifications if $C_i^- = 0$
Total volume is not constant	D: Eqs.(25) and (27) D_i: Eq. (30)	Eq.(27) is to be preferred Eq. (30) reduces to Eq. (18)
Total volume is constant; partial molal volumes are unequal	D: Eqs. (4) and (8) D_i: Eq. (17)	Eq. (17) reduces to Eq. (18)
Total volume is constant; partial molal volumes are equal	D: In Eqs.(4) and (8) C_i is replaced by N_i D_i: In Eq. (17), C_i is replaced by N_i	In Eq.(18), C_i is replaced by N_i

2.4. DIFFUSION IN MULTIPHASE BINARY SYSTEMS

2.4.1. Determination of the diffusion coefficients

Diffusion between two components A and B will cause a discontinuous penetration curve if at the diffusion temperature a two-phase region is present in the phase diagram (fig.2.7).

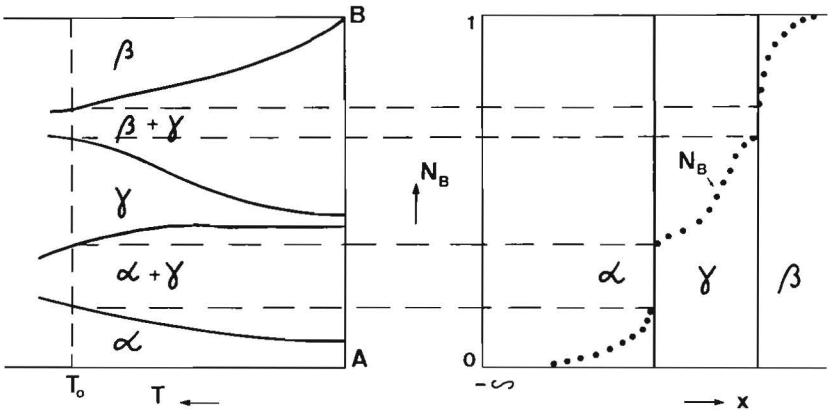

Fig.2.7,a. A fictitious phase diagram of the metals A and B, rotated over 90 deg.

Fig.2.7,b. The diffusion couple A-B with layers of α, γ and β and the penetration curve of component B after t seconds at temperature T_o.

The absence of two-phase regions in a binary diffusion couple can be explained by means of the phase rule, since then no degree of freedom would be left for the concentration to adapt itself. The most simple way to see why two-phase regions are forbidden is the form of the penetration curve that would be obtained in such a region. This form would be alternating rising and falling instead of continuously falling, at least on a microscopic scale. Such an alternating penetration curve is impossible in view of the diffusion laws.

The determination of the diffusion coefficient by means of the equations of table 2.2 is still justifiable, since the only condition is an integrable penetration curve (see Jost[34]).

Approximate solutions to these equations have been derived on the basis of a linear concentration gradient in a diffusion layer[35] or of the assumption of a constant diffusion coefficient[36]. These approximations are often valuable since they admit of calculating in a simple way a reasonable result for the diffusion coefficients.

Recently, Wagner[24] made an interesting contribution to the problem concerning phases with narrow homogeneity ranges. If these compounds exist in a diffusion couple, the concentration gradient in this phase approaches zero. The equations referred to in table 2.2 then give rise to infinite values for the diffusion coefficient. Wagner defines a new variable, which we will call an integrated diffusion coefficient:

$$D_{int.} = \int_{N_i(\gamma')}^{N_i(\gamma'')} D dN_i \qquad (34)$$

where $N_i(\gamma')$ and $N_i(\gamma'')$ represent the - unknown-limiting mole fractions of the compound γ.
If $N_i(\gamma') \cong N_i(\gamma) \cong N_i(\gamma'')$, Wagner derives from Eq.(25):

$$D_{int.} = \frac{(N_i(\gamma) - N_i^-)(N_i^+ - N_i(\gamma))}{N_i^+ - N_i^-}\left(\frac{d_\gamma^2}{2t}\right) +$$

$$+ \frac{d_\gamma}{2t}\left[\frac{N_i^+ - N_i(\gamma)}{N_i^+ - N_i^-}\int_{-\infty}^{x(\gamma-1,\gamma)} \frac{V_m(\gamma)}{V_m}(N_i - N_i^-)dx + \frac{N_i(\gamma) - N_i^-}{N_i^+ - N_i^-}\int_{x(\gamma,\gamma+1)}^{+\infty} \frac{V_m(\gamma)}{V_m}(N_i^+ - N_i)dx\right] \qquad (35)$$

where d_γ = width of phase γ
$x(\gamma-1,\gamma)$ = coordinate of the left-hand boundary of phase γ
$x(\gamma,\gamma+1)$ = coordinate of the right-hand boundary of phase γ

For several cases Eq.(35) can be simplified, particularly when there is no concentration gradient, either inside or outside the γ - layer in question. Then, the term in square brackets becomes zero.

An important quantity occurring implicitely in Eq.(35) is the penetration constant k, defined for a layer γ as

$$k_\gamma = d_\gamma^2/t \qquad (36)$$

For a particular diffusion couple and temperature the value of k_γ is a constant, since each concentration moves parabolically with time (see page 18), and so will the concentrations $N_i(\gamma-1,\gamma)$ and $N_i(\gamma,\gamma+1)$. In other words, the width of a particular layer increases parabolically with time.

From Eq.(35) (and also from equations derived by Kidson[37]) it can be shown that k_γ depends on composition of starting materials and on all the interdiffusion coefficients in the entire diffusion region. Contrary to the integrated diffusion coefficient, k_γ is only a valuable quantity if the starting materials are known and it is obviously no material constant. However, in many practical problems the value of k_γ can be of great use.

2.4.2. Determination of the phase diagram by way of multiphase diffusion

As will be evident from the preceding section, multiphase diffusion is an important tool in investigating phase diagrams. However, there are several restrictions:

(a) In deriving the previous equations it was assumed that at the interface two adjacent phases are in thermodynamic equilibrium.

In practice this requirement is often fulfilled, if the diffusion duration is sufficiently long[1,38]. Especially in intermetallic compounds, however, the measured concentration at the interfaces can deviate from that given in the phase diagram. The reasons for this are not fully understood at the moment. Evidence is obtained for the influence of internal stresses on the phenomenon[1,39]. These stresses can easily be built up since the differences in molar volume between two adjacent phases are sometimes great. Apart from this there are theoretical grounds for expecting such deviations. They are based on the conception that we actually have to do with a ternary system consisting of two metals and vacancies[40]. If the vacancies are not equilibrium throughout the diffusion couple, differences occur between the interface concentrations in a diffusion couple and in an equilibriated, two-phase alloy.

It is also mentioned in the literature[41] that a certain supersaturation is necessary to provide the driving force for the lattice transformation. However, the deviations are small and probably within experimental error.

(b) In some cases not all the compounds predicted by the phase diagram occur in the diffusion couple.

One reason might originate from the growth kinetics of the several layers. From an analysis of Kidson[37] it appears that the penetration constant of a particular layer may reach zero value, dependent on the several diffusion coefficients. It is assumed in this case that the phase is present in a very thin and therefore indetectable layer, since complete absence seems to be in contradiction with the thermodynamic requirement that the chemical potential should be continuous across a two-phase interface (see e.g. Shewmon[3] p.132). If for this reason a layer does not show up, it can often be formed in a diffusion couple at a more favourable temperature or when using other starting materials. In the former case the layer will vanish again when exposed to the origial conditions (see section 6.2).

(c) Another reason why some phases do not show up in a diffusion couple can be a very pronounced Kirkendall effect. Especially if several phases are involved, great differences may occur in the diffusion rate of both components. It is then possible that this results in a supersaturation of vacancies, especially near a phase boundary. This finds expression in the formation of a large number of pores, easily becoming a gap. In that case the supply of the diffusing component stops and the phases already formed can be consumed and vanish. Of course, cracks arising from other sources (e.g. volume effects, different coefficients of thermal expansion) can bring about the same effect.
The effect can be distinguished from that mentioned in (b) by applying an external pressure. This will generally prevent gap formation and as a result, layer growth becomes normal as shown by Heumann[42] in the Cu-Sb system.

(d) Baird[43] argues that in some cases a phase is absent in a diffusion couple because of difficulties in the nucleation of the new phase. We agree with him that this mostly resolves itself into the influence of impurities or oxide scales which prevent nucleation.

(e) It is possible that a non-equilibrium phase nucleates in a diffusion couple, as is found in the system Ag-Zn[44]. According to Baird[43], this may be caused by a surface energy contribution which might favour an actually unstable phase.

2.5. ANALYSIS OF THE APPROXIMATIONS USED IN THE PRECEDING SECTIONS

From Eq.(10), the intrinsic diffusion coefficient $D_i(C_i^*)$ can be defined by

$$J_i^m = -D_i \left(\frac{\partial C_i}{\partial x} \right) \tag{37}$$

where J_i^m represents the flux of component i across the marker interface at the concentration C_i. Actually, this equation is based on experimental facts and in the Matano-Boltzmann analysis it is assumed that D_i does not depend on time or concentration gradient. It can easily be verified if this condition is met with. Experiments of different duration or using different starting materials must yield the same value for D_i at a particular concentration independent of its gradient. If this is indeed true, the preceding analysis is correct. However, if this is not the case, the entire analysis is in fact worthless.

One could try to find a mathematical formulation for the diffusion process, which is theoretically more soundly based than Eq.(37). It must then be remembered that the necessary and sufficient condition for equilibrium in a binary system is that throughout the whole system temperature, pressure and each of the chemical potentials shall be uniform (omitting external forces).

If the system is displaced slightly from equilibrium it is assumed that the rate of return to equilibrium is proportional to the deviation from equilibrium. For an isothermic and isobaric diffusion process the most general equations for the fluxes with respect to a marker interface are given by [1,14,45]

$$\left.\begin{aligned}
J_1^m &= -L_{11} \frac{\partial \mu_1}{\partial x} - L_{12} \frac{\partial \mu_2}{\partial x} - L_{1v} \frac{\partial \mu_v}{\partial x} \\
J_2^m &= -L_{21} \frac{\partial \mu_1}{\partial x} - L_{22} \frac{\partial \mu_2}{\partial x} - L_{2v} \frac{\partial \mu_v}{\partial x} \\
J_v^m &= -L_{v1} \frac{\partial \mu_1}{\partial x} - L_{v2} \frac{\partial \mu_2}{\partial x} - L_{vv} \frac{\partial \mu_v}{\partial x} \\
J_1^m + J_2^m + J_v^m &= 0
\end{aligned}\right\} \tag{38}$$

where the subscript v denotes vacancies; L_{ij} are the phenomenological coefficients, independent of $\partial\mu_i/\partial x$ and related by the Onsager equation $L_{ij} = L_{ji}$. From the definition of the chemical potential it follows that

$$\left.\begin{aligned} \frac{\partial\mu_1}{\partial x} &= RT\,\frac{\partial \ln a_1}{\partial x} = \frac{RT}{N_1}\left(\frac{\partial N_1}{\partial x}\right)\frac{\partial \ln a_1}{\partial \ln N_1} \\ \frac{\partial\mu_2}{\partial x} &= RT\,\frac{\partial \ln a_2}{\partial x} = \frac{RT}{N_2}\left(\frac{\partial N_2}{\partial x}\right)\frac{\partial \ln a_2}{\partial \ln N_2} \end{aligned}\right\} \qquad (39)$$

$$\text{where } \frac{\partial \ln a_1}{\partial \ln N_1} = \frac{\partial \ln a_2}{\partial \ln N_2} = \text{thermodynamic factor}$$

In Eq.(38) it is assumed that:

(a) diffusion proceeds isothermically and isobarically provided other external forces are absent;
(b) internal stresses and viscous effect are neglected;
(c) time-dependent effects like recrystallisation are neglected;
(d) the relations hold irrespective of the magnitude of $\partial\mu_i/\partial x$.

It is further assumed that the vacancies are in thermodynamic equilibrium in the entire diffusion range. In fact, it is shown by Balluffi[46] that a deviation of 1% from the equilibrium value is enough to maintain the flux of vacancies. This assumption means $\partial\mu_v/\partial x \cong 0$. Then, combination of Eqs.(38) and (39) leads to

$$\left.\begin{aligned} J_1^m &= \left[-L_{11}\frac{RT}{N_1} + L_{12}\frac{RT}{N_2}\right]\frac{\partial \ln a_1}{\partial \ln N_1}\left(\frac{\partial N_1}{\partial x}\right) \\ J_2^m &= \left[+L_{21}\frac{RT}{N_1} - L_{22}\frac{RT}{N_2}\right]\frac{\partial \ln a_1}{\partial \ln N_1}\left(\frac{\partial N_2}{\partial x}\right) \end{aligned}\right\} \qquad (40)$$

From this equation and from Eq.(37) it is clear that

$$D_1 = \left[\frac{L_{11}}{N_1} - \frac{L_{12}}{N_2}\right] RT\,\frac{\partial \ln a_1}{\partial \ln N_1}\left(\frac{V_m^2}{\bar{V}_2}\right), \text{ or}$$

$$\left.\begin{aligned} D_1 &= +\left[\frac{L_{11}}{C_1} - \frac{L_{12}}{C_2}\right] RT \frac{\partial \ln a_1}{\partial \ln N_1}\left(\frac{V_m}{\bar{V}_2}\right) \\ D_2 &= -\left[\frac{L_{21}}{C_1} - \frac{L_{22}}{C_2}\right] RT \frac{\partial \ln a_1}{\partial \ln N_1}\left(\frac{V_m}{\bar{V}_1}\right) \end{aligned}\right\} \quad (41)$$

From Eq.(41) it is seen that the intrinsic diffusion coefficients indeed depend only on temperature and concentration, and are independent of concentration gradient or time. In fact, it is found that the simple equation (37) is just as correct for describing the diffusion process as the complicated Eq.(38) or (40). As a distinct advantage, however, the Eqs.(38-41) can be used in trying to relate the intrinsic diffusion coefficient to other physical quantities in the homogeneous alloy, more particularly to the self-diffusion coefficient D_i^s. The latter governs the diffusion in the absence of a chemical concentration gradient, and can be determined e.g. by means of tracers of component i.
Since the derivation of these relationships is not relevant in this thesis, only the results as taken from Manning[14] are given here.

Supposing D_1^s is larger than D_2^s, and making some simplifying assumptions, it is found that:

$$\left.\begin{aligned} D_1 &= D_1^s \left[1 + \frac{2}{M_o}\left(1 - \frac{D_2^s}{N_1 D_1^s + N_2 D_2^s}\right)\right] \frac{\partial \ln a_1}{\partial \ln N_1} \\ D_2 &= D_2^s \left[1 + \frac{2}{M_o}\left(1 - \frac{D_1^s}{N_1 D_1^s + N_2 D_2^s}\right)\right] \frac{\partial \ln a_1}{\partial \ln N_1} \end{aligned}\right\} \quad (42)$$

where M_o is a constant, dependent on the crystal structure (e.g. 7.15 in f.c.c. crystals, 5.33 in b.c.c. crystals).

The terms which are proportional to $2/M_o$ arise from the vacancy flow effect. This gives all constituents the tendency to flow in a direction opposite to the flow of vacancies. Hence, the vacancy flow effect tends to increase the intrinsic diffusion coefficient of the faster component and decreases that of the other one.

Experimental verification of Eq.(42) was recently carried out by Levasseur et al.[47] for the systems Fe-Ni and Fe-Co. They conclude that the equation is not obeyed: the devations are larger than the experimental errors. However, Badia and Vignes[48] argue that Levasseur's experiments were not properly performed, so that the results are not reliable. They carried out experiments and these do prove the validity of Eq.(42).

2.6. INFLUENCE OF DISTURBING EFFECTS ON THE VOLUME DIFFUSION PROCESS

In the preceding sections it is assumed that the diffusion coefficient must be a single-valued function of the concentration. This is always the case, if an undisturbed single diffusion mechanism is operating, no matter whether this is volume diffusion or e.g. grain-boundary diffusion. According to Baird[43], in a polycrystalline metal grain-boundary diffusion is unimportant in regard to volume diffusion, if

$$\frac{D_g}{D_v} < \frac{\text{grain diameter}}{\text{grain boundary width}}$$

where D_g represents the grain boundary diffusion coefficient and D_v the volume diffusion coefficient. In most metals this requirement is fulfilled at temperatures higher than half the absolute melting point. It will be clear that in this case the normal diffusion laws can be applied. When the requirement mentioned above is not fulfilled, then a different situation arises, in which both volume as well as grain-boundary diffusion will be operating.
Lidiard and Tharmalingam[49] state that the total diffusion process will in this case still appear to obey Fick's law, if

$$D_c t \gg a_g^2 \qquad (43)$$

where D_c = macroscopic or apparent diffusion coefficient for the solid as a whole,
a_g = mean radius of a grain or half the mean distance between dislocation pipes,
t = diffusion duration.

Hart[50] formulates a more restrictive condition

$$D_v t \gg a_g^2 \tag{44a}$$

Harrison[51] presents in his review article on this subject a more quantitative expression

$$D_v t \geqslant 10^5 a_g^2 \tag{44b}$$

In this type of diffusion process the grain boundaries and dislocation pipes accelerate the overall diffusion process[52,53]. There will be no marked concentration difference, however, between bulk and grain boundaries. Condition (44b) is often fulfilled, if long diffusion times or small grains are involved, or if diffusion along the grain boundaries is not much faster than in the bulk.

Since Fick's laws hold for this type of diffusion, in each experiment one must take into account the possibility of not measuring a true volume diffusion coefficient. Especially in experiments where new compounds are formed during the diffusion process the grains of this new phase will be small at the beginning. Large measured values for an apparent diffusion coefficient together with small energies of activation must, therefore, be seriously suspected (see section 2.7.). On the other hand, for a number of reasons deviations of Fick's laws may present themselves:

(a) If short-circuit diffusion occurs, and condition (44) is not fulfilled, then a very complex situation arises. Several models have been proposed[49,51,54,55] but no satisfactory solution has been found. According to Baird[43] and others[49] the displacement of a plane of constant concentration is in this case roughly proportional to $t^{1/n}$, where n is a number between 2 and 4; the layer growth will then show a similar time dependence. However, this type of diffusion mechanism can be easily recognised, since then there exists a marked concentration difference between grain boundary and bulk. This means that the phase boundary of a layer, formed in this way, will show a typical structure (fig.2.8).

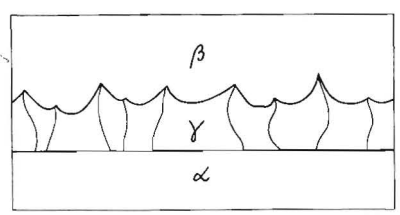

Fig.2.8. Layer γ grows by diffusion of material from α to β. The $\gamma - \beta$ boundary shows the typical form obtained if grain boundary diffusion plays a significant part (condition $D_c t \cong a_g^2$).

(b) There may be a poor contact between the starting materials due to an oxide layer or a crack parallel to the interface. Baird[43] states that after a certain incubation period layer-growth rate is intermediate between linear and parabolic. After longer periods of heating, the growth rate is parabolic. Baird's conclusion does not agree with Lustman and Mehl's statement[44] that transfer through an oxide film produces a linear growth rate.

(c) If during the diffusion process a gap is formed e.g. by the combination of pores caused by the Kirkendall effect, layer growth may be drastically diminished.

(d) At elevated temperatures reaction rates may become sufficiently high to affect the temperature of the diffusion couple. Deviations in layer growth will then result. The effect seems to be unimportant in most practical cases.

(e) The formation of the lattice of a compound may be the rate determining step, as is probably the case if solid titanium reacts with liquid aluminium[56]. Then a linear layer growth rate will result since the reaction rate is independent of time. During the process the diffusion rate diminishes continuously because of the thickening of the layer. After some time, diffusion becomes the rate-controlling step, and the growth rate will become parabolic.

(f) Small amounts of impurities may affect the diffusion behaviour of a particular couple considerably.
In the titanium-nickel system, for instance, there is a marked influence of impurties on the diffusion process[57]. Several reasons for this can be given. First, one has is fact to do with a ternary system; the diffusion path in the latter may deviate considerably from that in a binary system. As a result, the boundaries of the layers need no longer be straight interfaces. Besides, inclusions of various compounds may arise in the layer[58].
Secondly, the impurities may affect the diffusion process when interacting with vacancies, or by segregation to dislocations or grain boundaries.

2.7. TEMPERATURE DEPENDENCE OF THE DIFFUSION PROCESS

2.7.1. Volume diffusion

In the case of self-diffusion in pure cubic metals, it is for atomic reasons reasonable, as it has also been experimentally verified, that Arrhenius' rule applies:

$$D_i^s = D_{i,o}^s e^{-Q/RT} \tag{45}$$

Here $D_{i,o}^s$ is called the frequency factor, independent of temperature. Theoretically[1], for a vacancy mechanism, its value is expected to vary between 10^{-2} and 10 cm^2/sec. Q is the activation energy for diffusion, and is a constant if the lattice does not transform.

For diffusion by a vacancy mechanism, the activation energy can be written as

$$Q = \Delta H_f + \Delta H_m \tag{46}$$

where ΔH_f is the enthalpy of formation and ΔH_m the enthalpy of motion of the vacancies. Q can be determined from the slope of a log D_i^s vs. 1/T plot.

Proceeding successively from this simplest of diffusion processes to more intricate ones, the temperature dependence becomes more and more complex.

(a) Self-diffusion in a homogeneous alloy

In this case temperature-dependent correlation effects arise in the process[14]. Since these effects vary approximately exponentially with 1/T, Eq.(45) often applies all the same.

(b) Intrinsic diffusion coefficients

As shown by Eq.(42), the temperature dependence of e.g. D_1 arises from both D_1^s and D_2^s and from the thermodynamic factor $\partial \ln a_1 / \partial \ln N_1$. In principle, all these factors depend in a different way on temperature, so one would not expect Arrhenius' rule to apply.

(c) Interdiffusion coefficient and marker displacement

These are linear functions of D_1 and D_2 (see Eqs.(12) and(13)), so the same remarks as made in (b) are valid in a still larger measure.

(d) Penetration constant

This depends on all the diffusion coefficients throughout the whole diffusion couple. Besides, at different temperature, different equilibrium concentrations at the phase boundaries may arise.

It is remarkable that in many experiments Arrhenius' rule can still be applied in cases (a)-(d)[16]. It is obvious that the value of Q, found by plotting the logarithm of the quantity in question vs. 1/T, must be regarded as an empirical one, not related to well-defined physical quantities in a simple way.

2.7.2. Short-circuit diffusion

In the case of grain boundary or dislocation pipe diffusion a low value of both the activation energy and the frequency factor occur, the latter despite the high value found for the diffusion coefficient[1] (see fig.2.9). A plot of ln D vs. 1/T showing a bend as demonstrated in this figure, is an indication that short-circuit effects may be present. For self-diffusion in polycrystalline silver the bend appears at approximately 700°C[59].

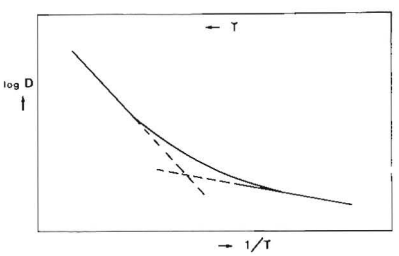

Fig.2.9. Typical plot of log D vs.1/T for polycrystal samples, showing the domination of volume diffusion at high temperatures and of grain boundary diffusion at low temperatures.

CHAPTER III

CONSTITUTION OF THE Ti-AL SYSTEM AND PROPERTIES OF ITS PHASES

3.1. THE EQUILIBRIUM DIAGRAM

Fig.3.1 shows the equilibrium diagram of the Ti-Al system as given by Hansen[62]. This diagram, however, is not complete. Especially on the Ti-rich side of the system many investigations have been carried out in the last few years[63-83]. The most important results are represented in fig.3.2, a-e. Publications, mentioning compounds such as Ti_9Al, Ti_6Al and Ti_2Al[63-67] are omitted since these phases have not been comfirmed in later investigations[72-82].

Fig.3.1 is also incomplete in the region between 25 and 35 at% Ti. Schubert et al.[84-86] report the existence of the compound $TiAl_2$, the

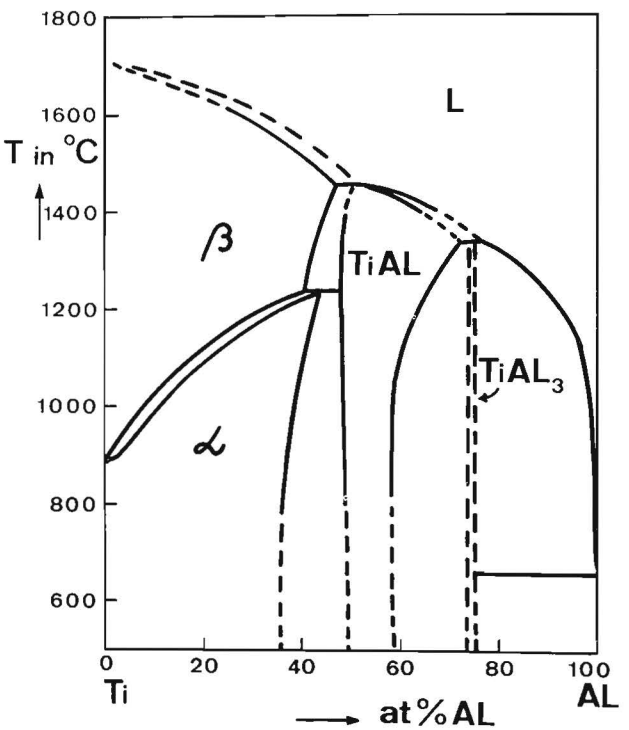

Fig.3.1.
Equilibrium diagram of the Ti-Al system according to Hansen[62].

high-temperature phase Ti_5Al_{11} and a compound described as Ti_9Al_{23}. Their view on this composition region is shown in fig.3.3.

One of the aims of the present work has been to give more experimental data on the phase diagram. As will be discussed in chapter VI, these data support the work of Blackburn[78] on the Ti-rich side. The results obtained by Schubert et al. are confirmed by our experiments only so far as $TiAl_2$ is concerned.

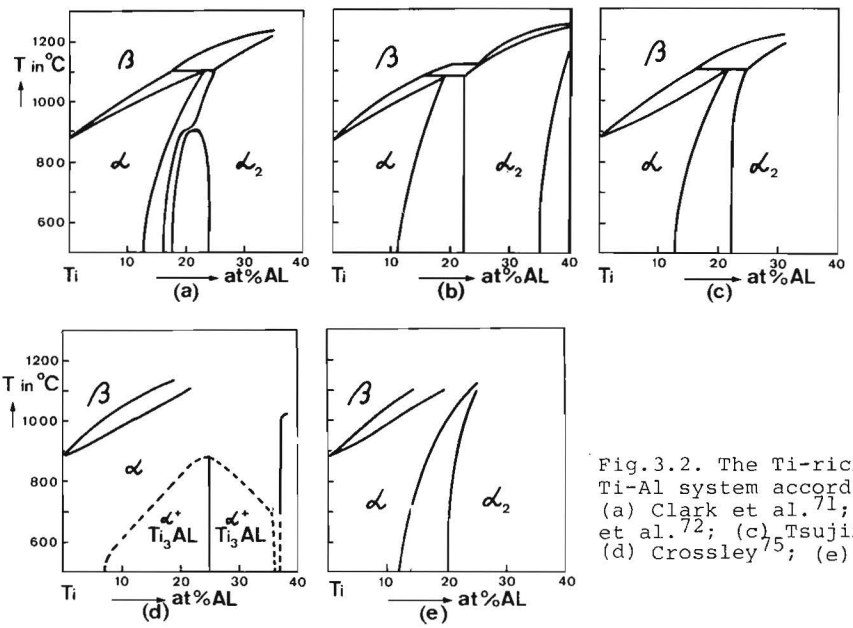

Fig.3.2. The Ti-rich side of the Ti-Al system according to (a) Clark et al.[71]; (b) Kornilov et al.[72]; (c) Tsujimoto et al[74]; (d) Crossley[75]; (e) Blackburn[78].

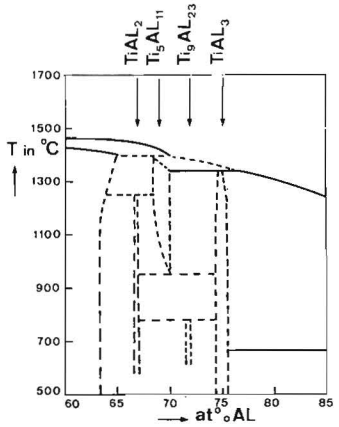

Fig.3.3. The Al-rich side of the Ti-Al system according to Raman and Schubert[86].

3.2. THE STRUCTURE OF THE VARIOUS PHASES

At 882.5° C the low-temperature h.c.p. structure of pure titanium transforms into the b.c.c. structure. The transition temperature rises when small amounts of Al are present. The region of the solid solution of Al in Ti widens as the temperature rises. The lattice parameters a and c of the h.c.p. structure are reduced by the presence of Al[87-90]. Hardness and high-temperature strength increase with increasing Al content[91]. Up to 6 at% Al the strength augments without substantial decrease in plasticity. At higher Al contents, however, a considerable decrease in plastic properties is reported. Addition of Al also increases the resistance of titanium to oxidation[92]. The oxidation rate of an alloy containing 8 at% Al in air at 850° C is 40% lower than that of pure Ti, other conditions being equal.

The structure of Ti_3Al is ordered-hexagonal, Mg_3Cd type[72,75,78]. As shown by fig.3.2, a-e, the region of homogeneity is not known with certainty at the moment.

The structure of TiAl is tetragonal, CuAu type, with a considerable homogeneity region[88,93,94]. The lattice parameter a decreases and c increases with augmentation of the Al content, which means an increase in tetragonality or c/a ratio. Other investigators[87], however, state a decrease of a as well as c with increasing Al content.
At Al contents greater than 50 at% it is found that Ti atoms are replaced by Al atoms[95], contrary to NiAl where Ni atoms are replaced by vacancies at compositions with more than 50 at % Al[96,97].

$TiAl_3$ as well as the compounds mentioned by Schubert et al. also have a tetragonal structure [84-86]. In fact, there is a rather close relationship between the structure of pure Al and that of $TiAl_3$, $TiAl_2$ and TiAl (see fig.3.4). According to Schubert, the compounds "Ti_9Al_{23}" and Ti_5Al_{11} also belong to this series of structures [86](see table 3.1).
It must be mentioned that our results differ from those reported by Schubert. We found that the "Ti_9Al_{23}" phase appears to be a low-temperature modification of the $TiAl_3$ phase (exactly 25 at% Ti) (see section 5.1.6.). The lattice parameters are somewhat different from those reported for Ti_9Al_{23}.
Contrary to TiAl and Ti_3Al, compounds with more Al are very brittle and hardly machinable. The oxidation resistance of $TiAl_3$ is very good and therefore this compound is used for protective coatings[9,10,13]. Since

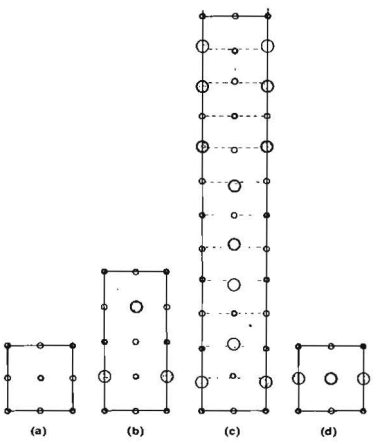

Fig.3.4. Simplified representations on the same scale of the structures of: (a)Al, (b)$TiAl_3$, (c)$TiAl_2$, (d)TiAl (Pötzschke and Schübert[84]). For lattice parameters see table 3.1. Small circles denote Al atoms, large circles Ti atoms; fat circumferences of the circles represent coinciding projections of two atoms.

the low-temperature phase of $TiAl_3$ is not reported in the literature, it is not known what consequences this structure change has on the properties of the coating.

The solubility of Ti in the f.c.c. lattice of Al is very small. The melting point of Al rises when small amounts of Ti are present[62].

Fig. 3.5 shows a plot of molar volume vs. mole fraction. The data correspond to the lattice parameters in table 3.1, except for the high and low temperature modifications of $TiAl_3$, which originate from experiments reported upon in this thesis.

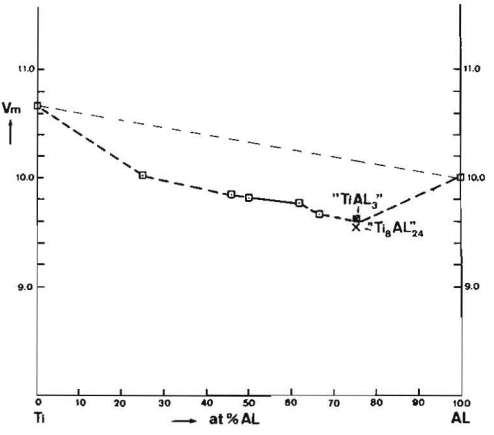

Fig.3.5. A plot of molar volume V_m vs. composition in the Ti-Al system. The squares correspond to the values of the lattice parameters in table 3.1. The values for the high and low temperature modifications of $TiAl_3$, denoted by x, result from the present work.

TABLE 3.1

Summary of the structures of the phases occurring in the Ti-Al system. The Vickers hardness numbers have been determined by the author.

phase	structure	lattice parameters Å	hardness V.H.100	remarks, literature
Ti	$<$ 882,5°C h.c.p.	a= 2.950 c= 4.683	81-143	Clark[98]
	$>$ 882,5°C b.c.c.	a= 3.313		T= 900°C[99]
Ti_3Al	hex.Mg_3Cd type	a= 5.765 c= 4.625	260-380	Blackburn[78]
TiAl	tetr.CuAu type	a= 3.998 c= 4.076	240-260	50 at%[94]
$TiAl_2$	tetr.$HfGa_2$type	a= 3.976 c= 6x4.060	478	Pötzschke-Schubert[84]
Ti_5Al_{11}	tetr.	a= 3.917 c= 4x4.131		Schubert et al.[85]
Ti_9Al_{23}	tetr.	a= 3.843 c= 8x4.183		Schubert et al.[85] (not confirmed in this thesis)
$TiAl_3$	tetr.	a= 3.851 c= 2x4.304	660-750	Dagerhamn[94] (confirmed in this thesis)
Al	f.c.c.	a= 4.0494	19-22	ASTM 4-0787[100]

CHAPTER IV

THE EXPERIMENTAL METHODS

4.1. PREPARATION OF THE DIFFUSION COUPLES

During this investigation a large number of different diffusion couples were prepared and several methods used.

In table 4.1 the various diffusion couples are arranged and their way of preparation is given. In fact, in a number of cases

TABLE 4.1

Summary of the diffusion couples used in the present investigation

couple \ preparation	hot dipping	cold pressing	vacuum furnace	arc furnace	through diffusion	vapour metallising
Ti-Al	32	29	25	7		
Ti(2½%Al)-Al			5			
Ti(5%Al)-Al			12			
Ti(10%Al)-Al			17	10		6
Ti_3Al-Al			16	8		
TiAl-Al			12			
$TiAl_2$-Al			4			
Ti-$TiAl_3$			1	1	19	
Ti-$TiAl_2$			11			
Ti-TiAl			20	4		
Ti(2½%Al)-TiAl			2			
Ti(5%Al)-TiAl				5		
Ti_3Al-$TiAl_3$			5	1		
Ti_3Al-$TiAl_2$			5			
TiAl-$TiAl_3$			6	2	1	
Ti-Ti_3Al			9			
Ti_3Al-TiAl			8			
TiAl-$TiAl_2$			3	1		
$TiAl_2$-$TiAl_3$				1		

TABLE 4.2

The titanium and aluminium, used in this investigation

titanium	supplier	shape	purity	hardness V.H.100	
				as received	annealed 850°C
I	Drijfhout(Holl)	sheet 0.5 mm	99.7	151	142
II	V.D.M.(Germ.)	sheet 1 mm	99.5	147	143
III	Koch-Light(Eng.)	sheet 1.25 mm	99.9	154	135
IV	M.R.C.(U.S.A.)	rod, 10 mm dia.	99.97	164	81
aluminium					annealed 600°C
I	Drijfhout(Holl.)	sheet 2 mm	99.99		19
II	Merck 1058(Germ)	ribbon,0.4 mm	99.99		22
III	Drijfhout(Holl.)	thread,4 mm dia.	99.99		

TABLE 4.3

Typical analysis of titanium and aluminium in weight % as furnished by the supplier

	H	C	N	O	Si	Al	Ti	Fe	Cu
titanium									
I	0.015	0.08	0.05	?	0.04		99.7	0.12	
II	0.013	0.08	0.05	0.10			99.5	0.20 *	
III	0.006						99.9	0.07 *	
IV	0.0004	0.0078	0.0006	0.0063	0.00035		99.97	0.005	0.0008
aluminium									
I						99.99			
II						99.99	0.005	0.006	0.005
III						99.99			

* The amount of Fe has been determined by Mr.Bachus Eindhoven.
For Ti II this was found to be 0.063 ± 0.002, for Ti III 0.071 ± 0.002.

sandwich couples consisting of three different materials were prepared e.g. TiAl-Ti-$TiAl_2$. In each column the number of couples are given from which the results were used in the investigation. A rather large number of samples broke down owing to several causes mentioned further on. Several couples are listed in which only one phase boundary develops during diffusion; they were used to obtain a more accurate value for the concentrations at this phase boundary.

Atomic percentages are used throughout this thesis unless stated otherwise.

In tables 4.2 and 4.3 details are given about the titanium and aluminium used in this investigation. On the ground of the remark in table 4.3 together with the fact that the hardness values of Ti I and II are equal, it seems justifiable to consider their purities to be likewise equal. Both will be referred to as Ti 99.7. The purity of Ti III as given by the supplier seems to be too high in view of its hardness. In this investigation any significant difference in diffusion behaviour between the titanium grades I, II and III was never noticed.

The aluminium was used as received, the titanium was annealed for three days in an evacuated quartz capsule at 850°C.

The alloys were prepared by melting Ti 99.7 and Al III in the proper weight ratio in an argon-arc melting furnace. For each sample melting was repeated five times in order to obtain the desired homogeneity. The loss of weight is less than 0.1 wt%. Two portions each of 10 g were remelted in the same furnace in a special mould to obtain a bar of 10 mm diameter. The bar was annealed in a quartz capsule for three days at a temperature of 850°C to obtain homogenisation and to relieve internal stresses.As has been verified several times, there was no significant difference whether using annealed or unannealed alloys.

Using either a 1-mm carborundum or a diamond blade, dependent on the nature of the material, the bar was sawn into 2-mm thick sheets. After this, the sheets were ground on silicon carbide papers of various grades, the finest being the 600 grade.

Before the preparation of the diffusion couple the sheet of starting material was pretreated in different ways:

(a) by abrasion on 600-grade silicon carbide paper;
(b) as (a), followed by etching with Kroll's reagent (2% HF, 2% HNO_3, 96% H_2O);
(c) as (a), followed by polishing with 3- μm diamond on nylon cloth;

(d) as (c), followed by soft cloth polishing with 0.05-μm Al_2O_3;
(e) as (d), followed by etching with Kroll's reagent.

After each treatment the material was rinsed with alcohol, dried and then stored in chloroform.

In the five cases mentioned above no significant difference in diffusion behaviour was found. Therefore, in all the following methods of preparation the samples were pretreated by the simplest method (a).

(a) Hot dipping

Aluminium III, cleansed in a 10% NaOH solution for one minute, was melted in an alundum crucible in an argon atmosphere, using a vertical furnace. At 850°C a strip of the base material, i.e. the material to be coated, was dipped into the molten aluminium for 10 sec. An irregular but adhesive layer of Al was formed on the base material. Microscopically, no diffusion layer could be detected.

The method of hot dipping has particularly been used at the beginning of our investigations.

(b) Cold pressing

A heating device for temperatures up to 420°C was placed in a Buehler mounting press. Circular sandwich couples Al-Ti-Al of 10 mm. diameter were prepared by pressing at this temperature a Ti disc between two Al discs, applying a pressure of 1500 kg/cm^2 for 30 minutes. During preparation the thickness of the Ti disc was reduced to half the original value.
In nearly all the samples good contact between Al and Ti was achieved. This method was used in a period of change-over to method (c) which offered more possibilities.

(c) Vacuum furnace

In cooperation with Ir.G.F.Bastin a special vacuum furnace was designed in our laboratory. This allowed us to prepare diffusion couples in vacuo, using an external pressure to ensure good contact between the starting materials.
By using a thermocoax heating element, a temperature up to 1000°C with a variation limit of $\pm$ 2°C was obtained. The external pressure was made variable by means of a set of weights (max.50 kg). Vacuum was from 10^{-6} to 10^{-7} mm Hg , measured close to the specimen. The temperature and duration of the heating varied, dependent on the proper diffusion couple. In this way, in most cases a very thin

diffusion layer was formed during preparation. Details of the furnace will be given in a publication by Bastin.

Although originally designed for preparing such couples, the furnace has later also been used for annealing the diffusion couples.

d) Joining by means of an arc furnace

In our final experiments a new method of preparing diffusion couples, developed by Den Broeder[101], was used. In this method the tungsten electrode of the arc furnace is replaced by a copper one, between which and the cooled copper bottom plate the sandwich is clamped and heated by a direct current of 200 - 400A at 4 - 5 V. Since the electric resistance of the couple was too low, it had to be placed between two graphite bars to obtain the desired temperature. Heating was carried out until a few drops were formed at the interfaces. In most of the couples so prepared no diffusion layer could be detected. However, in some cases the temperature rose too high, resulting in the formation of rather thick diffusion layers. These couples have been used for special investigations (see section 5.2.2.).

(e) Diffusion

A "diffusion method" was readily applied with couples of $TiAl_3$ and any other material. This material was first coated with a layer of pure aluminium. By annealing at approximately 625°C for a few days, the aluminium was converted into $TiAl_3$. (As will be seen in the next chapter, $TiAl_3$ is the only compound formed during this experiment). The contact between $TiAl_3$ and the other material is excellent, since, as a result of the Kirkendall effect, possible contaminations disappeared to the Al-side of the $TiAl_3$ layer during its formation.

(f) Vapour metallising

This technique has been used in some special cases (see section 5.1.6.). In an evacuated chamber (vacuum 5.10^{-5} mm Hg) a sheet of Ti (10% Al) was brought a temperature of 625°C by laying it on a ribbon of molybdenum heated by direct current. The temperature was measured by means of a thermocouple Pt-Pt(10% Rh).. About 1 cm above the alloy sheet, a length of aluminium wire wound around a tungsten filament was held. The aluminium evaporated when heating the filament to a sufficiently high temperature. The thickness of the aluminium layer on the alloy varied between 20 and 100 μm.

No diffusion layer of $TiAl_3$ was formed in the procedure which lasted about half a minute.

4.2. HEAT TREATMENT AND MICROSCOPIC EXAMINATION OF THE DIFFUSION COUPLES

The diffusion couples were annealed at temperatures between 540 and 1200°C in a small quartz-glass capsule, evacuated to less than 0.1 mm Hg or filled with helium. Temperature was measured by means of a Pt-Pt(10% Rh) thermocouple with an accuracy of ± 1.5°C. Fine pieces of pure titanium or niobium as getter materials were regularly heated in the capsules together with the diffusion couples. The presence of these materials was not found to affect the experimental results, thus proving the sufficiently good conditions of atmosphere in the capsule. During annealing at temperatures above 800°C some evaporation occurred, which was detected by the appearance of a thin diffusion layer at the outside of the sandwich couple (see section 5.2.1.).

In some couples the outside layers originated from surface diffusion, especially when pure aluminium was involved (see section 5.1.2.)

After the heat treatment each couple was embedded in transparent resin. To this end, the contact surface of the couple was held perpendicularly to the bottom of the mould. The embedded couple was then ground up to 600-grade silicon carbide paper, and polished for 20 to 30 minutes with 3-μm diamond on nylon cloth. In some cases a fine polishing with 0.05 -μm Al_2O_3 for 5 min on soft cloth was desirable. The samples were washed and then etched with Kroll's reagent.

Microscopic examination of the diffusion layer was carried out with a Reichert microscope using a calibrated filar micrometer eyepiece, allowing of measuring with an accuracy of ± 0.15 μm. Photographs were made using the Reichert Me F microscope.

In a number of experiments the couple was removed from the mounting resin after microscopic examination and heated at the original temperature again to investigate the growth kinetics of the diffusion layer. Rather often a couple broke down as a result of crumbling of one of the brittle starting materials like $TiAl_2$ or $TiAl_3$ or cracks owing to the diffusion behaviour (see section 5.1.1.).

4.3. MICROPROBE ANALYSIS

The penetration curve was measured by means of electron probe X-ray microanalysis (or microprobe analysis), using an S.E.M.IIA apparatus of Associated Electrical Industries, Manchester, England. A calibration curve was made, using 15 alloys between 25 and 100 at% titanium (this is the region of interest in our investigations). The alloys were made by argon-arc melting and after grinding, polishing and light etching mounted in rectangularly shaped Wood's metal.

A calibration curve was made for Ti as well as for Al (fig.4.1). A representative value for the whole surface of the alloy was obtained by scanning 50 different squares each 100 x 100 μm and counting the pulses of TiKα and AlKα radiation, respectively, for

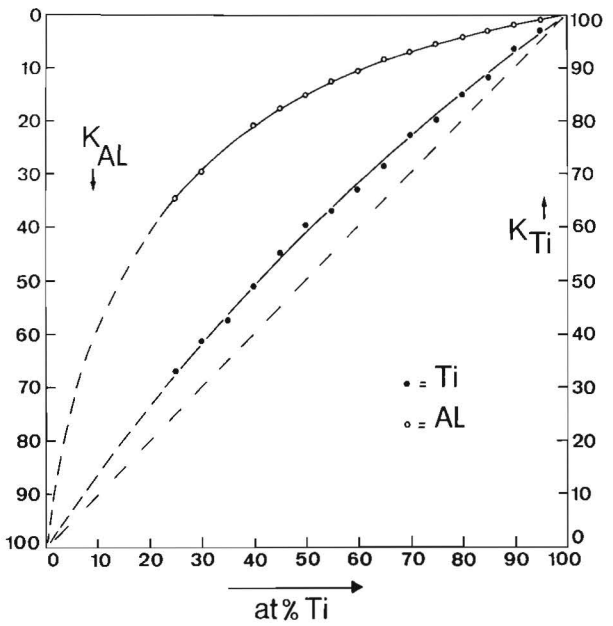

Fig.4.1. Calibration curves in microprobe analysis for Ti and Al. Operating conditions for:
Ti: accelerating voltage 25kV; probe current 0.2 μA; TiKα radiation; LiF crystal.
Al: accelerating voltage 30 kV; probe current 0.2 μA; AlKα radiation; KAP crystal.

10 sec. In no sample was a significant difference found between the composition of the central area and the edge of the sample. Before and after each measurement, 10 squares of 100 x 100 μm of pure titanium (or aluminium) were examined. In both cases correction for background radiation was made. The resulting value of $K = I/I^{O}$ can be written as a function of the mole fraction N:

$$\frac{1 - K}{K} = A \times \frac{1 - N}{N}$$

The value of A was for titanium 0.70 ± 0.04 and for aluminium 5.7 ± 0.10.

When recording the penetration curve in a diffusion couple, point measurements were carried out under the same operating conditions as in the calibration measurements.

The counting time was 10 sec at every point; the minimum distance over which the sample was moved between two point measurements was 2.5 μm.

In order to prevent failures due to differences in absorption of radiation, the plane formed by the incident electron beam and the direction in which the X-rays are taken off was kept parallel to the interface between the diffusing materials. Despite this precaution, the concentration at the interfaces is not accurately determinable within a distance of 3 μm owing to several edge effects. The latter arise from metallographic sources as well as from the volume of the material excited, the volume being strongly dependent on the acceleration voltage and on the nature of the material[102-105].

4.4. X-RAY DIFFRACTION

In order to identify the various phases formed in the diffusion couples, the layers have been successively ground parallel to the contact interface between the starting materials. After each abrasion of various amounts of material, a CuKα - diffractogram in the region $10^{O} < 2\theta < 85^{O}$ was made from the surface of the sample, using a Philips X-ray diffractometer and a goniometer speed of ½ or 1 degree/minute.

This method was used for qualitative investigations in the couples $Ti\text{-}TiAl_3$; in couples in which aluminium was one of the starting materials the diffractograms were used in a semi-quantitative sense (see section 5.1.6.).

4.5. MICRO-INDENTATION HARDNESS TESTING

Hardness testing has been carried out on the titanium and aluminium used in this investigation to get an impression about their purity, applying a load of 100 g on the Vickers diamond, using a Leitz "Durimet" hardness tester (see table 4.2). It is a well-known fact that especially the hardness of titanium is dependent in a high degree on the concentration of impurities like oxygen and nitrogen. Micro-indentations have also been used in testing the hardness of the various phases in the Ti-Al system (see tables 3.1 and 4.2) and in qualitative studies of the diffusion zone in certain couples.

Before making the indentations, the sample was polished carefully, using 3-μm diamond and 0.05 - μm Al_2O_3, respectively. Afterwards the sample was lightly etched in order to make visible the individual grains and phase boundaries. The etching did not affect the value of the micro-indentation hardness.

CHAPTER V

THE EXPERIMENTAL RESULTS

5.1. DIFFUSION COUPLES OF WHICH ONE OF THE STARTING MATERIALS IS PURE ALUMINIUM

5.1.1. Ti-Al diffusion couples

5.1.1.1. Couples made by hot dipping or cold pressing

Couples of Ti-Al made by hot dipping or cold pressing, have been annealed at temperatures varying from 580 to 640°C. In all cases the result was the formation of a single diffusion layer of composition $TiAl_3$, as confirmed by microprobe analysis (section 5.1.5., fig.5.12). The crystal structure of this layer will be discussed in section 5.1.6.

The growth process of the $TiAl_3$ layer was very peculiar. In the initial stages of varying duration the layer growth was roughly proportional to time (see fig.5.1, a and b). More precisely,

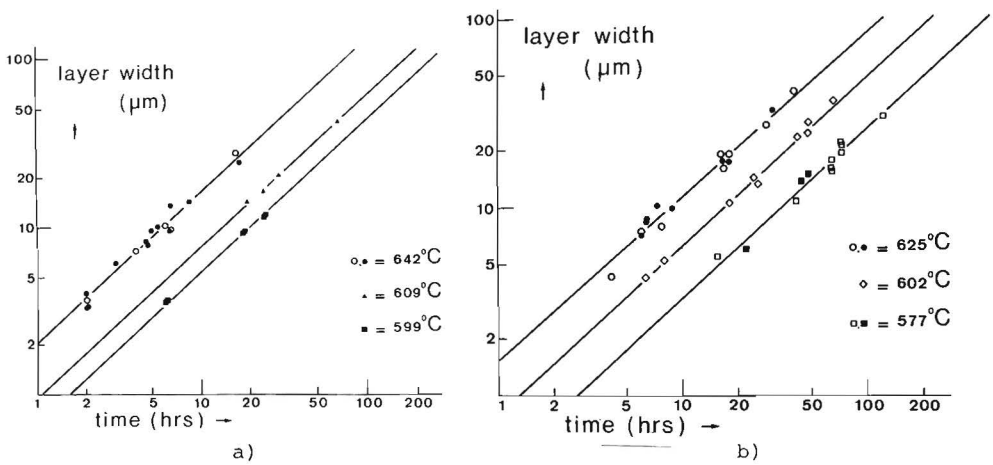

Fig.5.1, a,b. Plot of the logarithm of the layer width of $TiAl_3$ vs. the logarithm of diffusion time in Ti (99.7)-Al couples at various temperatures. Open symbols refer to cold pressing, the others to hot dipping.

$d^{1.1} = kt$ where d denotes the layer width and k is the penetration constant. These initial stages will henceforth be referred to as the "linear" stages or periods. In fig.5.2 a plot of log k vs.1/T is represented; the data, calculated from this plot are to be found in table 5.4.

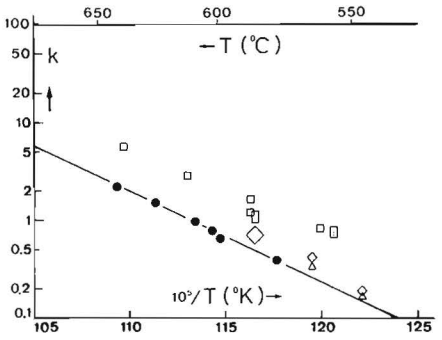

Fig.5.2. Plot of log k vs.1/T for the $TiAl_3$ layer in various couples. In Ti-Al couples k is defined by the relation $d^{1.1}=kt$, in the other couples by $d = kt$.
= Ti-TiAl; = Ti(5%Al)-Al;
= Ti(10%Al)-Al; = Ti_3Al-Al.

The microscopic aspect of the linear stage is characterised by the regular shape of the $TiAl_3$ layer and by small inclusions of pure aluminium (see fig.5.3,a). The identification of the inclusions was confirmed by X-ray diffraction. The linear period ended abruptly in a break-through, followed by a much faster growth process in which a pure $TiAl_3$ layer was developed irregular in shape and free from inclusions (fig.5.3,b). The change-over between the two

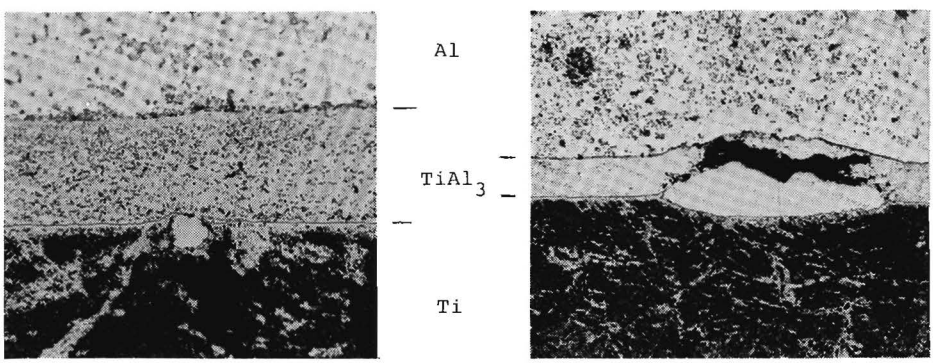

a) b)

Fig.5.3,a,b. Ti-Al diffusion couple, annealed for 40 h at 625°C. The thickness of the $TiAl_3$ layer is 41 μm. The process of break-through sets in.

processes was visible in the layer as a series of smaller or larger pores . Often the diffusion couple broke down at this "pore interface" during subsequent annealing.

It was not possible to describe mathematically the growth rate of the $TiAl_3$ layer after the break-through, since the latter did not set in at the same time for each point. Therefore, the resulting layer was very irregular.

5.1.1.2. Couples made in the vacuum furnace and in the arc furnace

Using the vacuum furnace or the arc furnace for preparing the Ti-Al couples, the results were different from those mentioned in section 5.1.1.1. The initial linear stage was very short, in fact hardly measurable. Consequently, nearly the whole $TiAl_3$ layer was created by the much faster subsequent growth process and was therefore relatively thick and rather regular in shape.

When annealing such a couple again at the same temperature, the $TiAl_3$ layer did not grow any more. Actually, in most cases the couple broke down at the $TiAl_3$-Al interface after the first annealing (see section 5.1.2.).

5.1.2. Diffusion couples of the types Ti(2½%Al)-Al; Ti(5%Al)-Al; Ti(10%Al)-Al; Ti(25%Al)-Al

The couples mentioned in the heading have often been prepared in sandwich form, using both aluminium I and II in various numbers of

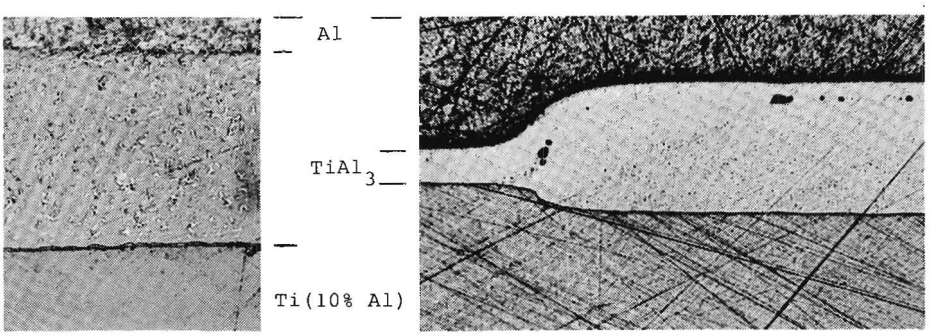

a) b)

Fig.5.4,a. Ti(10%Al)-Al diffusion couple, annealed for 68.5 h at 588°C. The $TiAl_3$ layer is in the "linear growth period". Thickness 60 µm. Notice the Al inclusions in the $TiAl_3$ layer.

Fig.5.4,b. The same couple, showing the transition from the linear to the parabolic growth period.

sheets in order to obtain the desired thicknesses. No difference in diffusion behaviour of the two grades of aluminium was observed.

The initial linear stage was found again in the growth of the $TiAl_3$ layer formed in all the couples (fig.5.4,a). When the layer width reached a certain value d_1, then a break-through occurred, resulting in a regular layer, thus proving that this process started at the same point of time t_1 in nearly the whole diffusion couple (fig.5.4,b).

The thickness of the layer at the moment of break-through, d_1, was visible from the row of pores which were formed on the Ti-rich side of the layer (figs.5.5, a-c).

The reproducibility of the value for d_1 and t_1 was poor. However, qualitatively the results can be summarised as follows:

(a) the lower the temperature the longer and the more reproducible is the duration of the linear stage and the slower the linear growth rate;
(b) the more aluminium is present in the starting alloy the longer is the duration of the linear growth stage;
(c) the more aluminium is present in the starting alloy the faster is the linear growth rate;
(d) the distance between aluminium and the row of pores remained constant on subsequent annealing. Growth occurred exclusively on the Ti-rich side of the layer (fig.5.5, a-c).

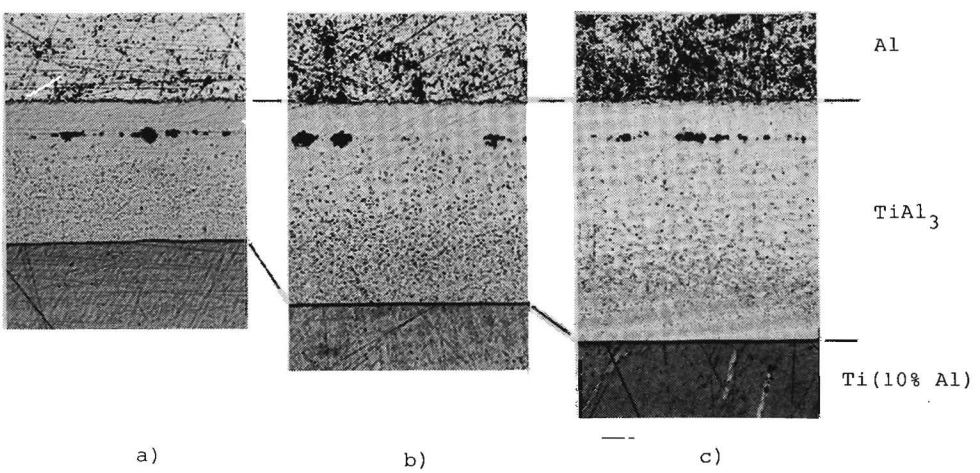

Fig.5.5,a-c. Ti(10%Al)-Al diffusion couple, annealed at 639°C for 15,28 and 40 h, respectively. The distance between the row of pores and the Al-$TiAl_3$ boundary is constant.

A difficulty in determining the linear growth kinetics was the relatively short duration of this period. It appeared to be possible to determine only one or a few data in one particular couple. The results are, therefore, not very accurate, but qualitatively they are unambiguous. This is shown in fig.5.6 for Ti(25%Al)-Al couples.

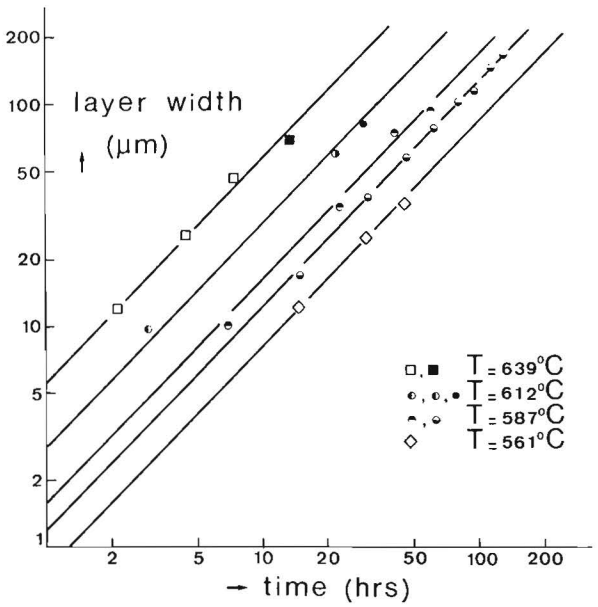

Fig.5.6. Plot of the logarithm of the layer width of $TiAl_3$ vs. log t for the "linear growth period" in Ti_3Al-Al couples at various temperatures. The black block and dot denote measuring data obtained from fig.5.7,a.

Since the row of pores originates closer to the aluminium side of the couple in proportion as less aluminium is present in the starting alloy, the "pore interface" coincides with the $TiAl_3$-Al phase boundary, when using pure Ti as a starting material. This often results in the formation of a gap (see section 5.1.1.2.). The gap also often occurred in Ti(2½% Al)-Al couples at higher Al content this annoying phenomenon did not show up.

It must be mentioned that in some diffusion couples a very thin, hardly observable layer was present between $TiAl_3$ and the titanium-

rich starting alloy. The occurrence and width of the interjacent layer depended on the particular grain in the starting material from which the layer was growing. Actually, also the linear growth rate of the $TiAl_3$ layer and the point of time of break-through differed slightly from grain to grain in the starting material. There might be a relationship between the presence of the interjacent thin layer and the moment of break-through. However, this could not be confirmed unambiguously.

In fig.5.2 the logarithm of the penetration constant k_1 for the linear growth is plotted vs. the reciprocal absolute temperature. There is a distinct connection between the results for Ti(25%Al)-Al and those for Ti-Al couples made by hot dipping or cold pressing. In Ti (5%Al)-Al and Ti(10% Al)-Al it was possible to perform only a few measurements for k_1 at low temperatures.

The growth kinetics after the break-through is difficult to determine. If the layer becomes thicker, irregularities occur because of cracks in the brittle $TiAl_3$, probably introduced by the several mechanical and heat treatments of the couple. Besides, only a limited number of data could be obtained from one particular couple, since the diameter of a couple did not permit more than approximately five or six subsequent annealings and abrasions. As a matter of fact, for each measurement an appreciable part of the couple had to be removed by grinding in order to avoid effects originating from surface diffusion on the outside of the couple.

Surface diffusion was sometimes very well observable. In that case, the Ti-rich starting alloy plates were coated all around with a rapidly growing layer of $TiAl_3$. The layer formed in this way did not show the relatively slow linear growth rate but it grew fast from the first moment. Therefore, the layer was sometimes even thicker than the one created inside the couple between pure aluminium and the starting alloy, viz., when the latter layer was in its linear stage.

Contrary to phenomena to be discussed in section 5.2., evaporation effects cannot be the cause of the formation of such $TiAl_3$ layers on the outside of the starting alloy. This has been verified by heating a piece of the same alloy together with the couple in the same quartz capsule. This piece remained uncoated.

Unfortunately, the surface-diffusion effect was not reproducible and in most experiments it was absent. The conditions, required in order to avoid or to favour it, could not be sufficiently investigated during the present investigation. Because of the possible practical

importance, a more thorough investigation in this phenomenon is desirable.

Despite these difficulties it is obvious that especially at higher temperatures the total layer growth becomes parabolic with time after the break-through. Examples of this are shown in figs. 5.7,a and b, where the square of the total layer width, d^2, is plotted vs. diffusion duration. In the same figures, the value of $(d^2 - d_1^2)$ is plotted, too. The straight line connecting the experimental data in the latter case intersects the abscissa at time t_1.

The values of d_1 and t_1 for the Ti(25% Al)-Al couples calculated in this way are represented in fig.5.6 and agree reasonably well with the direct measurements of the linear period. When Ti(10% Al) or still Ti-richer starting materials are used, the results are not reliable any more, since high degrees of inaccuracy arise because of the small values of d_1 and t_1 involved.

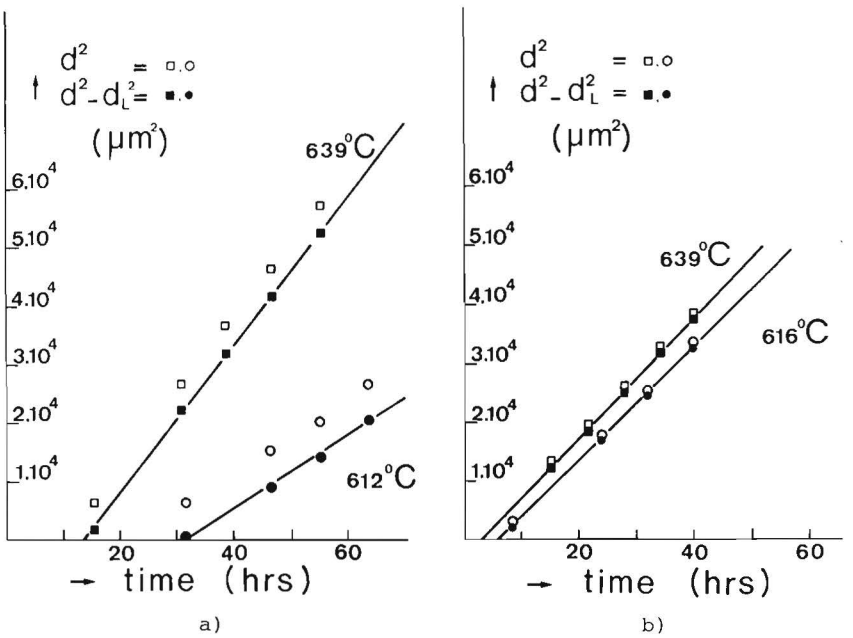

Fig.5.7,a. Plot of the square of the layer width of $TiAl_3$ vs.diffusion time in Ti_3Al-Al couples at two temperatures.

Fig.5.7,b. The same plot for Ti(10%Al)-Al couples. For an explanation of the plot for the black blocks and dots see text.

The values obtained for the parabolic penetration constant agree satisfactorily with the results to be discussed in section 5.1.3. (see figs. 5.11 and 6.2). The appearance of the $TiAl_3$ layer was peculiar. Microscopically, the very small grains did not show any preferred orientation. In the vicinity of the row of pores they were often needle-shaped in random directions, elsewhere the grains appeared to be equiaxed (see fig.5.8).

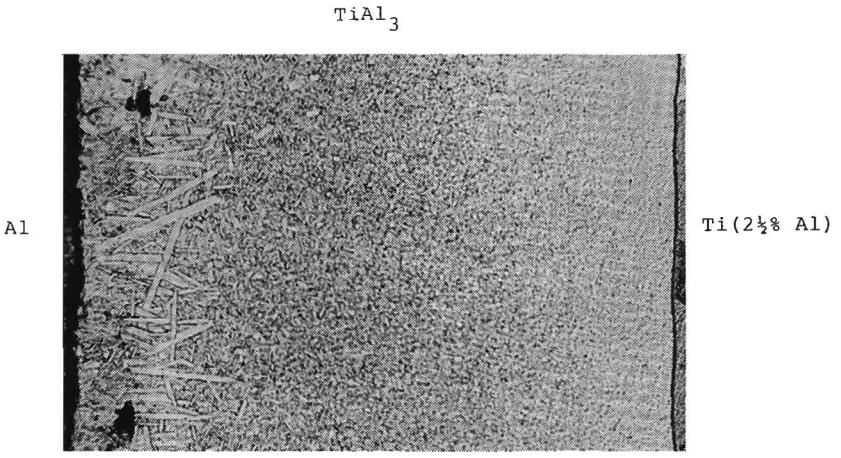

Fig.5.8. Ti(2½%Al)-Al diffusion couple, annealed for 68.5 h at 588°C. Layer width of $TiAl_3$ is 167 µm. Notice the pores and the needle-shaped crystals at the Al-side of the couple.

In two cases distinct deviations of the results mentioned before occurred:

(i) Vapour metallising was used as a preparation method for the couples. Then, the duration of the linear period was shorter, in fact hardly measurable. Unfortunately, the experiments were not reproducible enough to obtain more quantitative data for the layer growth.

(ii) The purest Ti IV was used for the preparation of the starting alloy. The deviation was verified in particular for Ti(25% Al) at 585°C. In this case, the initial linear period was very short and, in fact, the results resembled very closely those for Ti-Al couples as mentioned in section 5.1.1.2. Also breakdown at the $TiAl_3$-Al interface often occured.

5.1.3. Diffusion couples of the types TiAl (54%Al)-Al and $TiAl_2$-Al.

The results of the experiments using TiAl and $TiAl_2$ as starting alloys as represented in fig.5.9 showed no initial linear stage. Layer growth was parabolic with time right from the beginning of the experiment, apart from small deviations originating from the situation at t = 0.(For instance, a thin $TiAl_3$ layer may have been formed during the preparation of the couples; short incubation times may have arisen because of insufficient contact). The appearance of the layer was also different from that mentioned in the previous section. In TiAl-Al and $TiAl_2$-Al couples the grains in the $TiAl_3$ layer were, although very small, more or less columnar in the diffusion direction (see fig.5.10).

Sometimes cracks were formed at the boundary between $TiAl_3$ and TiAl. They were obviously caused by the cooling after annealing, since the layer thickness was not affected by the presence of the cracks. They were removed by continued grinding.

The thin interjacent layer mentioned in section 5.1.2. was not present in this kind of diffusion couples.

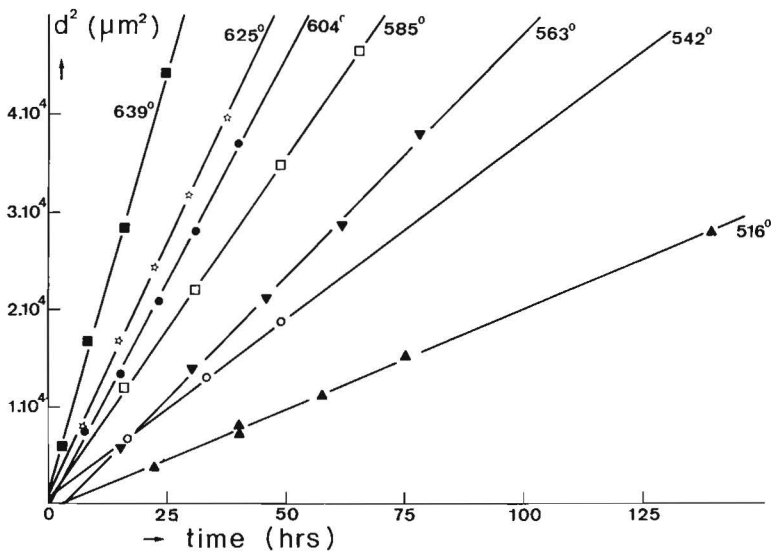

Fig.5.9. Plot of the square of the layer width of $TiAl_3$ vs.diffusion time in TiAl-Al couples at various temperatures.

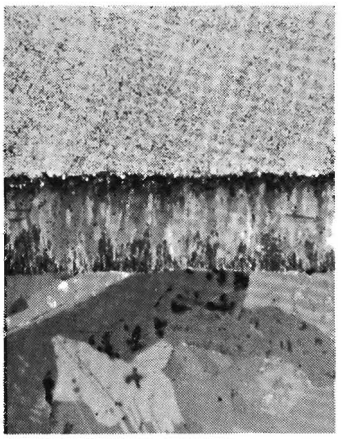

Fig.5.10. TiAl-Al diffusion couple (polarised light), annealed for 7 h at 600°C. Thickness of the $TiAl_3$ layer is 72 μm. Notice the regular layer without pores, and the columnar appearance of the crystals.

The $TiAl_2$-Al couples were very difficult to prepare owing to the brittleness of $TiAl_2$ and so have not been investigated thoroughly. The diffusion layer had the same appearance as that in TiAl-Al, but was only formed in a few places where good contact was made.

In fig.5.11 the logarithm of the penetration constant $k_p = d^2/t$

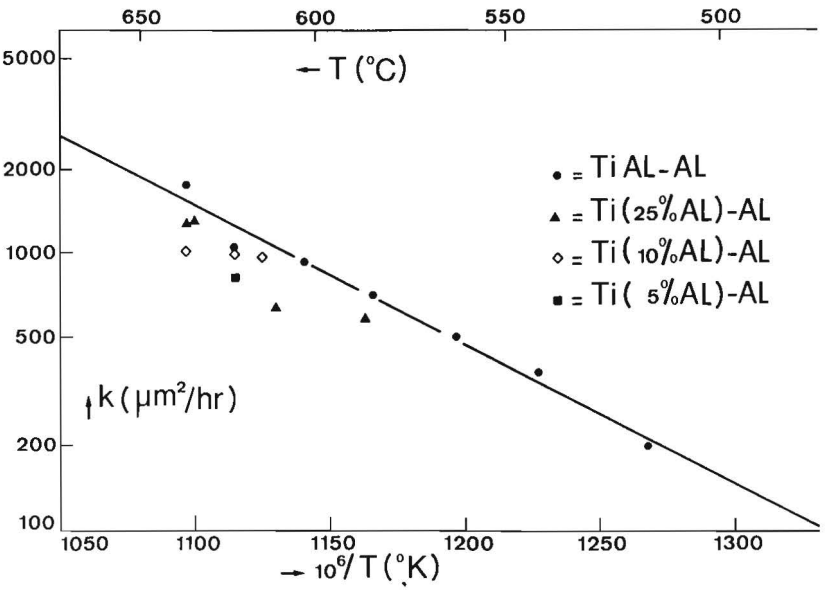

Fig.5.11. Plot of log k vs.1/T for the $TiAl_3$ layer in various couples. The penetration constant k is defined by $d^2 = kt$.

is plotted vs. the reciprocal temperature. A reasonably straight line connects the several data. The values for k_o and Q are represented in table 5.4.

5.1.4. Marker experiments

In all diffusion couples in which aluminium is used as a starting material, marker experiments proved that aluminium was the only diffusing component in all stages of layer growth. This is rather peculiar, since in the linear stage pure aluminium is found on both sides of the markers. The latter fact can not be the result of the markers being pushed into the soft aluminium during the preparation of the couple, in view of the great distance over which pure aluminium was found in the $TiAl_3$ layer. Besides, after preparation the position of the markers was checked and found to be correct. As markers, 10 micron molybdenum wire as well as very fine ZrO_2powder were used. The Mo wire was observed microscopically, the ZrO_2powder was observed better when using the microprobe.

Another proof that Al is the only diffusing component is found by reannealing a couple at the original temperature. Then, the new-grown part of the layer $TiAl_3$ is situated on the Ti-side of the layer. This is observable because of the brighter appearance of the new-grown layer after etching.

5.1.5. Microprobe analysis

Microprobe analysis has been performed in practically all the couples mentioned in the previous sections. In fig. 5.12 three examples are given. The analysis has proved the following points:

(a) In the $TiAl_3$ layer, grown in the parabolic growth period, no homogeneity range was detected; the layer was found to be of a stoichiometric composition, independent of the temperature at which the layer was formed.

(b) During the initial linear growth period of the layer the overall content of Al was found to be higher, varying from 75-80 at%. This percentage agrees with 0-20 vol % of pure Al inclusions. Generally, the inclusions were more in evidence on the Al side of the layer.

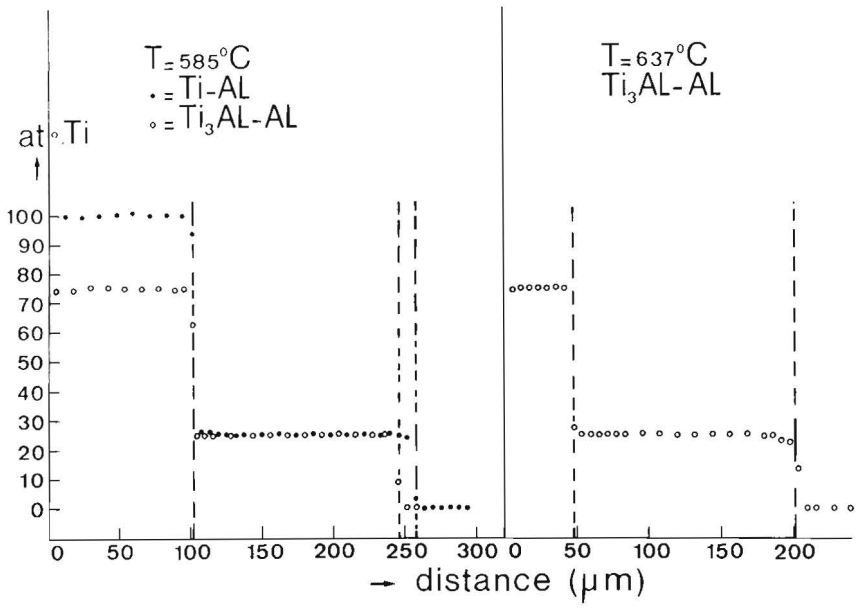

Fig.5.12. Penetration curves for Ti in the couples:Ti-Al, annealed for 87 h at 585°C; Ti_3Al-Al, 87 h at 585°C; Ti_3Al-Al 21.5h at 637°C.

Actually, they were too small to be reliably identified by microprobe analysis, but microscopic as well as X-ray diffraction analysis confirmed the inclusions to consist of pure Al.

(c) In no case was a solid solution of Al in Ti formed in these experiments. Neither did the starting alloys already containing 2½, 5, 10, 25 or 54 at% Al, enrich their Al content during diffusion annealing.

(d) The thin interjacent layer mentioned in section 5.1.2. was unfortunately too thin to be identified by microprobe analysis.

5.1.6. X-ray diffraction investigation of $TiAl_3$ formed in diffusion couples

The structure of $TiAl_3$ formed in couples of different starting materials and annealed at different temperatures, was investigated using X-ray diffraction (see section 4.4.). The results were sur-

prising and can be summarised as follows:

(a) At temperatures of about 638°C the diffusion layer consists almost entirely of the pure phase $TiAl_3$, as follows from a comparison between the lattice parameters found in this work and those, given in the literature for the phase "$TiAl_3$", spatial group D_{4h}^{17} I 4/ mmm, containing 2 molecules/cell. (Standard deviations are stated in the parameter values found by us).

Our investigations	Dagerhamn[94]
$a = 3.849 \pm 0.004$ Å	$a = 3.851 \pm 0.003$ Å
$c = 8.610 \pm 0.008$ Å	$c = 8.608 \pm 0.004$ Å
$c/a = 2.237$	$c/a = 2.235$
$V_{cell} = 127.56$ Å^3	$V_{cell} = 127.66$ Å^3

The reflections and observed values of 2θ, obtained by averaging the values of 18 different couples are listed in table 5.1 together with the values of 2θ (for Cu Kα radiation), calculated using the lattice parameters, found by us.
The same lattice parameters were also found in $TiAl_3$ coatings, annealed at temperatures > 760°C, and in $TiAl_3$ made by melting in an arc furnace.

In the diffractograms some small additional peaks were found, which is attributable to the phenomenon mentioned in (b) below.

(b) At temperatures of about 585°C the diffusion layer consists of a mixture of two modifications of $TiAl_3$, viz., the one mentioned in (a), which will henceforth be denoted as "$TiAl_3$", and a hitherto unknown modification, which can be described as a superstructure of "$TiAl_3$", with a cell parameter, c, four times as long, thus containing 8 molecules/cell. The lattice parameters of this phase which will be denoted as "Ti_8Al_{24}", resemble rather closely those of the compound Ti_9Al_{23} as given by Schubert et al.[86].

Our investigations	Schubert et al.[86]
$a = 3.875 \pm 0.004$ Å	$a = 3.85$ Å
$c = 33.84 \pm 0.04 = 4 \times 8.46$ Å	$c = 33.46 = 4 \times 8.365$ Å
$c/a = 4 \times 2.183$	$c/a = 4 \times 2.173$
$V_{cell} = 4 \times 127.01$ Å^3	$V_{cell} = 4 \times 123.99$ Å^3

TABLE 5.1

Observed and calculated reflections for

"$TiAl_3$" (tetragonal, a = 3.849 Å, c = 8.610 Å) and

"Ti_8Al_{24}" (tetragonal, a = 3.875 Å, c = 33.835 Å)

The standard deviation in 2θ obs. is at most ±0.04 deg.

$TiAl_3$			Ti_8Al_{24}		
reflection	2θ obs.	2θ calc.	reflection	2θ obs.	2θ calc.
002	20.62	20.61	008	20.99	20.99
			101	23.07	23.08
			103	24.28	24.27
101	25.33	25.32			
			105	26.48	26.48
			107	29.50	29.52
110	32.89	32.88	110	32.66	32.65
			10$\underline{11}$	37.32	37.29
112,103	39.12	39.12	118	39.15	39.14
004	41.96	41.94	00$\underline{16}$	42.74	42.72
200	47.18	47.19	200	46.85	46.85
			208	51.87	51.86
			213	53.48	53.45
114,211	54.31	54.30	11$\underline{16}$	54.78	54.79
			10$\underline{19}$	56.89	56.85
105	58.70	58.68			
			21$\underline{11}$	61.37	61.35
213	62.92	62.90			
204,006	64.95	64.94	20$\underline{16}$	65.24	65.26
220	68.93	68.95	220	68.39	68.42
116,301	74.73	74.73	11$\underline{24}$	75.81	75.82
215,310	78.51	78.51			
312,107,303	82.24	82.23	318	81.73	81.75
224,206	84.06	84.07	22$\underline{16}$	84.09	84.12

Microprobe analysis has shown unambiguously that the composition of the "new compound" is indeed $TiAl_3$ ($=Ti_8Al_{24}$) within the experimental error of $\pm$ 0.5 at%.

The reflections together with the observed and calculated values of 2θ, averaged over 13 couples, are listed in table 5.1.

(c) No significant change in the structure of the $TiAl_3$ layer was detected in the direction of diffusion. This was verified by abrading various quantities of the layer, and examining the liberated surface after each abrasion: the peaks in the diffractogram remained unaltered.
It was also found that the structure of $TiAl_3$, formed during the linear period, was not different from the structure of $TiAl_3$, formed in the subsequent parabolic period.

(d) $TiAl_3$, formed in couples at 638°C, does not change its structure on subsequent annealing at 585°C. On the other hand, $TiAl_3$ formed at 585°C and subsequently annealed at 638°C does not change its crystal structure either. In these experiments the aluminium was removed from the couple by abrasion in order to prevent further growth of the diffusion layer during subsequent annealing.

(e) The ratio between the quantities of the two modifications, "$TiAl_3$" and "Ti_8Al_{24}", depends not only on temperature, but also on other variables (see tables 5.2 and 5.3), viz.,

(i) in couples of Al vs. an alloy containing between 0 and 25 at% Al, in which Ti 99.7 has been used in the preparation, the quantity of Ti_8Al_{24} is higher than in couples TiAl-Al, as shown in table 5.3.
The percentages given in this table characterise the fraction of Ti_8Al_{24} present in the diffusion layer and must be considered to be a rough estimate. They have been calculated by assuming that

$$\text{fraction } Ti_8Al_{24} = \frac{\Sigma\ Ti_8Al_{24}}{\Sigma\ Ti_8Al_{24} + \Sigma\ \text{"}TiAl_3\text{"}}$$

where $\Sigma\ Ti_8Al_{24}$ denotes the sum of the peak heights of all the reflections of Ti_8Al_{24}, and Σ "$TiAl_3$" is the sum of the peak heights of all the reflections of "$TiAl_3$".

TABLE 5.2

Relative intensities of the reflections of "$TiAl_3$" for various circumstances, compared with literature values[106]

temperature	639°C		564 - 585°C				
%"$TiAl_3$" in layer	95	95	43	24	27	84	
starting material	TiAl	Ti(≤25%Al)	TiAl	Ti(≤25%Al)	Ti(25%Al)	*	
number of couples	1	7	3	10	1	3	
purity of Ti	99.7	99.7	99.7	99.7	99.97	*	
reflection							Brauer[106]
002	15	20	13	8	6	0	4
101	10	9	6	5	0	10	8
110	6	2	2	0	0	9	2
103,112	96	83	100	100	100	87	100
004	100	100	89	56	32	5	22
200	81	40	85	33	6	100	31
114,211	4	3	4	2	1	4	2
105	0	2	0	0	0	0	0.4
213	0	0.2	0	0	0	0	0.6
006,204	20	24	24	21	16	6	22
220	12	10	9	8	3	24	9
116,301	32	38	24	13	28	4	14
215,310	0	0.3	0	0	0	0	0.3
107,312,303	36	20	24	16	0	23	22
206,224	6	7	4	8	0	5	10

* In this column the results are tabulated for one couple Ti(25%Al)-Al annealed under the same conditions as the couple in the foregoing column, viz. 66 hours at 585°C and using Ti 99.97 in the preparation of the starting material. Besides, two couples Ti(10%Al)-Al, prepared using vapour metallising and heated at 585°C for 6 hours and 66 hours, respectively, have been added. In the latter two couples, Ti 99.7 has been used in the preparation of the starting materials. The resulting relative intensities for these three couples appeared to be equal.

TABLE 5.3

Relative intensities of the reflections of "Ti_8Al_{24}" formed at 564°C or 585°C, prepared in the vacuum or in the arc furnace. These intensities are compared with those for Ti_9Al_{23} given by Schubert et al[86].

% Ti_8Al_{24} in layer	57	82	73	20	
starting material	TiAl	Ti($\leqslant$25%Al)	Ti(25%Al)	Ti(25%Al)	
number of couples	3	13	1	1	
purity of Ti	99.7	99.7	99.97	99.97	
Reflection					$I^{86}_{rel.}$
008	14	5	5	0	VVW
101	0	0.5	0	0	0
103	2	5	0	0	VW
105	0	0.5	0	0	VVW
107	0	$<$0.2	0	0	0
110	0	8	6	6	VW
10$\underline{11}$	0.5	1	2	0	VVW
118	42	100	100	100	VVS
00$\underline{16}$	100	31	18	10	VS
200	34	62	11	94	VS
208	0	0.5	0	8	-
213	0	2	0	0	-
11$\underline{16}$	0	0.5	1	0	-
10$\underline{19}$	1	0.5	0	0	-
21$\underline{11}$	0	0.5	0	0	-
20$\underline{16}$	8	18	20	12	VS
220	1	24	12	12	S
11$\underline{24}$	17	11	14	0	S
318	8	21	8	23	S
22$\underline{16}$	2	9	22	8	S

In the summations the reflections at $2\theta = 39.13$ and $2\theta \cong 84.09$ have been omitted because at these values of 2θ two reflections of the two structures coincide.

(ii) When aluminium is applied by vacuum metallising, the occurrence of Ti_8Al_{24} at 585°C reduces considerably, as verified for two couples Ti(10%Al)-Al (see table 5.2).

(iii) Two couples Ti(25%Al)-Al annealed for 66 hours at 585°C and in which Ti 99.97 was used in preparing the starting alloy, have been investigated by means of X-ray diffraction. In one of them the amount of Ti_8Al_{24} was roughly the same as when Ti 99.7 was used in the alloy. In the other couple, however, a much smaller amount of Ti_8Al_{24} was found (see tables 5.2 and 5.3).

(f) In tables 5.2 and 5.3 the relative intensities of the observed reflections are represented for various circumstances and compared with those given in the literature. Our values are only rough estimates; each represents the mean value of the peak height of its corresponding reflection. Besides, there are two other factors which affect the significance of the observed relative intensities:

(i) The strongest reflections of the modifications "$TiAl_3$" and Ti_8Al_{24} practically coincide at $2\theta = 39.13$. Therefore, it is difficult to estimate the true intensity of the reflection for each structure separately, except for the case in which one of them is almost absent, e.g. at 638°C.

Therefore, the following procedure has been used in which it is assumed that the intensity of the reflection at $2\theta = 39.13$ is equal for both modifications. This assumption is the result of our experiments in which nearly pure modifications have been formed and which, indeed, showed the practically equal absolute intensity of the two reflections. The absolute intensity of the various reflections is then found by multiplying their peak height by $100/p$, in which p denotes the fraction of the modification in question formed in the diffusion couple, except for the coinciding reflections at $2\theta = 39.13$ and 84.09, which are given as measured.

After this, all intensities are normalised to obtain the relative intensities.

(ii) The intensities are given in separate columns since in some cases a pronounced texture is present in the diffusion layer. The occurrence of a texture has been confirmed with a texture goniometer for one couple TiAl-Al, annealed for 4 hours at 638°C. In fact, the reflection (004) was found to be much stronger in the direction of diffusion than in any other.

5.2. DIFFUSION COUPLES OF WHICH NEITHER STARTING MATERIAL IS PURE ALUMINIUM

5.2.1. Type Ti-TiAl (54%Al)

At first, the couples Ti-TiAl were prepared in the vacuum furnace, afterwards the arc furnace was used in order to investigate the influence of the preparation method on the diffusion process. Between 768-880°C one diffusion layer was formed, which it is possible to describe as Ti_3Al with a rather wide homogeneity range (see figs. 5.13 and 5.14). No solid solution of aluminium in titanium was detected, except for a small region round the site where a grain boundary of titanium met the Ti_3Al-layer (fig.5.13). Because of the large grain size in titanium relative to the width of the diffusion layer, this type of grain boundary diffusion hardly affected the overall layer growth. Above the transition temperature of 880°C the

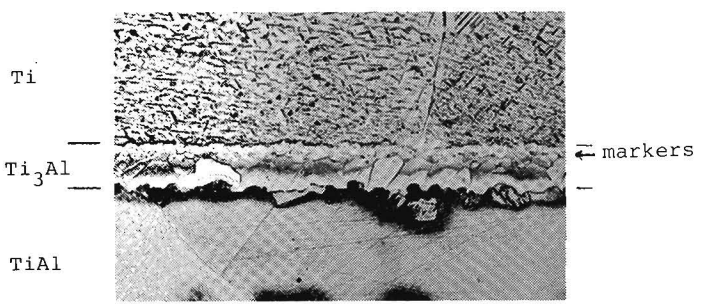

Fig.5.13. Ti(II)-TiAl diffusion couple, annealed for 163.5 h at 816°C. Thickness of the Ti_3Al layer is 17 μm.

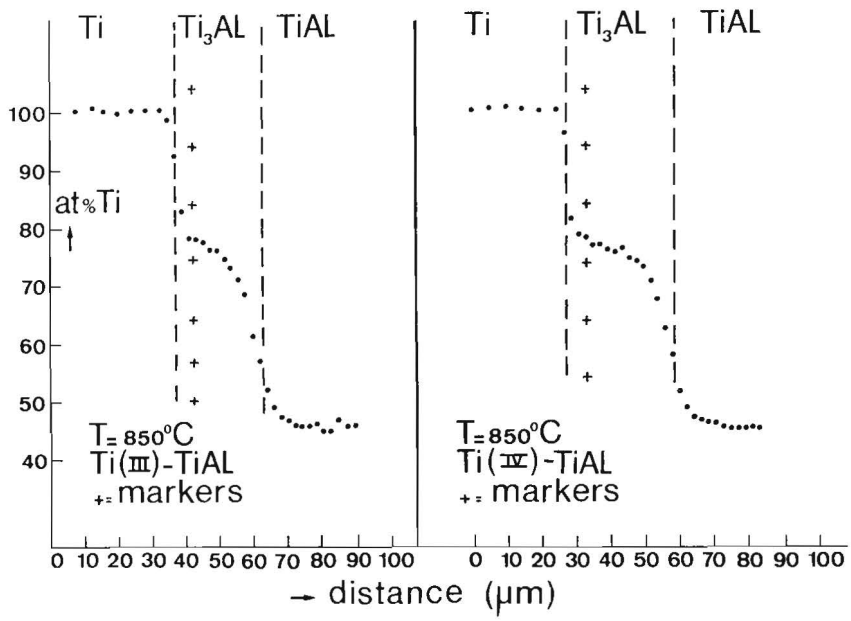

Fig.5.14. Penetration curves for Ti in Ti(III)-TiAl and Ti(IV)-TiAl couples, annealed for 303 h at 850°C.

situation was different. Then the phases β-Ti, α-Ti as well as Ti_3Al were formed in the diffusion couples, although the designation Ti_3Al was in this case, in fact, no longer justified (figs. 5.39 and 6.1). At 1200°C the α-Ti phase did not occur any more.

In TiAl a thin Ti-rich region was found. This was microscopically observed since the layer appeared as a striated zone after etching. These striated regions also occurred in the TiAl alloy after melting and it took very long annealing times at high temperatures to homogenise the alloy. Actually, in most cases these inhomogeneities were still present in the TiAl used in the diffusion couples. Heating at the relatively low temperatures used in this investigation hardly exerted any influence on the inhomogeneous appearance of the starting alloy. The thickness of the diffusion layer was not affected measurably by the rather small local variations in composition of the TiAl from which it was growing, as was to be expected from a theoretical point of view.

Using 10 μm Mo-wires, marker experiments proved titanium to be the faster moving component at the Kirkendall interface (see section 6.3.1.). Below 880°C, this interface was situated at a concentration of 78 at% Ti. Actually, it was visible without using markers, since the grains of the diffusion layer Ti_3Al on the Ti side of the interface were much smaller than those on the TiAl side (fig.5.13). Above 880°C, the markers were present in the Ti-rich solid solution. After some experience neither in this case were the Mo-wires necessary any longer, since a line of very small "grinding debris" marked the Kirkendall interface (fig.5.15).

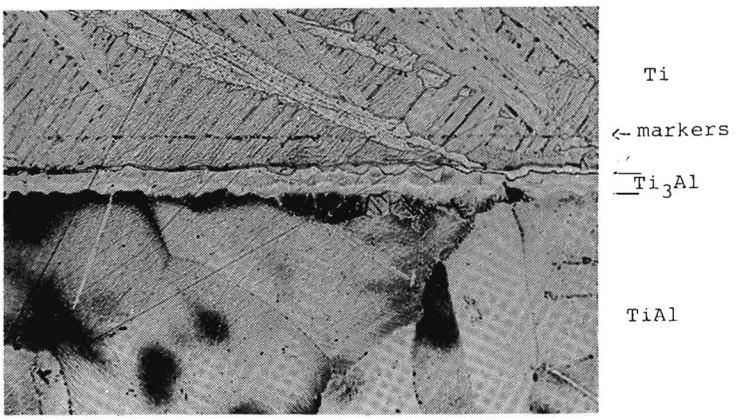

Fig.5.15. Ti(II)-TiAl diffusion couple, annealed for 15.25 h at 969°C. Thickness of layer "Ti_3Al" is 10 μm.

At first, the determination of the growth rate of the diffusion layer was obstructed by the presence of a 4-5μm thick Ti_3Al layer at time t = 0 as a result of the preparation of the couple in the vacuum furnace. Two methods have been used to overcome this difficulty:

(i) When using the vacuum furnace for the preparation as well as for the annealing of the couple, no problem arose. Whether the external pressure required during the first hour for assuring good contact, was present or not during further annealing, was immaterial for further layer growth.

(ii) When preparing the couples in the arc furnace, no initial layer was formed.

If the preparation period was included in the total diffusion time and both preparing and annealing temperatures were the same, the results for the couples in which a Ti_3Al layer was present at t = 0 agreed with those of the two methods mentioned above. If the temperatures differed, the "effective" duration of the preparation period was estimated on the basis of values at other temperatures. This rather rough estimation is permissible because of the relatively short corrections in time involved.

In figs.5.16-18 are given the results for the growth of the Ti_3Al layer for various methods of preparation and grades of titanium. The reproducibility is remarkable and in all cases the same time-dependence of the layer growth is found, viz., $d^{3.3} = kt$.

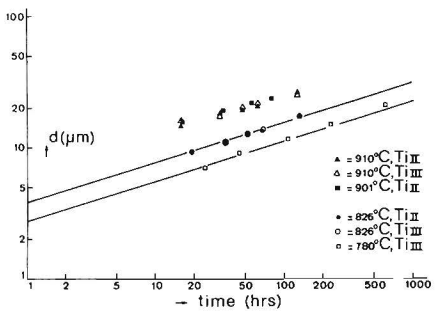

Fig.5.16. Plot of the logarithm of the layer width of Ti_3Al vs. log t for Ti-TiAl couples at various temperatures. Both Ti (II) and (III) have been used as starting material in the couples.

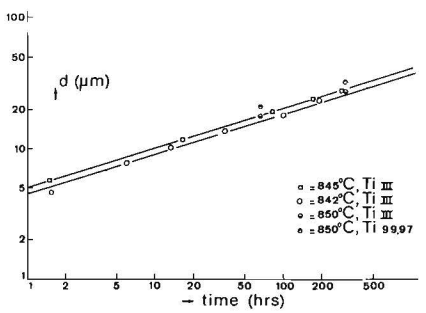

Fig.5.17. Plot of the logarithm of the layer width of Ti_3Al vs. log t for Ti-TiAl couples at various temperatures. Both Ti (III) and Ti (IV) = Ti 99.97 have been used as starting material in the couples.

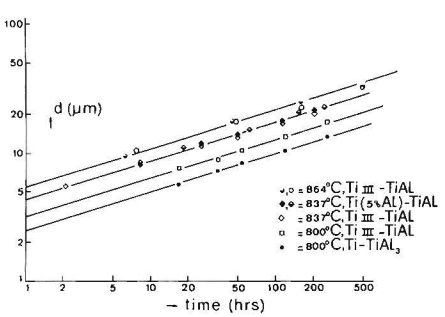

Fig.5.18. Plot of the logarithm of the layer width of Ti_3Al vs. log t for various couples and temperatures.

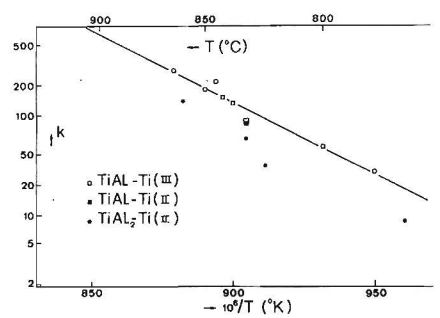

Fig.5.19. Plot of log k vs.1/T for the Ti_3Al layer in various couples. The penetration constant k is defined by $d^{3.3} = kt$.

In fig.5.19 and table 5.4 the temperature dependence of k is represented.

For temperatures above the transition point of 880°C the growth kinetics is determined quantitatively in only a few cases, mainly because of the irregularity of the diffusion layers (fig. 5.15). Up to 910°C the layer growth was measured and is found to follow the relationship $d^4 = kt$ (fig.5.16). In this case, the width of the solid solution in Ti was variable from 10 to 30 μm. At higher temperatures, the solid solution width grew rapidly and irregularly at the expense of the Ti_3Al layer, which was thinner than at 910°C.

The experiments discussed in this section were performed using Ti II and III. No significant difference between the two grades was found (see fig.5.16). In order to investigate the influence of impurities, one sandwich couple was prepared consisting of Ti IV-TiAl-Ti III, in which the alloy TiAl was prepared using Ti IV and Al I. The results for the growth of the Ti_3Al layer are given in fig. 5.17. Microprobe analysis demonstrated that solid solution of aluminium in both grades of titanium was not formed. Therefore, we may conclude, although there is a slight difference in layer thickness, that the general diffusion behaviour is essentially the same for both Ti III and Ti IV.

Another point which must be mentioned is the evaporation found to occur in the quartz capsules at temperatures < 800°C in all couples mentioned in section 5.2. This was visible because of the brownish colour of the quartz and the production of thin diffusion layers on the outside of the couples and on pieces of pure Ti being annealed together with the couple in the same capsule. Our measurements have probably not been affected by this phenomenon, since evaporation from the centre of the couple is very unlikely. Only at the ends of the diffusion layer a slight thickening was sometimes observed.

5.2.2. Types Ti(2½%Al)-TiAl and Ti(5%Al)-TiAl

The diffusion couples Ti(2½%Al)-TiAl and Ti(5%Al)-TiAl were made in the arc furnace. The observed layer growth of Ti_3Al agrees very well with the results given in section 5.2.1., as was to be expected (see in fig.5.18 the couples, heated at 837°C). Again, no aluminium penetrates the Ti-rich starting alloy (fig.5.20).

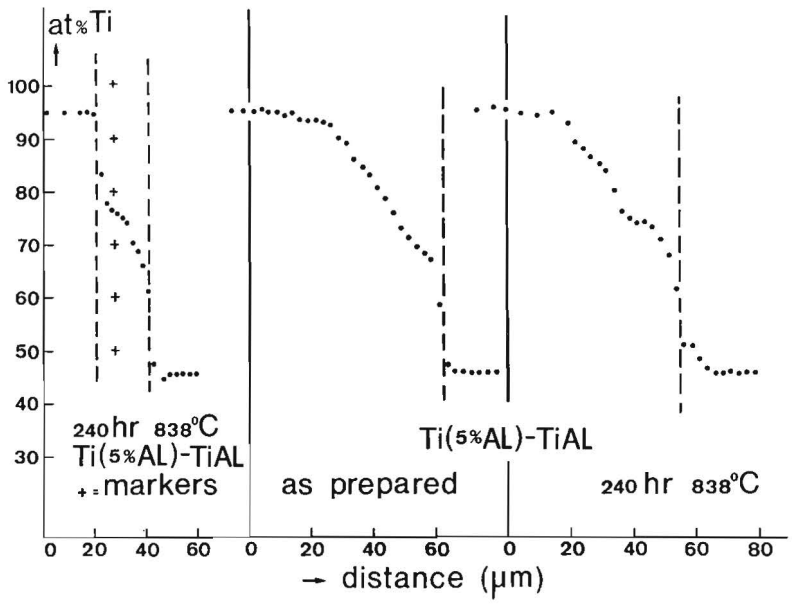

Fig.5.20. Penetration curves for Ti in Ti(5%Al)-TiAl couples. For a discussion of these experiments see section 5.2.2.

An interesting experiment was performed using a couple in which during the preparation a 40 μm thick solid solution in Ti(5%Al) was formed as a result of an accidental temperature rise. Microprobe analysis showed a smooth penetration curve in a concentration region in which, strictly speaking, a two-phase region ought to have formed during cooling. After annealing at 838°C for 240 hours, no change in thickness of the diffusion layer was detectable. The penetration curve, too,hardly showed any alteration, although a slight tendency to developing a phase boundary α-Ti—Ti_3Al might be concluded from fig. 5.20 . This experiment proves that at temperatures below the transition point of titanium diffusion proceeds very slowly in the Ti-rich solid solution and in the compound Ti_3Al.

5.2.3. Type Ti-$TiAl_2$

The couples Ti-$TiAl_2$ were made together with those mentioned in section 5.2.1.in a sandwich form: TiAl-Ti-$TiAl_2$. At temperatures below the transition point of Ti, two diffusion layers were formed,

viz., a thin layer of TiAl and a thicker one of Ti_3Al (see figs. 5.21 and 5.30). No solid solution of Al in Ti was found. In $TiAl_2$ a thin Ti-richer region may have formed but this could not be confirmed with certainty. Marker experiments proved that, again, Ti is the faster diffusing component.

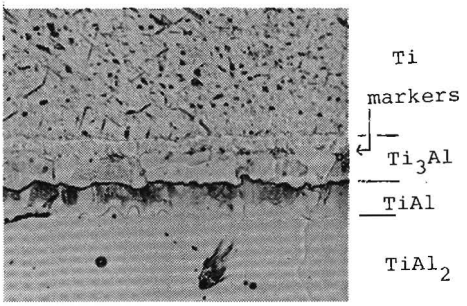

Fig.5.21. Ti(II)-$TiAl_2$ diffusion couple, annealed for 119 h at 818°C. Thickness of the total layer (Ti_3Al+TiAl) is 22 μm.

Concerning the growth kinetics of the two layers, the same remarks as given in section 5.2.1. may apply: the period during which the couple was prepared in the vacuum furnace must be included in the total diffusion time. In figs. 5.22 and 5.23 the results are given for various temperatures below 880°C. For the Ti_3Al layer the relation between thickness and diffusion time can be described in the same way as in the previous section, viz., $d^{3.3} = kt$. For TiAl this relation is found to be $d^{2.7} = kt$. The temperature dependence of k is given in figs. 5.19 and 5.24, respectively.

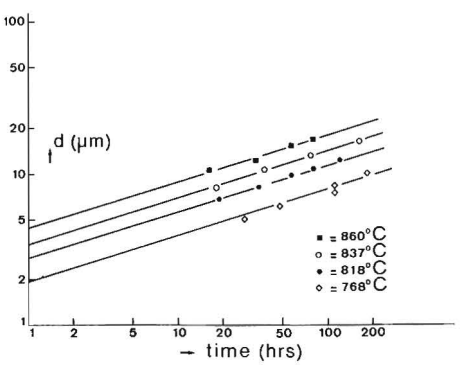

Fig.5.22. Plot of the logarithm of the layer width of Ti_3Al vs. log t for Ti(II)-$TiAl_2$ couples at various temperatures.

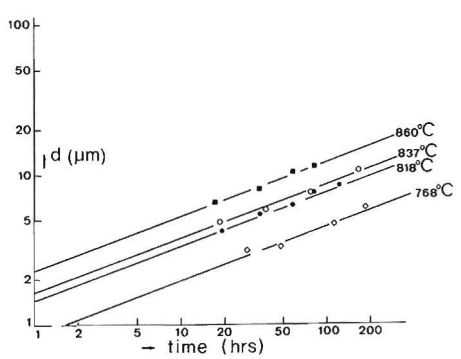

Fig.5.23. Plot of the logarithm of the layer width of TiAl vs. log t for Ti(II)-$TiAl_2$ couples at various temperatures.

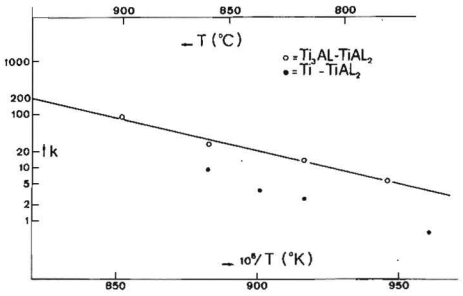

Fig.5.24 Plot of log k vs.1/T for the TiAl layer in Ti_3Al-$TiAl_2$ and Ti-$TiAl_2$ couples. The penetration constant k is defined by $d^{2.7} = kt$.

5.2.4. Type Ti-$TiAl_3$

The couples Ti-$TiAl_3$ were made by annealing Ti-Al couples at 625°C, in which process the Al is converted into $TiAl_3$. The method does not allow insertion of markers between Ti and $TiAl_3$. Three layers were formed after annealing below 880°C, viz., $TiAl_2$, TiAl and Ti_3Al (see fig. 5.25).

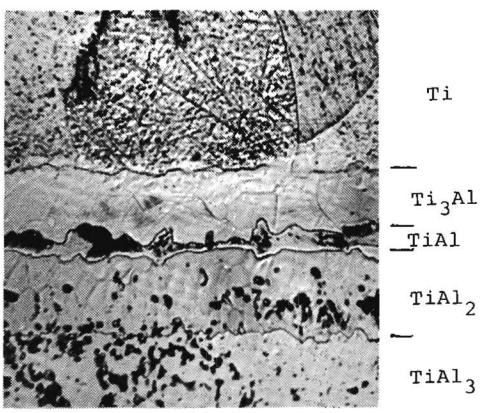

Fig.5.25. Ti(II)-$TiAl_3$ diffusion couple, annealed for 114 h at 870°C. Total layer thickness (Ti_3Al+TiAl+$TiAl_2$) is 43 μm.

The TiAl layer was the thinnest and the most irregular. Often it was very difficult to observe microscopically the boundaries between the three layers, especially between TiAl and $TiAl_2$. Because of this problem it was hardly possible to give accurate values of the layer width of the three layers separately. Therefore, in fig. 5.26 only the total thickness is given as a function of time. The time dependence of the total layer width is given by $d^{2.5} = kt$.

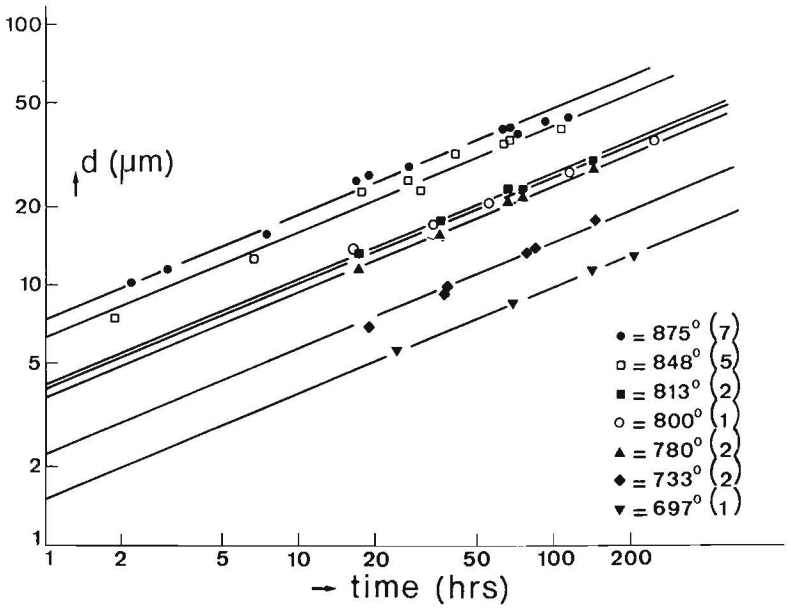

Fig.5.26. Plot of the logarithm of the total layer width (Ti_3Al+TiAl+$TiAl_2$) vs.log t for Ti(II)-$TiAl_3$ couples at various temperatures, given in °C. The numbers in brackets denote the numbers of couples from which the measuring points have been taken.

The temperature dependence of k is given in fig. 5.27 (see also table 5.4). The reproducibility is striking, the more so as the layer widths in question are small.

In our final experiments a couple Ti-$TiAl_3$ was heated together with a couple Ti-TiAl at 800°C and owing to our greater experience in etching techniques at that time, it appeared to be possible to measure the three layers in Ti-$TiAl_3$ separately. In fig. 5.18 the results show the same time relation for the Ti_3Al layer growth in the two couples. The growth of the $TiAl_2$ layer was also completely comparable with the results in couples using other starting materials and is represented in fig.5.28. The TiAl layer was too thin to obtain reliable results.

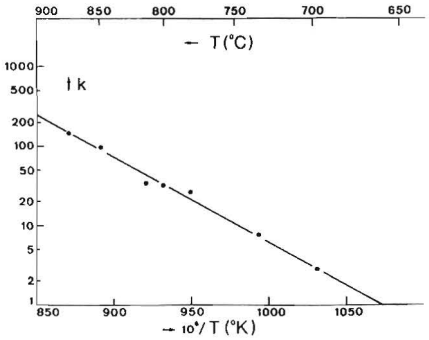

Fig.5.27. Plot of log k vs.1/T for the total diffusion layer in Ti-$TiAl_3$ couples. The penetration constant k is defined by $d^{2.5}=kt$.

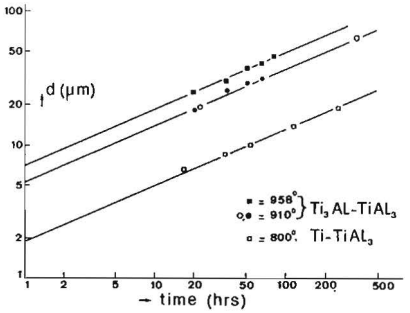

Fig.5.28. Plot of the logarithm of the layer width of $TiAl_2$ vs. log t for various couples and temperatures.

5.2.5. Type Ti_3Al-$TiAl_2$

The couples Ti_3Al-$TiAl_2$ were difficult to prepare because of the brittleness of $TiAl_2$.

Between 784-972°C one diffusion layer, TiAl, was formed as expected (figs. 5.29 and 5.30), showing the same kind of striation as mentioned in section 5.2.1. In Ti_3Al as well as in $TiAl_2$ hardly any change in concentration was found.

The markers at the Kirkendall interface were situated at 48±1 at%Ti.

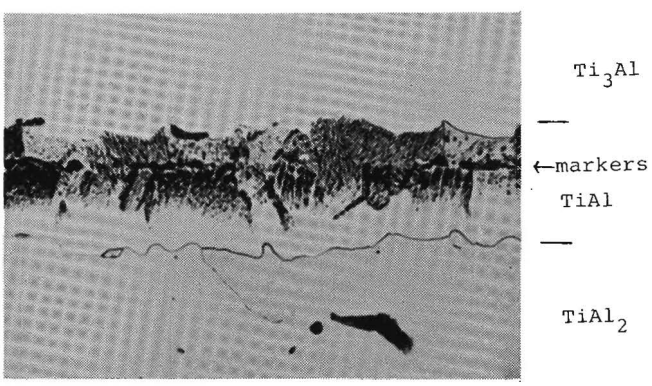

Fig.5.29. Ti_3Al-$TiAl_2$ diffusion couple, annealed for 98 h at 972°C. Thickness of the TiAl layer is 42 μm.

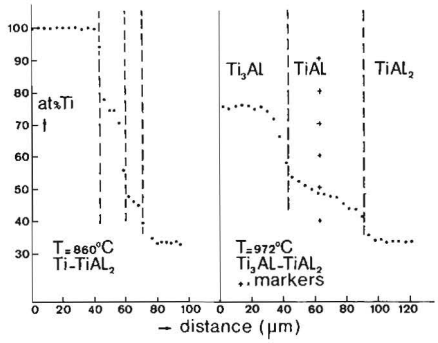

Fig.5.30. Penetration curves for Ti in a Ti(II)-$TiAl_2$ couple, annealed for 80 h at 860°C and Ti_3Al-$TiAl_2$ couple, annealed 98 h at 972°C. In the former case the "Ti_3Al" and "TiAl" layers were formed.

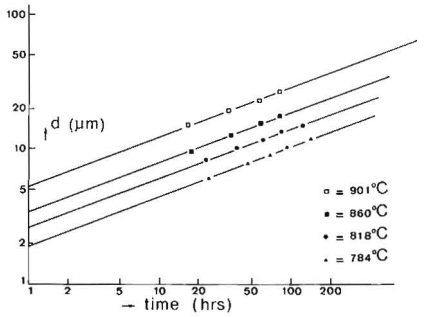

Fig.5.31. Plot of the logarithm of the layer width of TiAl vs. log t for Ti_3Al-$TiAl_2$ couples at various temperatures.

In fig. 5.31 the growth rate of TiAl is given for various temperatures. Following the same arguments as in section 5.2.1. the preparation period is included in the total diffusion time. The growth of the layer TiAl follows the relation $d^{2.7} = kt$.

In fig.5.24 a plot of log k vs. 1/T is represented and table 5.4 shows the data calculated from this plot.

5.2.6. Type TiAl(54%Al)-$TiAl_3$

The couples TiAl-$TiAl_3$ were prepared in the vacuum furnace in sandwich form together with those mentioned in the following section. The brittleness of $TiAl_3$ certainly did not facilitate processes like sawing and grinding, and the preparation of a perfect diffusion couple was difficult.

Between 784-958°C one single diffusion layer, viz.$TiAl_2$, was found (fig.5.32). A typical penetration curve is given in fig.5.33. The Kirkendall interface is situated near the middle of the layer (see section 6.3.2.). The growth rate of the $TiAl_2$ layer is represented in fig. 5.34. The relationship between thickness d and time t can be described as $d^{2.4} = kt$.

In fig. 5.35 a plot of log k vs.1/T is given; table 5.4 shows the data calculated from this plot.

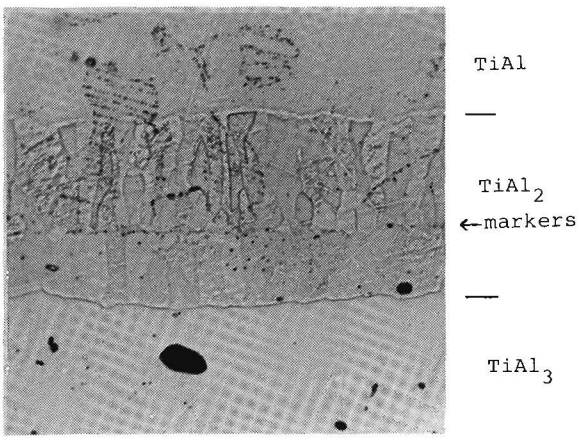

Fig.5.32. TiAl-$TiAl_3$ diffusion couple, annealed for 81 h at 958°C. Thickness of the $TiAl_2$ layer is 56 μm.

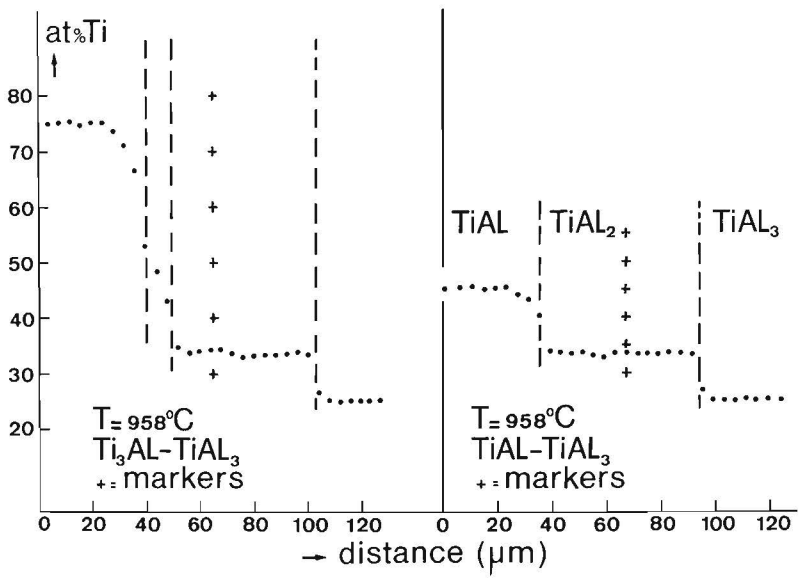

Fig.5.33. Penetration curves for Ti after 81 hours annealing at 958°C for a Ti_3Al-$TiAl_3$ couple (where the layers TiAl and $TiAl_2$ were formed) and a TiAl-$TiAl_3$ couple.

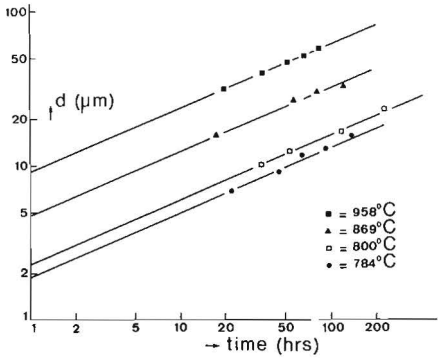

Fig.5.34. Plot of the logarithm of the layer width of $TiAl_2$ vs. log t for TiAl-$TiAl_3$ couples at various temperatures.

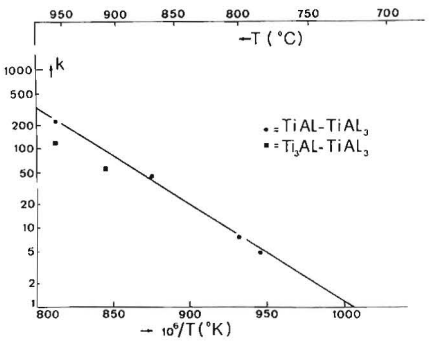

Fig.5.35. Plot of log k vs.1/T for the $TiAl_2$layer in TiAl-$TiAl_3$ and Ti_3Al-$TiAl_3$ couples. The penetration constant k is defined by $d^{2.4} = kt$.

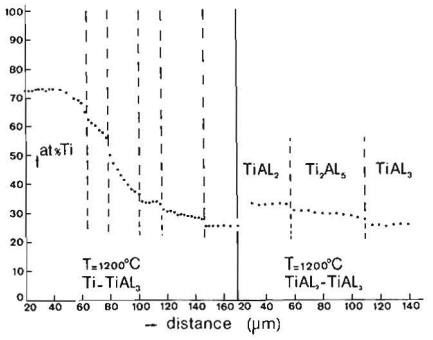

Fig.5.36. Penetration curves for Ti in a Ti(25%Al)-$TiAl_3$ and a $TiAl_2$-$TiAl_3$ couple, annealed for 23 h at 1200°C. In the former case, the phases occurring in the couple after annealing are from left to right: ß-Ti,"Ti_3Al", "TiAl", $TiAl_2$, Ti_2Al_5 and $TiAl_3$.

At 1200°C a new compound was formed between 27.5 and 30.5 at%Ti, probably the same as the compound Ti_5Al_{11} reported by Schubert et al.[86] (see fig.5.36). No further investigations on this compound have been carried out.

5.2.7. Type Ti_3Al-$TiAl_3$

Between 800 and 958°C two diffusion layers in the couples Ti_3Al-$TiAl_3$ were formed viz., TiAl and $TiAl_2$ as shown in figs.5.33 and 5.37. Grinding debris again marks the Kirkendall interface, situated in the $TiAl_2$ layer.

The TiAl layer was much thinner and showed a striated appearance. The growth rate of TiAl was not determinable with sufficient accuracy; that of the $TiAl_2$ layer can be described by (see fig.5.28) $d^{2.4} = kt$.

In fig.5.35 a plot of log k as a function of 1/T is represented. At 1200°C the compound between 27.5 and 30.5 at%Ti was again found.

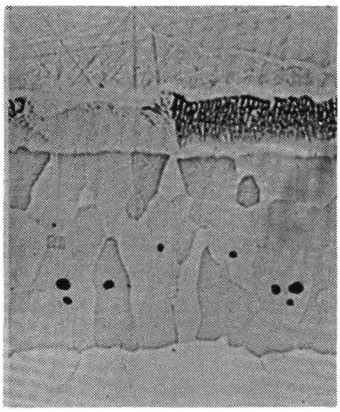

Fig.5.37. Ti_3Al-$TiAl_3$ diffusion couple, annealed for 349 h at 910°C. Thickness of the total layer (TiAl+$TiAl_2$) is 81 μm.

5.2.8. Couples in which only one phase boundary occurs

In order to determine the concentration at the phase boundaries more accurately, a number of couples were investigated in which only one phase boundary was present. Figs. 5.38 and 5.39 show the penetration curve for some of these couples. Generally, no marked difference in concentration at the boundaries was found between these couples and those in which a new phase was formed (see fig.6.1).

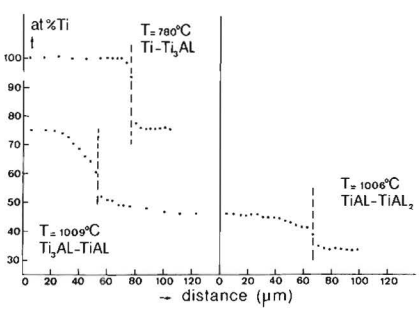

Fig.5.38. Penetration curves for Ti in the following couples: Ti-Ti_3Al, annealed for 143 h at 780°C, Ti_3Al-TiAl, 143 h at 1009°C, and TiAl-$TiAl_2$, 136 h at 1006°C.

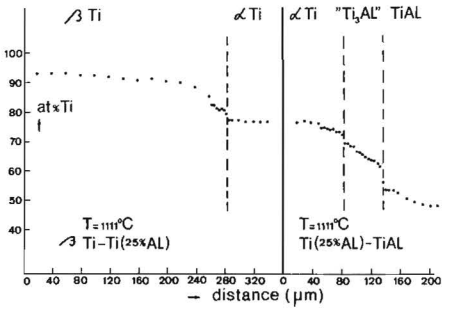

Fig.5.39. Penetration curve for Ti in a Ti-Ti(25%Al)-TiAl sandwich couple, annealed for 94 h at 1111°C.

5.3. REMARKS ON THE VALUES OF THE PENETRATION CONSTANT k AND THE ACTIVATION ENERGY Q AS REPRESENTED IN TABLE 5.4

Because of the non-parabolic layer growth found in most of the couples, the dimensions of the penetration constant k are cm^n/sec instead of the customary cm^2/sec.

When writing the relation between layer thickness and time in the form $d = k' t^{1/n}$ and, consequently, $k' = k'_o e^{-Q'/RT}$, it is clear that $Q' = Q/n$.

As may be seen from table 5.4 the value of Q is variable between 65.5 and 49.0 kcal for couples of which Al is no starting material. On the other hand, the value of Q/n is the same for all these couples within the experimental error. At the moment we do not know whether the constancy of Q/n is purely accidental or not.

TABLE 5.4

Results of the layer growth in various diffusion couples.
The layer width d follows the relation $d^n = kt$; the penetration contant k can be described as $k_o e^{-Q/RT}$ (see section 5.2.9.)

couple	temp. range °C	layer	n	$^{10}\log k_o$ (cm^n/sec)	Q kcal	Q/n kcal	reference to figs.
Ti-Al	580-640	$TiAl_3$	1.1±0.1	+2.6 ±0.4	42.9±1.4	38.3±4.0	5.1 and 2
TiAl-Al	516-640	$TiAl_3$	2	-2.9±0.3	22.7±1.2	11.4	5.9 and 11
Ti-TiAl	768-880	Ti_3Al	3.3±0.3	-1.9±1.1	65.5±5.2	-9.7±2.6	5.16 - 19
Ti-$TiAl_2$	768-880	Ti_3Al	3.3±0.3				5.22
		TiAl	2.7±0.3				5.23
Ti_3Al-$TiAl_2$	784-972	TiAl	2.7±0.3	-2.2±0.9	56.0±4.5	20.6±3.1	5.24 and 31
TiAl-$TiAl_3$	784-958	$TiAl_2$	2.4±0.3	-0.8±0.5	57.0±2.6	23.4±3.1	5.34 and 35
Ti_3Al-$TiAl_3$	800-958	$TiAl_2$	2.4±0.3				5.28
Ti-$TiAl_3$	700-875	Ti_3Al+ TiAl+ $TiAl_2$	2.5±0.3	-2.1±0.4	49.0±2.0	19.6±2.6	5.26 and 27

CHAPTER VI

EVALUATION OF THE EXPERIMENTAL RESULTS

6.1 PHASE DIAGRAM OF THE Ti-AL SYSTEM

In fig. 6.1 the phase diagram as determined by our polyphase diffusion experiments is shown. Despite the rather inaccurate results respecting the concentrations at some boundaries, particularly the Ti_3Al-(Ti_3Al + TiAl) boundary, the diagram seems reliable.

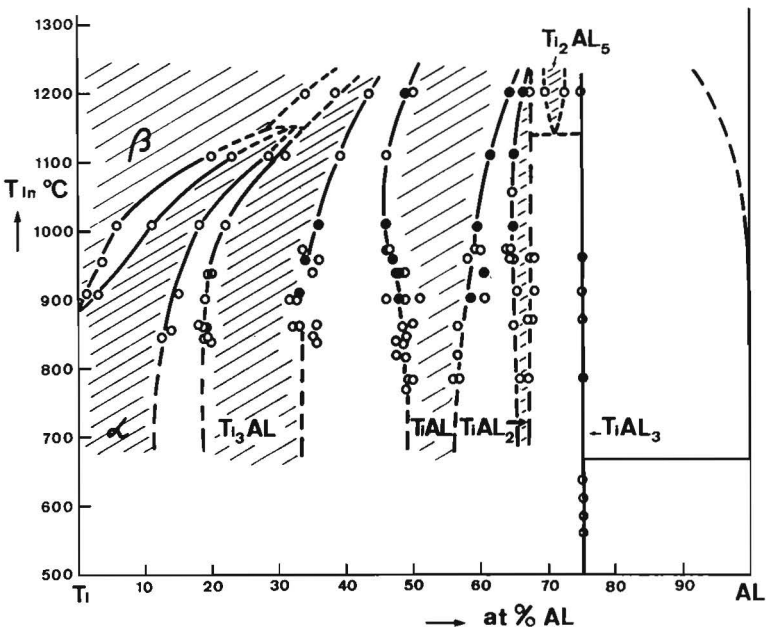

Fig.6.1. Tentative phase diagram of the Ti-Al system, determined by means of the diffusion couple technique in the present investigation. Black dots denote concentration measurements at phase boundaries in couples in which no new phase has been formed, e.g. in Ti_3Al-TiAl at 1009°C. Open circles denote concentration measurements at phase boundaries in couples in which one or both phases in question were formed during diffusion annealing.

In the Ti-rich region it agrees remarkably well with the results of Blackburn [78]. Both the shape of the homogeneity regions and the very slow diffusion process at temperatures below the transition point of Ti, are probably responsible for the large differences between the findings of the various investigators. It is, for instance, clear from fig.6.1 that at 950°C the phase "Ti_9Al" exists, at 1000°C the phase "Ti_6Al" and at 1075°C the phase "Ti_2Al". In actual fact, however, Ti_9Al and Ti_6Al are identical with α-Ti, while Ti_2Al corresponds with the "Ti_3Al" phase. Because of the slow diffusion it is very well possible that a phase formed at a higher temperature does not attain its equilibrium structure on annealing at a lower temperature and remains in a metastable state.

Concerning the homogeneity range of the TiAl-phase it seems justifiable to assume that the Ti-rich boundary at temperatures below 750°C is situated at a content of approximately 50 at% Ti. This follows from the shape of the boundary in fig. 6.1 as well as from the clear two-phase appearance of an alloy containing 50-54 at% Ti (see section 5.2.1.).

The $TiAl_2$ phase offers no problems and occurs in all suitable couples, showing a very small homogeneity range.

The phase "Ti_5Al_{11}", reported by Schubert et al.[86], is present at 1200°C between 27.5 and 30.5 at% Ti and might therefore better be described as "Ti_2Al_5". The homogeneity range has not been further investigated, neither has its crystal structure.

The occurrence of two modifications of the $TiAl_3$ phase has already been discussed in section 5.1.6. It is not quite clear yet under what conditions each modification exists. If there at one fixed temperature a transition is involved, no „mixed" layers containing both structures would be possible. It seems propable, therefore, that there is a certain transition range, maybe under the influence of impurities. It is well known that AB_3 structures, like $TiAl_3$, are very sensitive to impurities affecting the electronic configuration [86,107-110].

Another possibility is that there is actually a sharp transition temperature between the two phases, but that in diffusion couples these phases are stable in the "forbidden" temperature range for energetic reasons. The latter may be found in surface energy or strain contributions as mentioned in section 2.4.2., possibly influenced by a texture that might favour an actually unstable phase.

Once formed, the modifications do not transform into the equilibrium structure, probably because of the low temperatures involved.

This will also be the reason why the "low-temperature" modification has not been found up to now by others: in all former investigations the temperature at which the phase was formed, was higher than say 640°C and therefore only the"high-temperature" phase was found.

The solubility of Ti in solid Al is so small that microprobe analysis could not be used in determining it. This means that the solubility is probably below 10^{-3} at% Ti.

6.2. DIFFUSION COUPLES OF WHICH ONE OF THE STARTING MATERIALS IS PURE ALUMINIUM

6.2.1. Discussion of the results

When we first direct our attention to the experiments in which the customary diffusion behaviour holds, we have to start with the TiAl-Al couples, in which the diffusion layer grows according to the parabolic law.

When calculating the diffusion coefficient for the $TiAl_3$ phase in these couples, we must use the equation (35) as given by Wagner[24] since we have to do with a line-compound. In the present case, the equation can be simplified considerably, there being no concentration gradient in the adjacent phases. Then, Eq.(35) reduces to:

$$D_{int.} = \int_{N_i(\gamma')}^{N_i(\gamma'')} D \, dN_i = \frac{(N_i(\gamma)-N_i^-)(N_i^+-N_i(\gamma))}{(N_i^+-N_i^-)} \left(\frac{d_\gamma^2}{2t}\right)$$

When substituting $k = d_\gamma^2/t$, we obtain:

$$D_{int.} = \frac{(N_i(\gamma)-N_i^-)(N_i^+-N_i(\gamma))}{(N_i^+-N_i^-)} \left(\frac{k}{2}\right)$$

In TiAl(54%Al)-Al this equation yields:

$$D_{int.} = 6.87 \, k$$

In fig.6.2 the logarithm of the integrated diffusion coefficient is plotted vs.1/T. It also shows the integrated coefficients for some other couples in which a parabolic growth rate occurs. These values are found on the same line of argument as above:

for Ti(25%Al) : $D_{int.} = 8.33$ k
for Ti(10%Al) : $D_{int.} = 9.03$ k
for Ti(5%Al) : $D_{int.} = 9.21$ k
for pure Ti : $D_{int.} = 9.375$ k

From fig.6.2 it can be concluded that the integrated diffusion coefficient obeys Arrhenius' rule:

$$D_{int.} = 8 \times 10^{-3} e^{-22700/RT} cm^2/sec$$

when only the TiAl-Al couples are involved, and

$$D_{int.} = 7 \times 10^{-3} e^{-22600/RT} cm^2/sec$$

when the results of the other couples are included. The accuracy of the activation energy is $\pm$ 1200 cal; the frequency factor has a value between 2×10^{-3} and 16×10^{-3} cm^2/sec (see table 5.4).

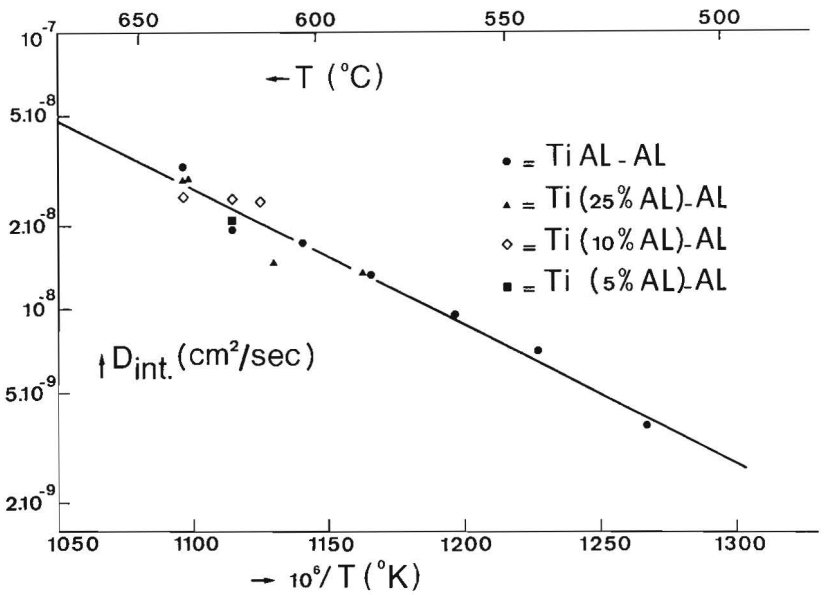

Fig.6.2. Plot of the logarithm of the integrated diffusion coefficient for the $TiAl_3$ layer vs.1/T for various couples.

The values for the activation energy as well as for the frequency factor are low. As discussed in section 2.6., this is a strong indication for the presence of grain boundary or, more generally, short-circuit diffusion. The indication is still corroborated by the very small grains formed. Another explanation of the low values for the activation energy and frequency factor might be the very fast diffusion along a lattice direction with an abnormally high vacancy concentration as proposed by Kidson et al.[111] and Heumann et al.[112-114]. In the present case this seems less probable in view of the very small grains in the layer and the lack of an unambiguously clear texture in the diffusion layers. Besides, we feel that Kidson's as well as Heumann's results can equally well be explained by the contribution of grain boundary diffusion.

In section 2.4.2. the reasons have been discussed why not all the layers predicted by the phase diagram necessarily occur in a diffusion couple. In the present case it appears that the formation of only one phase, $TiAl_3$, arises from kinetic causes, as is verified by the following experiment. A Ti-$TiAl_3$ couple was annealed at 800°C in order to create the interjacent phases Ti_3Al, TiAl and $TiAl_2$. Then, a plate of pure Al was joined on to the outside of the remaining $TiAl_3$ layer and the following situation was achieved: Ti-Ti_3Al - TiAl - $TiAl_2$ - $TiAl_3$ - Al. This system was then annealed at 625° for 15 hours. The interjacent layers (total thickness 12 µm) were found to have completely vanished, and the situation was changed to Ti-$TiAl_3$-Al. This proves that difficulties in nucleation of one of the interjacent phases cannot be the cause of their absence in the diffusion couples in question. Obviously, diffusion in the $TiAl_3$ phase is very much faster than in the interjacent phases, and therefore these are present in only immeasurably small layers.

Let us now discuss the deviations from the normal diffusion laws which we have found in couples, using Al as one of the starting materials. The facts which must be explained are (see section 5.1.):

(a) the existence of an initial linear growth period,
(b) the occurrence of inclusions of pure Al in the $TiAl_3$ layer during this period,
(c) the dependence of the duration of the period of linear growth on the composition of the starting material,
(d) the dependence of the duration of this period on the method of preparation of the couples,

(e) the dependence of the linear growth rate on the composition of the starting material,
(f) the formation of the row of pores which mark the change-over between the linear and the - much faster - parabolic growth.

In addition, experiments in our laboratory on diffusion the Ti-Ni system by Bastin[57] and the Ni-Al system by Janssen[115,116] using the same quality Ti an Al as in the present work, do not show the phenomena described above, and the normal diffusion laws are found to be valid.

On the other hand, the interdiffusion experiments by Kidson et al.[111] between pure Zr and Al show some agreement with our work. They found that $ZrAl_3$ was the only phase formed during diffusion, and also that a row of pores in the $ZrAl_3$ layer was formed near to the $ZrAl_3$-Al boundary. Besides, the growth of the layer was irregular, very fast, and dropped at longer annealing periods. Their results, however, are too inaccurate and their article is too vague to compare their experiments in more detail with ours. The same remarks can be made on the paper of Tiwari and Sharma[117] on diffusion in the Zr-Al system.

Finally, it is known from experiments of Mackowiak and Shreir[118,119] that diffusion between Ti and Al at temperatures above the melting point of Al results in a layer growth directly proportional to time. The diffusion layer consists of both $TiAl_3$ and Al particles as in our experiments, but in their case the Al-percentage is larger.

The most obvious explanation of the phenomena observed in our experiments is the presence of a thin oxide film on the surfaces of Al and/or Ti which are pressed together during the preparation of the couple. Then, Al penetrates this film (marker experiments!) and reacts with Ti to form $TiAl_3$. We will examine whether this assumption accounts for the facts mentioned before.

Ref.(a) It is possible that the rate of formation of the $TiAl_3$ phase is determined by the chemical reaction between Ti, Al and the obstructing oxide scale. If so, the layer growth is linearly dependent on time. It is also possible that the penetration of Al through the oxide film is rate-determining. Since the effect has not been found in e.g. Ni-Al diffusion experiments[116], the oxide film must then

be present on the surface of the Ti or the Ti-rich alloy, as is also concluded from item (c). From this point of view, the much smaller Ni-atoms in Ti-Ni diffusion couples cross the scale in question without much difficulty.

Ref.(b) It is possible that parts of the Al, enveloped by some kind of oxide scale, are enclosed in the growing $TiAl_3$ layer. The fact that oxygen causes locally a ternary system may also give rise to the two-phase region which is formed.

Ref.(c) The starting alloys might be coated with an oxide film which is thicker as the Al content rises from 0 to 25at%,and which is practically absent or inactive when TiAl is involved.

Ref.(d) This is most obvious for pure Ti, when preparing the couples by hot dipping or cold pressing on the one hand and in the vacuum or arc furnace on the other hand. It is possible that the oxide film thickens during preparation in the former two methods, or that the film is partly removed during the latter methods.

Ref.(e) Because of the Al content already present, Ti(25%Al) will form a layer of $TiAl_3$ which is 1.125 times as thick as when pure Ti is used, when the same supply of free Al is present. However, this is not enough to account for the rather large differences as shown in fig. 5.2. Perhaps, the oxide film on Ti(25%Al) is more permeable to Al than the film on pure Ti. It is also possible that the chemical reaction mentioned at Ref.(a) is faster in the case of Ti(25%Al).

Ref.(f) At a certain moment the oxide scale is saturated with Al and breaks down. The Al, present in the $TiAl_3$ layer, diffuses rapidly to the liberated Ti or alloy surface; the $TiAl_3$ particles in the layer stick together and the spaces previously filled with Al combine to form an interface of pores, parallel to the contact interface.

A point which cannot be satisfactorily explained is the very short linear period found when the layer on the Ti-rich alloy is formed by surface diffusion (see section 5.1.2.), since the obstructing oxide film must then be present, too. It is possible that in this case the fast flowing Al "rolls up" the oxide scale, since the direction of arrival of free Al atoms is parallel to the surface of the alloy instead of perpendicular to it, as in a normal diffusion couple.

When looking for other possible explanations of the abnormal growth behaviour of the $TiAl_3$ layer one could think of the influence of impurities, present in the starting material. In that case, this influence would terminate when the break-through to parabolic time dependence occurs. Experimental verification of this influence is possible by heating a couple under such conditions that the break-through arises. Then, the whole $TiAl_3$ layer is abraded in such a way that a fresh surface of the alloy is just liberated. A new plate of Al is then joined to this surface and the growth rate determined once more. Exactly the same time dependence is found as before: an equally long linear period, followed by break-through and the parabolic period. This proves that impurities have nothing to do with the deviations in question.

Finally, a third possibility may be mentioned, viz., difficulties in nucleation of the $TiAl_3$ layer, perhaps caused by:

(i) the entirely different structures of $TiAl_3$ and Ti or the Ti-rich alloy (in contradiction to the closely resembling structures in TiAl-Al couples!),
(ii) differences in molar volume,
(iii) the presence of a transition temperature between two $TiAl_3$ modifications in the vicinity of the diffusion annealing temperature.

This assumption, however, is not very likely since then especially item (d) cannot be explained. Besides, in Ti-Al couples the linear period is found to be very short when using the vacuum or arc furnace for preparation purposes, while differences in molar volume between $TiAl_3$ and Ti are larger than e.g. between $TiAl_3$ and Ti(25%Al) (see fig.3.5).

Mackowiak and Shreir[119], on the other hand, use this possibility of rate-determining reaction between Ti and Al to explain the linear layer growth found by them. However, the circumstances in their experiments are quite different from those in ours, since they used molten Al and therefore higher temperatures in their experiments. The effect of thin oxide film will then probably be much smaller and diffusion proceed much faster. The low values of the activation energy for the process found by them (23000 cal/mole) might indicate that the mechanism is indeed different from that found by us in which the activation energy is nearly twice as much. (Actually, this criterion

cannot be simply applied because of the different physical state of the Al involved).

Heumann and Dittrich[112] also mention the possibility of difficulties in nucleation of the Fe_2Al_5phase as a reason for the "incubation period" in the growth of the layer in an Fe-Al diffusion couple. They support this conclusion by experiments on heavily worked starting materials, which indeed showed layer growth starting at a lower temperature than when undeformed materials were used. This effect of deformation on the diffusion behaviour was not found in our experiments, as is demonstrated by the same results obtained with Ti-Al couples when using either the hot-dip or the cold-pressing method. In the latter, the plate of Ti is heavily deformed, in the former, Ti is in the annealed condition.

6.2.2. Conclusions from section 6.2.

Diffusion experiments carried out below 640°C in which Al is one of the starting materials have shown that only one phase develops, viz. $TiAl_3$. Two modifications of this compound are found to exist, the already known "high-temperature" phase and a hitherto unknown "low-temperature" modification. The latter can be described as a superstructure of the high-temperature phase with a c-parameter four times as long.

Layer growth obeys the parabolic time dependence for the TiAl-Al couples. When using Ti-richer starting materials, an initial layer is formed which grows linearly with time. The duration of the linear period and the rate of the layer formation have been investigated. The existence of this period is assumed to be caused by a more or less thin film of oxide scale on the surface of Ti or the Ti-rich alloy. The change-over between the linear and the subsequent parabolic period is marked by a row of pores parallel to the contact interface.

The low values of diffusion coefficient and activation energy in the parabolic growth period indicate that grain boundary diffusion is the dominant mechanism in the mass transport through the $TiAl_3$ layer. Marker experiments have proved that Al is the only diffusing component in this transport.

6.3. DIFFUSION COUPLES OF WHICH NEITHER STARTING MATERIAL IS PURE ALUMINIUM

6.3.1. Couples in which Ti is one of the starting materials

Below the transition temperature of Ti, diffusion in couples as referred to in the heading, is characterised by two facts, viz., the absence of a solid solution of Al in Ti and the non-parabolic growth of the phases arising.

Concerning the first mentioned fact one might in the first place think of the influence of an oxide film as mentioned in the previous section. However, we feel that the assumption of such scale gives no explanation of the absence of the solid solution of Al in Ti. This follows from the fact that in couples in which a solid solution is already formed by raising their temperature, annealing at temperatures below 880°C produces no further extension of the layer of solid solution (see section 5.2.2. and fig.5.20). We therefore believe that the absence of the solid solution is caused by an abnormally low volume diffusion coefficient in this phase.

The conclusion of low diffusivity of Al in α-Ti is in sharp disagreement with the findings of Goold[120]. He claims for the diffusion couple Ti(6.9%Al)-Ti(13.4%Al) at 834°C a frequency factor of 1.6×10^{-5} cm^2/sec and an activation energy of 23700 cal. This indicates a diffusion zone of about 200 μm. Goold himself, however, doubts of the accuracy of his own measurements, and we feel he is right, since his method of preparation of the couples is very questionable. In our opinion, the diffusion zone claimed by him may have been formed as a result of the preparation of the couple.

The values for D_o and for the activation energy for self-diffusion in α-Ti as reported in the literature are very low[121-123]. Indications for grain boundary diffusion in these experiments are present. Further, diffusion in α-Zr shows the same diffusion charactistics, as follows from a review made by Kidson[124]. He supposes the short-circuit effects also to be present in most of the experiments described by him.

The second characteristic point is the growth of the Ti_3Al layer in accordance with $d^n = kt$, in which n is 3.3 in all the couples

investigated (also when different starting materials are used).

The most obvious explanation is a considerable contribution of grain boundary diffusion in the material transport through the Ti_3Al layer. This gives rise to enhanced growth in the first stage of annealing since then the grains in the layer are small. When the diffusion duration increases, the grains will grow, leading to a reduced contribution of grain boundary diffusion, which eventually becomes negligible after very long annealing times. This model will indeed cause time-dependence as has been found in the couples in question.

We strongly feel that this model holds in principle for most polyphase diffusion measurements. Sometimes, the devations from the parabolic time dependence will be clearly observable. In other cases, however, this may be difficult as e.g. in our experiments. Because of the small layer widths involved, a plot of the square of layer width vs. time often gives a reasonably straight line, intersecting the ordinate at some initial thickness. Especially when an initial layer thickness (as in couples prepared in the vacuum furnace) is indeed found experimentally, it is difficult to check whether the parabolic time dependence is real or not. Actually, in our investigations we have for a long time considered the growth rate to follow the parabolic time law; as recently as when the new preparation and annealing methods were introduced (see section 5.2.1.) we found that our assumption was not justifiable.

The model for layer growth referred to above resembles closely the theory, proposed by Meyering et al.[125] on the oxidation kinetics in the case of ageing CuO films on Cu_2O. The experimental methods of checking the correctness of the model is more difficult in our case and, in fact, impossible in view of the very low diffusivity which occurs if only volume diffusion is at hand. The low activation energy found by us supports the model, since the ageing of the layer proceeds faster with increasing temperature, thus effectively opposing the faster short-circuit diffusion process.

In the literature only a few data are given on polyphase diffusion in which α-Ti is one of the starting materials. We have come across experiments on the Ti-Ag system[126-128] demonstrating the same diffusion behaviour as in our couples: layer growth of TiAg and Ti_3Ag according to $d^n = kt$, in which $n > 2$, and probably absence of a solid solution of Ag in Ti.

Concerning the mobility of the two components with respect to each other at the Kirkendall interface, it is clear that Ti is the more mobile one. Assuming that the molar volume is constant in the Ti_3Al layer (no data are available in the literature), Eq.(17) can be used in a simplified form to obtain a value for the factor D_{Ti}/D_{Al} at the Kirkendall interface. Since parabolic time dependence does not apply, this ratio is not a material constant and has no general value. It must be considered a description of the mobilities of the two components in the particular couples under discussion.

Using Eq.(17) in the form

$$\frac{D_{Ti}}{D_{Al}} = \frac{N_{Ti}^{+}\int_{-s}^{x_m}(N_{Ti}-N_{Ti}^{-})\,dx - N_{Ti}^{-}\int_{x_m}^{+s}(N_{Ti}^{+}-N_{Ti})\,dx}{N_{Al}^{+}\int_{-s}^{x_m}(N_{Al}-N_{Al}^{-})\,dx - N_{Al}^{-}\int_{x_m}^{+s}(N_{Al}^{+}-N_{Al})\,dx}$$

we find for the couples in figs.5.4 and 5.20 the values for D_{Ti}/D_{Al} as given in table 6.1. Within the temperature range stated in the table, no significant differences in this ratio occur.

6.3.2. Diffusion couples of the types Ti_3Al-$TiAl_2$, $TiAl$-$TiAl_3$ and Ti_3Al-$TiAl_3$

The results of layer growth in the couples mentioned in the heading agree in at least one point, viz., their non-parabolicity. The reason must be the same as mentioned in the previous section: a smaller or larger contribution of grain boundary diffusion in the mass transport, probably steadily decreasing with increasing diffusion duration. A conspicuous aspect is the constancy of the power n in the relation $d^n = kt$ for each layer, independent of the starting materials. Apparently, the importance of grain boundary diffusion is the same in all cases, which means that the ratio between layer thickness and mean grain radius is not dependent on the starting materials. Because of the thinness of the layers and consequent delicate etching process, this is difficult to verify quantitatively.

The mobilities of the two components in the various couples at the Kirkendall interface can be determined in the same way as in the previous section. The values of D_{Ti}/D_{Al} for the couples in

figs.5.30 and 5.33 are given in table 6.1. They are roughly constant within the given temperature range. As is understandable on account of the closely resembling structures of $TiAl_2$ and $TiAl_3$, this ratio is the same for both phases, viz., Al is the only diffusing component. In TiAl, Al is roughly three times as mobile as Ti, whereas in Ti_3Al, Ti is by far the most mobile component.

TABLE 6.1

Values of D_{Ti}/D_{Al} at the Kirkendall interface in various couples

couple	temp. range in ^{o}C	Kirkendall interface in the phase	at% Ti at Kirkendall interface	D_{Ti}/D_{Al}
TiIII-TiAl	768-865	Ti_3Al	78	7.7 $\pm$ 1
TiIV-TiAl	768-865	Ti_3Al	78	8.5 $\pm$ 1
Ti(5%Al)-TiAl	768-865	Ti_3Al	77	8.5 $\pm$ 1
Ti_3Al-$TiAl_2$	784-972	TiAl	48	0.37 $\pm$ 0.06
TiAl-$TiAl_3$	784-958	$TiAl_2$	33.3	0
Ti_3Al-$TiAl_3$	784-958	$TiAl_2$	33.3	0
Ti($<$ 67%Al)-Al	516-640	$TiAl_3$-Al boundary	--	0

6.3.3. Conclusions from section 6.3.

In diffusion experiments, carried out above $700^{o}C$ and using pure Ti or alloys as starting materials, have been developed the phases in accordance with the phase diagram represented in fig.6.1. The growth of the various diffusion layers is non-parabolic; the reason is supposed to be the influence of grain boundary diffusion, steadily decreasing with increasing annealing duration as a result of grain growth in the layer.

In the composition range $\lesssim$ 25 at% Al, Ti is the faster diffusing component. The phase diagram in this region is found to agree with the work of Blackburn[78].

In the TiAl compound, Al is the faster diffusing component, at least at the Kirkendall interface. In the $TiAl_2$ phase, Al is the only diffusing component at the Kirkendall interface.

6.4. THE USE OF $TiAL_3$ AS A COATING MATERIAL

Concerning the applicability of $TiAl_3$ as a coating material for Ti-alloys, some points must be particularly mentioned:

(a) The interface of pores, formed in the $TiAl_3$ layer dependent on the coating method and composition of the base alloy, might easily cause a break-down of the coating.

(b) The influence of the transition temperature at about 600°C in the $TiAl_3$ phase on the coating properties has yet to be investigated.

(c) A favourable condition is the low diffusivity at temperatures $<$ 880°C, together with the virtually total absence of Al in the α-Ti phase. Above the transition temperature, however, the coating will soon be consumed by the very fast diffusion in β-Ti. Besides, the properties of the base metal will then be seriously affected by the penetrating Al atoms.

SUMMARY

A study of the influence of concentration-dependent partial molal volumes on the calculation of diffusion coefficients in a binary metal system has led to the conclusion that the equation proposed by Balluffi[25] is equivalent to that proposed by Sauer and Freise[19]. A discussion of the applicability of the various equations is added, and new, simple relations for the calculation of intrinsic diffusion coefficients are presented.

Interdiffusion phenomena have been investigated in the Ti-Al system, using the diffusion couple technique. A number of methods have been used to achieve proper contact between the starting materials, for which the pure elements as well as various Ti-Al alloys have been used. Dependent on the nature of the starting materials, annealing temperatures between 500-1200°C have been applied, using evacuated quartz capsules in order to avoid reactions with gases. Afterwards the couples were prepared by the usual metallographic methods.

The measuring techniques used in this investigation are microscopy, microprobe analysis, X-ray diffraction, and micro-indentation hardness testing.

The results prove that in diffusion experiments carried out below 640°C, in which Al is one of the starting materials, only one phase develops , viz., $TiAl_3$. Two modifications of this compound are found to exist, viz., the already known "high-temperature" phase and a hitherto unknown "low-temperature" modification. The latter can be described as a superstructure of the high-temperature phase with a c-parameter, four times as long.

Layer growth obeys the parabolic time dependence for the TiAl-Al couples. When using Ti-richer starting materials, an initial layer is formed which grows linearly with time. The duration of the linear growth period and the rate of the layer formation have been investigated. The existence of the linear growth is assumed to be caused by a more or less thin film of oxide scale on the surface of Ti or the Ti-rich alloy. The change-over between the linear and the subsequent parabolic period is marked by a row of pores parallel to the contact interface.

The low values of diffusion coefficient and activation energy in the parabolic growth period indicate that grain boundary diffusion is the dominant mechanism in the mass transport through the $TiAl_3$ layer. Marker experiments have proved that Al is the only diffusing component in this transport.

At temperatures above 700°C, using pure Ti or various Ti-Al alloys as starting materials, other phases develop according to the phase diagram given in fig.6.1. The growth of the various diffusion layers is non-parabolic; the reason for this is supposed to be the influence of grain boundary diffusion, steadily decreasing with increasing annealing duration as a result of grain growth in the layer.

In the composition range $\leqslant$ 25at% Al, Ti is the faster diffusing component. The phase diagram in this region is found to agree with the work of Blackburn[78].

In the compound TiAl, Al is the faster diffusing component, and in the compound $TiAl_2$, Al is the only diffusing component.

At 1200°C we have found the phase Ti_2Al_5, which is probably the same as the compound Ti_5Al_{11}, mentioned by Schubert et al.[86].

Finally, some remarks are made on the applicability of $TiAl_3$ as a coating material for Ti-alloys.

SAMENVATTING

De invloed van concentratie-afhankelijke partiële molaire volumina op de berekening van diffusiecoefficienten in een binair metaalsysteem is onderzocht. De vergelijkingen opgesteld door Balluffi[25] enerzijds en Sauer en Freise[19] anderzijds, blijken gelijkwaardig te zijn. De toepassingsmogelijkheden van de verschillende vergelijkingen zijn onderzocht en er zijn enkele eenvoudige relaties afgeleid voor de berekening van intrinsieke diffusiecoefficienten.

Interdiffusie-verschijnselen zijn onderzocht aan het systeem Ti-Al met behulp van de diffusiekoppeltechniek. Een zestal methoden zijn toegepast om een goede hechting te verkrijgen tussen de twee uitgangsmaterialen, waarvoor zowel de zuivere elementen als legeringen gebruikt zijn. Afhankelijk van de aard van de uitgangsmaterialen zijn temperaturen toegepast van 500-1200°C, waarbij de koppels in geëvacueerde kwartsglazen capsules zijn ingesmolten teneinde reacties met gassen te vermijden.

Als onderzoektechnieken zijn gebruikt metaalmicroscopie, microprobe analyse, röntgendiffractie en microhardheidsbepaling.

Bij diffusie-experimenten uitgevoerd beneden het smeltpunt van Al, waarbij Al een van de uitgangsmaterialen is, ontstaat slechts één intermetallische verbinding, nl. $TiAl_3$. Van deze verbinding blijken twee modificaties te bestaan, de alreeds bekende "hoge-temperatuur" vorm en een tot nu toe nog niet bekende "lage-temperatuur" vorm. De laatste kan beschreven worden als een superstructuur van de hoge-temperatuur-vorm met een verviervoudigde c-as.

Voor de koppels TiAl-Al wordt de parabolische laaggroei gevonden. Wanneer echter Ti-rijkere uitgangsmaterialen gebruikt worden, dan ontstaat eerst een laag, die lineair met de tijd aangroeit. De duur van deze lineaire groei en de snelheid van laagvorming zijn bestudeerd. De oorzaak van het optreden van deze lineaire groei wordt gezocht in de aanwezigheid van een meer of minder dun oxidehuidje op het Ti of de Ti-rijke legering. De overgang tussen de lineaire periode en de daarop volgende parabolische laaggroei wordt in de $TiAl_3$-laag gemarkeerd door een rij poriën evenwijdig aan het contactoppervlak.

De lage waarden voor de geïntegreerde diffusiecoefficient en de activeringsenergie gedurende de parabolische groei van de $TiAl_3$-laag zijn een sterke aanwijzing voor de overheersing van korrelgrensdiffusie bij het massatransport door de laag. Marker experimenten hebben aangetoond, dat Al de enig beweeglijke component is bij dit transport.

Bij temperaturen boven 700°C, waarbij zuiver Ti of Ti-Al legeringen als uitgangsmaterialen gebruikt zijn, worden in de diffusiekoppels de overige fasen gevormd, overeenkomstig het fasendiagram in fig.6.1. De groei van de diverse fasen is niet parabolisch. Verondersteld wordt, dat de oorzaak van deze afwijking gezocht moet worden in de bijdrage die korrelgrensdiffusie levert aan het groeiproces. Deze bijdrage neemt af naarmate de diffusietijd toeneemt t.g.v. korrelgroei in de laag.

Bij 1200°C is door ons gevonden de verbinding Ti_2Al_5, die waarschijnlijk dezelfde is als de door Schubert c.s.[86] gevonden fase Ti_5Al_{11}.

Bij samenstellingen $\leqslant$ 25 at% Al is Ti de snelst diffunderende component. Het door ons gevonden fasendiagram in dit gebied toont grote overeenstemming met het werk van Blackburn[78].

In de verbinding TiAl is Al de snelst diffunderende component, in de verbinding $TiAl_2$ is Al de enig diffunderende component.

Wat een eventueel gebruik van $TiAl_3$ als coating materiaal voor Ti-legeringen betreft, moet op enige punten de aandacht worden gevestigd:

(a) De poriën die afhankelijk van verschillende bereidingswijzen of uitgangsmaterialen in het $TiAl_3$ gevormd worden, kunnen gemakkelijk aanleiding geven tot afbrokkelen van een deel van de coating.
(b) De invloed van de overgangstemperatuur rond 600°C in de $TiAl_3$-fase op de eigenschappen van de coating zal bestudeerd moeten worden.
(c) Een gunstige omstandigheid is de lage diffusiesnelheid bij temperaturen $<$ 880°C. Boven de overgangstemperatuur van Ti zal echter t.g.v.de zeer snelle diffusie in β-Ti de coating spoedig verbruikt zijn. Bovendien zullen de eigenschappen van het materiaal dan sterk beinvloed worden door het binnendringende aluminium.

REFERENCES

1 Adda, Y., and J.Philibert: La Diffusion dans les Solides, P.U.F., Paris 1966.
2 Seith,W: Diffusion in Metallen, Springer-Verlag Berlin, Göttingen, Heidelberg, 1955.
3 Shewmon,P.G.: Diffusion in Solids,Mc Graw-Hill Book Co., Inc., New York 1963.
4 McQuillan,A.D., and M.K.McQuillan: Titanium, Butterworths Scientific Publications, London 1956.
5 The Science, Technology and Application of Titanium, Proceedings of an International Conference held at London, on 21-24 May 1968, Ed.by Jaffee, R.I., and N.E.Promisel, Pergamon Press, Oxford 1970.
6 Gray, A.G.: Met.Prog.94, 59-71 (Sept.1968).
7 Wiedemann, K.H.: Metall 24, 144-149 (1970).
8 Brick, R.M., R.B.Gordon and A.Phillips: Structure and Properties of Alloys, McGraw-Hill Book Company, New York 1965.
9 Nicholls, J.E.: Corrosion Technology 11, 16-21 (Oct.1964).
10 Nicholls, J.E.: Metallurgia 75, 57-66 (Febr.1967).
11 Jukes, R.A.in: The Science, Technology and Application of Titanium, see Ref.5, p.923-931.
12 Bowers, J.E., N.J.Finch and M.G.Burberry in: The Science, Technology and Application of Titanium, see Ref.5, p.1081-1096.
13 Zemskov, G.V., and P.F.Shulenok: Prot.of Metals 2,83-85(1966).
14 Manning, J.R.: Diffusion Kinetics for Atoms in Crystals, D.van Nostrand Company, Inc., London 1968.
15 Bakker, H.: Tracer Diffusion in Face Centered Cubic Metals, Thesis, University of Amsterdam, 1970.
16 Bolk, A.: Het Kirkendall-effect in het Systeem Goud-Platina, Thesis, Technical University Delft, 1959.
17 Boltzmann, L.: Ann. der Physik 53, 959-964(1894).
18 Matano, C.: Japan.J.Physics 8, 109-113(1933).
19 Sauer, F., and V.Freise: Z.Elektrochem.66, 353-363(1962).
20 Den Broeder, F.J.A.: Scripta Met.3, 321-326(1969).
21 Darken, L.S.: Trans.Met.Soc.AIME 175, 184-194(1948).
22 Wever, H.: Phys.Status Solidi 18, K25-K27(1966).
23 Levasseur, J., and J.Philibert: Phys.Status Solidi 21, K1-K4(1967).
24 Wagner, C.: Acta Met.17, 99-107(1969).
25 Balluffi, R.W.: Acta Met.8, 871-873(1960).
26 Crank, J.: The Mathematics of Diffusion, Oxford University Press,1967.
27 Guy, A.G., R.T.De Hoff and C.B.Smith: Trans.Am.Soc.Metals 61, 314-320(1968).
28 Guy, A.G.: Scripta Met.5, 279-282(1971).
29 van Loo, F.J.J.: Scripta Met.5, 287-288(1971).
30 van Loo, F.J.J.: Acta Met.18, 1107-1111(1970).
31 Prager, S.: J.Chem.Phys.21, 1344-1347(1953).
32 van den Broek, J.J.: Philips Res.Repts 25, 405-414(1970).
33 van den Broek, J.J.: Philips Res.Repts 26, 40-48(1971).
34 Jost, W.: Z.Physik 127, 163-167(1950).
35 Heumann, Th., Z.Physik.Chemie 201, 168-189(1952).
36 Wagner, C.in: Jost,W.: Diffusion, Darmstadt(1957)
37 Kidson, G.V.: J.Nucl.Mater.3, 21-29(1961).
38 Fara, H., and R.W.Balluffi: J.Appl.Phys.30,325-329(1959).
39 Beyeler, M., and Y.Adda: C.R.Acad.Sc.253, 2967-2969(1961).

40 Powell, G.W., and R.Schuhmann,Jr.: Trans.Met. Soc.AIME 245, 961-965(1969).
41 Eifert, J.R., D.A.Chatfield, G.W.Powell, and J.W.Spretnak: Trans.Met.Soc.AIME 242, 66-71(1968).
42 Heumann, Th. in: La Diffusion dans les Métaux, Comptes Rendus du Colloque à Eindhoven, 1956, p.59-75.
43 Baird, J.D.: J.Nucl.Energy, Part A,11, 81-88(1960).
44 Lustmann, B., and R.F.Mehl: Trans.Met.Soc.AIME 147, 369-395(1942).
45 Howard, R.E., and A.B.Lidiard: Reports on Progress in Physics 27, 161-240(1964).
46 Balluffi, R.W., and L.L.Seigle: Acta Met.3, 170-177 (1955).
47 Levasseur, J. and J.Philibert: C.R.Acad.Sci.267,1562-1565(1968), and Kohn,A., J.Levasseur, J.Philibert, and M.Wanin: Acta Met.18, 163-173 (1970).
48 Badia, M., and A.Vignes: Mém.Scient.Rev.Mét.66,915-927(1969).
49 Lidiard, A.B., and K.Tharmalingam: Disc.Faraday Soc.28, 64-68(1959).
50 Hart, E.W.: Acta Met.5, 597(1957).
51 Harrison, L.G.: Trans.Faraday Soc.57, 1191-1199(1961).
52 Frischat, G.H.: Z.angew.Phys.22, 281-287(1967).
53 Hässner, A.: Neue Hütte 12, 161-168(1967).
54 Fisher, J.C.: J.Appl.Physics 22, 74-77(1951).
55 Whipple, R.T.: Phil.Mag.45, 1225-1236(1954).
56 Mackowiak, J., and L.L.Shreir: J.Less-Common Metals 1, 456-466(1959) and 15, 341-346(1968).
57 Bastin, G.F.: private communication, to be published.
58 Clark, J.B.: Trans.Met.Soc.AIME 227, 1250-1251(1963).
59 Turnbull, D.: Atom Movement, ASM, Cleveland 1951,p.129.
60 Trimble, L.E., D.Finn and A.Cosgarea, Jr.: Acta Met.13, 501-507(1965).
61 Smigelskas, A.D., and E.O.Kirkendall: Trans.Met.Soc.AIME 171, 130-142(1947).
62 Hansen, M.: Constitution of Binary Alloys, McGraw-Hill Book Co., Inc., New York 1958.
63 Sagel, K., E.Schulz and U.Zwicker: Z.Metallkde 47,529-534(1956).
64 Anderko K., K.Sagel und U.Zwicker: Z.Metallkde 48,57-58(1957).
65 Ence, E., and H.Margolin: Trans.Met.Soc.AIME 221,151-157(1961).
66 Glazova, V.V.: Dokl.Chem.160, 11-13(1965).
67 Yao, Y.L.: Trans.Am.Soc.Metals 54, 241-246(1961).
68 Pietrokowsky, P.: Nature 190, 77-78(1961).
69 Goldak, A.J., and J.G.Parr: Trans.Met.Soc.AIME 221, 639-640(1961).
70 Clark, D., and J.C.Terry: Bull.Inst.Metals 3, 116 (1955-57).
71 Clark, D., K.S.Jepson and G.I.Lewis: J.Inst.Metals 91, 197-203(1962-63).
72 Kornilov, I.I., E.N.Pylaeva, M.A.Volkova, P.I.Kripyakevich, and V.Ya.Markiv: Dokl.Chem.161, 332-335(1965).
73 Kornilov, I.I., and M.A.Volkova: Russ.Metall.no 1,105-108(1968).
74 Tsujimoto, T., and M.Adachi: J.Inst.Metals 94, 358-363(1966).
75 Crossley, F.A.: Trans.Met.Soc.AIME 236, 1174-1185 (1966).
76 Crossley, F.A.: Trans.Am.Soc.Metals 60,714-716(1967).
77 Crossley, F.A.: Trans.Met.Soc.AIME 245, 1963-1968(1969).
78 Blackburn, M.J.: Trans.Met.Soc.AIME 239,1200-1208(1967).
79 Crossley, F.A.: Trans.Met.Soc.AIME 242, 726-728(1968).
80 Blackburn, M.J.: Trans.Met.Soc.AIME 242, 728-730(1968).
81 Margolin, H.: Trans.Met.Soc.AIME 242, 742-743(1968).
82 Blackburn, M.J.: Trans.Met.Soc.AIME 242, 743-744(1968).
83 Shunk, F.A.: Constitution of Binary Alloys sec.Suppl., McGraw-Hill Book Co., New York 1969.
84 Pötzschke, M., and K.Schubert: Z.Metallkde 53, 548-561(1962).

85 Schubert, K., H.G.Meissner, A.Raman and W.Rossteutscher: Naturwiss.51, 287(1964).
86 Raman, A., and K.Schubert: Z.Metallkde 56, 44-51(1965).
87 Ogden, H.R., D.J.Maykuth, W.L.Finlay and R.I.Jaffee: Trans.Met.Soc.AIME 191, 1150-1155(1951).
88 Bumps, E.S., H.D.Kessler and M.Hansen: Trans.Met.Soc.AIME 194, 609-614(1952).
89 Rostoker, W.: Trans.Met.Soc.AIME 194, 212-213(1952).
90 McHargue, C.J., S.E.Adair and J.P.Hammond: Trans Met.Soc. AIME 197, 1199-1203(1953).
91 Ogden, H.R., D.J.Maykuth, W.L.Finlay and R.I.Jaffee: Trans.Met. Soc.AIME 197, 267-272(1953).
92 Glazova, V.V.: Russ.Metall. no2, 116-118(1967).
93 Duwez, P., and J.L.Taylor: Trans.Met.Soc.AIME 194,70-71(1952).
94 Dagerhamn, T.in: Shunk, see Ref.83, p.45.
95 Elliot, R.P., and W.Rostoker: Acta Met.2, 884-885(1954).
96 Cooper, M.J.: Phil.Mag.8, 805-810(1963).
97 Cooper, M.J.: Phil.Mag.8, 811-821(1963).
98 Clark, H.T.: Trans.Met.Soc.AIME 185, 588-589(1949).
99 Eppelsheimer, D.S., and R.R.Penman: Nature 166, 960(1950).
100 Swanson H.E. and E.Tatge: JC Fel.Reports, NBS 1950(ASTM 4-0787).
101 Den Broeder, F.J.A.: Onderzoek naar de Diffusie in het Systeem Chroom-Wolfraam, Thesis, Technical University Delft, 1970.
102 Reed, S.J.B. in: X-Ray Optics and Microanalysis, IVe congrès international sur l'optique des Rayons X et la Microanalyse, Orsay 1965, Ed.by Castaing, R., P.Deschamps and J.Philibert, Hermann Paris VI, pp.339-349.
103 Hehenkamp, Th.: ibid pp.350-356.
104 Belk, A., and B.Clayton: ibid pp.409-417.
105 Henoc, M.J., Mlle F.Maurice and Mme A.Zemskoff in: Vth International Congress on X-ray Optics and Microanalysis, Tübingen 1968, Ed. by Möllenstedt, G., and K.H.Gaukler, Springer-Verlag Berlin, Heidelberg, New York, pp.187-192.
106 Brauer, G.: Z.anorg.allg.Chem.242, 1-22(1939).
107 Raman, A., and K.Schubert: Z.Metallkde 56, 40-43(1965).
108 Schubert, K.: Z.Metallkde 56, 93-98(1965).
109 Raman, A., and K.Schubert: Z.Metallkde 56, 99-103(1965).
110 Sinha, A.K.: Trans.Met.Soc.AIME 245, 911-917(1969).
111 Kidson, G.V., and G.D.Miller: J.Nucl.Mater.12,61-69(1964).
112 Heumann, Th., and S.Dittrich: Z.Metallkde 50,617-625(1959).
113 Heumann, Th.: Z.Metallkde 58, 168-174(1967).
114 Heumann, Th.: Z.Metallkde 59, 455-459(1968).
115 Janssen, M.M.P.: Reactiediffusie in het Systeem Nikkel-Aluminium, Thesis, Technical University Eindhoven,1966.
116 Janssen, M.M.P., and G.D.Rieck: Trans.Met.Soc.AIME 239, 1372-1385(1967).
117 Tiwari, G.P., and B.D.Sharma: Nature 204, 178-179(1964).
118 Mackowiak, J., and L.L.Shreir: J.Less-Common Metals 1, 456-466(1959).
119 Mackowiak, J., and L.L.Shreir: J.Less-Common Metals 15, 341-346(1968).
120 Goold, D.: J.Inst.Metals 88, 444-448(1959-60).
121 Libanati, C.M., and F.Dyment: Acta Met.11, 1263-1268(1963).
122 Murarka, S.P., and R.P.Agarwala: Acta Met.12, 1096(1964).
123 Dyment, F., and C.M.Libanati: J.Mater. Science 3,349-359(1968).
124 Kidson, G.V.: Electrochemical Technology 4,193-205(1966).
125 Meyering, J.L., and M.L.Verheijke: Acta Met.7, 331-338(1959).
126 Reinbach, R., and D.Fischmann: Z.Metallkde 54, 314-316(1963).
127 Shinoda, G., and H.Kawabe: Japan. J.Appl.Phys.3,662-663(1964).
128 Kawabe, H., M.Kaneko and G.Shinoda: Techn.Rep.Osaka Univ.17, 315-320(1967).

LEVENSBERICHT

12 febr.1938	: Geboren te Heerlen
1956	: Diploma H.B.S.-b behaald aan het St.Bernardinuscollege te Heerlen
1962	: Doctoraal examen afgelegd aan de Rijksuniversiteit te Utrecht, hoofdvak scheikunde, bijvakken fysische scheikunde en natuurkunde
1961 - 1963	: Leraar aan de R.K. H.B.S. te Wijk-Maastricht
1962 - 1966	: Leraar aan het St.Michiellyceum te Geleen
1966 - heden	: Wetenschappelijk medewerker in de sectie Fysische Chemie aan de Technische Hogeschool te Eindhoven

ERRATA TO "DIFFUSION IN THE TITANIUM-ALUMINIUM SYSTEM",
by F.J.J. van LOO, THESIS EINDHOVEN, 1971.

Page		reads	should read as follows
4	Line 5	Fysiche	Fysische
15	Fig.2.1.		left-hand part is Fig.2.1,a right-hand part is Fig.2.1,b
	Caption to Fig.2.1,b	V_2	$\bar{V}_2$
17	Fig.2.2.		left-hand part is Fig.2.2,a right-hand part is Fig.2.2,b
19	Caption to Fig.2.3.	Since the shaded areas are equal,..	Since area ACE is equal to area EGH,..
32	Fig.2.7.		left-hand part is Fig.2.7,a right-hand part is Fig.2.7,b
59	Caption to Fig.5.2.		● = Ti-Al; △ = Ti(5%Al)-Al ◇ = Ti(10%Al)-Al; □ = Ti_3Al-Al
80	Line 24	$<800^{\circ}$ C	$>800^{\circ}$ C
90	Table 5.4.	section 5.2.9.	section 5.3.
90	Table 5.4. (Ti-TiAl)	-9.7 ± 2.6	19.7 ± 2.6

STELLINGEN

1. Het gebruik van de volumefractie van een element als concentratie-eenheid in een homogene legering is onpraktisch, overbodig en vaak onmogelijk.

Guy,A.G.: Scripta Met. 5, 279-282 (1971).
van Loo, F.J.J.: Scripta Met. 5, 287-288 (1971).

2. Experimenten waarbij een intermetallische fase wordt gevormd tijdens het diffusieproces zijn in het algemeen niet geschikt om de volumediffusiecoefficient in deze fase te bepalen.

Dit proefschrift, hoofdstuk VI.

3. De formule waarmee Kolster de diffusiecoefficient meent te kunnen berekenen in een line-compound is onjuist. Zijn kritiek op Janssen en Rieck is dan ook ongegrond.

Kolster, B.H.: Proefschrift Delft 1968, par.6.7.5.
Janssen,M.M.P.: Proefschrift Eindhoven 1966, par.3.3.1.
Janssen, M.M.P., en G.D. Rieck: Trans. Met. Soc. AIME 239, 1372-1385 (1967).

4. De berekening van de intrinsieke diffusiecoefficienten door Kähkönen c.s. van Al en Ag in de fase Ag_2Al (door hen genoemd Ag_3Al) is foutief door een verkeerde bepaling van de markerverplaatsing. Uit de weergegeven penetratiecurve bij 535°C blijkt de verhouding D_{Al}/D_{Ag} ongeveer de helft te zijn van de door hen opgegeven waarde.

Kähkönen, H., en E. Syrjänen: J. Mater. Science 5, 710-712 (1970).

5. De methode van Heumann ter berekening van intrinsieke diffusiecoefficienten wordt vaak verkeerd toegepast, waardoor foutieve conclusies worden getrokken. Twee voorbeelden ter illustratie:

a. Uit markerexperimenten in een Ag-Ag (8% Mn) koppel trekken Barclay c.s. de conclusie dat $D_{Ag} \approx D_{Mn}$. In feite echter volgt uit hun experimenten dat $1 \leqslant D_{Mn}/D_{Ag} \leqslant \infty$.

b. Uit experimenten aan Ni-NiZn koppels trekken Andreani c.s. de conclusie dat D_{Zn}/D_{Ni} (bij 70 at% Ni) ≈ 3. In feite volgt uit de weergegeven penetratiecurve bij 800°C dat $D_{Zn}/D_{Ni} \approx \infty$. Hierdoor vervallen ook de door hen berekende waarden voor Q_{Zn} en Q_{Ni}.

Barclay, R.S., en P. Niessen: Trans. Am. Soc. Metals 62, 721-723 (1969).

Andreani, M, P. Azou en P. Bastien: Vth International Congress on X-Ray Optics and Microanalysis, Tübingen 1968, Ed. by Möllenstedt, G. and K.H. Gaukler, Springerverlag Berlin, Heidelberg, New York, pp. 519-530

6. De groei van de laag $NbAl_3$ in Nb-Al diffusie-koppels wordt door Steeb c.s. geinterpreteerd als evenredig met $\sqrt{t}$, voorafgegaan door een incubatieperiode. Het is echter veel waarschijnlijker dat de laaggroei in hun experimenten evenredig met de tijd verloopt en dat van een incubinatieperiode geen sprake is. Dit komt dan kwalitatief overeen met experimenten, die in ons laboratorium aan het systeem Nb-Al zijn uitgevoerd.

Steeb,S., en R. Keppeler: Z. Naturforsch. 24 a, 1601-1606 (1969).
Gischler, J.A.: Afstudeerverslag sectie Fysische Chemie, Juni 1968.

7. De methode die Waldmann c.s. voorstellen om de volumefracties van de afzonderlijke fasen in een tweefasige legering te bepalen met behulp van microprobe analyse is principieel onjuist.

Waldmann, J., M. Schwartz en S. Nash:
Trans. Am. Soc. Metals 62, 818-819 (1969).

8. Lidström geeft onvoldoende bewijzen voor de juistheid van zijn uitspraak dat kwartsdeeltjes met afmetingen tussen 1 en 8 µm zijn omgeven door een amorfe laag ter dikte van 0,12 µm.

Lidström, L.:
Acta Polyt. Scand., Chem. Met. Ser., no. 75, pp. 24-33 (1968).
Koopmans, K.: Proefschrift Eindhoven 1971 Hoofdstuk 2.

9. Voor de bepaling van het mechanisme van electrodereacties zijn de tweepunts- en de driepuntsmethode minder geschikt dan de conventionele methoden.

Barnartt, S. : Electrochim. Acta 15, 1313-1324 (1970).

10. Bij het uitzoeken en aanbrengen van coatings voor industriële doeleinden gaat men in het algemeen zeer empirisch te werk en houdt men te weinig rekening met de resultaten van het fundamentele onderzoek in deze materie.

Haupttagung der Deutschen Gesellschaft für Metallkunde, 1-4 Juni 1971, Lausanne.

Eindhoven, 17 september 1971. F.J.J. van Loo